universität wien

DISSERTATION

Titel der Dissertation

The role of Tyk2 in type I interferon signalling: identification and characterisation of novel target genes

angestrebter akademischer Grad

Doktor der Naturwissenschaften (Dr. rer.nat.)

Verfasserin:	Elisabeth Hofmann
Matrikel-Nummer:	9811902
Dissertationsgebiet (lt. Studienblatt):	Dr.-Studium der Naturwissenschaften Genetik - Mikrobiologie
Betreuerin/Betreuer:	Univ.-Prof. Dr. Mathias Müller

Wien, am 29. März 2010

ABSTRACT

The Janus kinase / signal transducer and activator of transcription (Jak/Stat) signalling cascade provides a fast way to transmit signals from cell surface receptors to target genes and is involved in numerous pathways including development, growth and immunity. The Jak tyrosine kinase 2 (Tyk2) is amongst others involved in type I interferon (IFNα/β) and IL-12 signalling, where it is required for full activation of Stats. Mice deficient for Tyk2 on the one hand show increased susceptibility to a number of pathogens, but on the other hand are resistant to e.g. lipopolysaccharide- (LPS-) induced shock. In the absence of Tyk2, peritoneal macrophages (PMs) show reduced expression of IFNβ, IFNα-4 and inducible nitric oxide synthase (iNOS) after LPS treatment.

The global impact of the absence of Tyk2 on the transcriptional response of PMs to LPS treatment was analysed in a whole genome microarray experiment. By reverse-transcription (RT) quantitative real-time PCR (qPCR) we could confirm the microarray data with respect to reduced expression levels of IFNβ and IFN-stimulated genes (ISGs) in the absence of Tyk2 as compared to WT. In addition, six genes, that had so far not been described to be regulated in response to LPS or IFN treatment, were found to be induced/repressed after LPS treatment in a Tyk2-dependent manner.

Within another expression profiling experiment, octamer-binding factor 6 (Oct-6; also known as Pou3f1, SCIP or Tst-1) was found to be induced in response to IFNβ in a Tyk2-dependent manner in fibroblasts. This transcription factor belongs to the family of Pit-Oct-Unc- (POU)- domain containing proteins and has been mainly described to be involved in developmental processes, but has not been related to immunity yet. We showed for the first time that Oct-6 is expressed in murine fibroblasts and macrophages after stimulation with IFNs. Oct-6 was also induced in response to poly(I:C) treatment and during viral infections, both in a strictly type I IFN-dependent manner. IFN-mediated induction of Oct-6 was largely dependent on the Jak/Stat signalling pathway and we could demonstrate Stat1 binding to the Oct-6 promoter in response to IFN treatment. With respect to the role of Oct-6, overexpression of Oct-6 resulted in prolonged expression of type I IFN mRNAs, but endogenous levels of Oct-6 did not impact on IFNα/β expression. However, we could demonstrate that endogenous Oct-6 is involved in regulating transcriptional responses to poly(I:C) treatment using microarray and RT-qPCR methods comparing the transcriptomes of WT and Oct-6-deficient macrophages. More detailed analyses will be required to fully elucidate the role of the novel ISG Oct-6 in innate immunity.

ZUSAMMENFASSUNG

Die Signaltransduktionskaskade der *Janus kinases* und *signal transducers and activators of transcription* (Jak/Stat) stellt eine schnelle Übertragung von Signalen ausgehend von Zelloberflächenrezeptoren zu Zielgenen sicher. Sie ist an zahlreichen Prozessen, wie zum Beispiel während der Entwicklung, des Wachstums und der Immunantwort, beteiligt. Die Jak *tyrosine kinase 2* (Tyk2) ist unter anderem in die Signaltransduktion von Typ I Interferonen (IFNα/β) und IL-12 involviert, wo es für die vollständige Aktivierung der Stats notwendig ist. Tyk2-defiziente Mäuse sind einerseits anfälliger auf verschiedenste Pathogene, andererseits resistent gegen Lipopolysaccharid- (LPS-) induzierten Endotoxinschock. Peritoneale Makrophagen weisen in Abwesenheit von Tyk2 eine reduzierte Expression von IFNβ, IFNα-4 und *inducible nitric oxide synthase* (iNOS) nach LPS Behandlung auf.

Der globale Einfluss der Tyk2-Defizienz auf die transkriptionelle Antwort peritonealer Makrophagen auf LPS-Behandlung wurde mittels Microarray-Technologie analysiert. Unter der Verwendung von reverser Transkription (RT) gekoppelt mit quantitativer real-time PCR (qPCR) konnten wir die Microarray-Daten bezüglich der reduzierten Expression von IFNβ und IFN-stimulierten Genen (ISG) verifizieren. Darüber hinaus wurden sechs weitere Gene gefunden, die bis jetzt nicht als LPS- oder IFN-reguliert bekannt waren und die eine Tyk2-abhängige Genregulation aufwiesen.

Während einer vorangegangenen Studie hatte sich gezeigt, dass *octamer-binding factor 6* (Oct-6, alias Pou3f1, SCIP, Tst-1) in Fibroblasten durch IFNβ-Behandlung Tyk2-abhängig induzierbar war. Dieser Transkriptionsfaktor zählt zu der Familie der Pit-Oct-Unc- (POU-) Domäne-enthaltenden Proteine und wurde bis jetzt nur im Zusammenhang mit Prozessen während der Entwicklung, nicht aber in Verbindung mit Abläufen im Immunsystem, beschrieben. Wir konnten zum ersten Mal überhaupt zeigen, dass Oct-6 durch Behandlung mit IFN in Fibroblasten und Makrophagen induziert wird. Außerdem wurde Oct-6 nach poly(I:C)-Behandlung sowie im Zuge von Virusinfektionen produziert, was wiederum abhängig von einem funktionierenden Typ I IFN-Signalweg war. Diese IFN-vermittelte Oct-6 Induktion war weitestgehend von der Jak/Stat-Signaltransduktionskaskade abhängig. Des Weiteren konnten wir belegen, dass Stat1 in Folge von IFN-Behandlung an den Oct-6-Promoter bindet. Die Funktion von Oct-6 im Kontext der angeborenen Immunität wurde in Überexpressions- und Deletionsexperimenten untersucht. Die Überexpression von Oct-6 führte zu einer verlängerten Expression von Typ I IFN mRNAs, allerdings hatte endogenes Oct-6 keinen Einfluß darauf. Dass Oct-6 eine Rolle im Zuge einer Immunantwort spielt, wurde gezeigt, indem die Antworten von WT und Oct-6-defizienten Makrophagen auf poly(I:C)-Behandlung mittels Microarrays und RT-qPCR verglichen wurden. Um die Rolle des neuen ISG Oct-6 im Zuge der angeborenen Immunität vollständig zu erfassen, sind weitere, detailliertere Analysen notwendig.

DANKSAGUNG

Viele Menschen waren in der einen oder anderen Form an der Entstehung dieser Arbeit beteiligt. Bei all jenen möchte ich mich an dieser Stelle bedanken:

Diese Arbeit entstand am Institut für Tierzucht und Genetik der Veterinärmedizinischen Universität Wien. Daher möchte ich mich zunächst ganz besonders bei Prof. Mathias Müller für die Möglichkeit, an seinem Institut an diesem überaus interessanten Thema arbeiten zu dürfen, bedanken. Darüber hinaus gilt ihm auch mein Dank für die konstruktiven Diskussionen im Zuge meiner Arbeit sowie für seine Unterstützung, nicht zuletzt in Form des Korrigierens meiner Dissertation.

Ganz besonderer Dank gilt meiner Betreuerin, Dr. Birgit Strobl, ohne deren Unterstützung und fundiertes Fachwissen diese Arbeit nicht Zustande gekommen wäre. Dank ihrer Anleitung, ihres Engagements, ihrer Ideen, der wertvollen Vorschläge und Diskussionen und nicht zuletzt auch ihrer Kritik habe ich in den letzten Jahren viel gelernt, wovon ich sicher auch in Zukunft sehr profitieren werde. Nicht weniger erwähnenswert sind ihre Geduld und Motivation auch noch während der Korrekturen meiner Arbeit – herzlichen Dank auch dafür.
Herzlichen Dank für alles!

Ebenso möchte ich mich bei all meinen Kolleginnen und Kollegen am Institut bedanken, die mir immer mit Rat und Tat zur Seite gestanden sind. Ohne euch wäre das Arbeiten auch nur halb so lustig gewesen.
Ohne jemanden benachteiligen zu wollen, sollte ich an dieser Stelle Dr. Ursula Reichhart besonders erwähnen, die immer ein wachsames Auge auf die Oct-6-Mauszucht hatte. Danke!

Doch all jenen, bisher erwähnten, Personen könnte ich an dieser Stelle nicht danken, wäre nicht meine Familie gewesen, ohne die mein Studium und damit auch diese Dissertation nicht möglich gewesen wären, und die mich immer in jeder Hinsicht unterstützt hat, und auf deren Unterstützung ich immer zählen kann, egal was ich noch vorhabe. Ein ganz großes Dankeschön euch allen dafür!

Schließlich möchte ich Christoph für sein Verständnis, seine Geduld, aber vor allem dafür, daß er das letzte Jahr zu einem für mich so besonderen Jahr gemacht hat, danken. Danke für alles!!

Table of contents

Abbreviations

BMM ..... bone marrow-derived macrophage
ChIP ..... chromatin immunoprecipitation
Ct ..... cycle threshold
DAVID ..... database for annotation, visualization and integrated discovery
Egr2 ..... early growth response 2
EMSA ..... electrophoretic mobility shift assay
FC ..... fold change
FLM ..... fetal liver-derived macrophage
GAS ..... IFNγ activated site
GFP ..... green fluorescent protein
GO ..... gene ontology
IFN ..... interferon
IL-12 ..... interleukin-12
IP ..... immunoprecipitation
Irf1 ..... IFN regulatory factor 1
ISG ..... IFN-stimulated gene
ISGF3 ..... IFN-stimulated gene factor 3
ISRE ..... IFN-stimulated response element
LPS ..... lipopolysaccharide
Lsm10 ..... U7 snRNP-specific Sm-like protein LSM10
MAPK ..... mitogen-activated protein kinase
MCMV ..... murine cytomegalovirus
MEF ..... murine embryonic fibroblast
MOI ..... multiplicity of infection
NES ..... nuclear export signal
NFκB ..... nuclear factor-κB
NLS ..... nuclear localisation signal
Oct-6 ..... octamer-binding factor 6
PM ..... peritoneal macrophage
pMEF ..... primary embryonic fibroblast
Pmp22 ..... peripheral myelin protein 22
poly(I:C) ..... polyinosinic-polycytidylic acid
POU-protein ..... Pit-Oct-Unc-domain containing protein
PRR ..... pattern recognition receptor

qPCR ..... real-time quantitative PCR
rcf ..... relative centrifugal force (g-force)
RLH ..... RIG-I-like helicase
rpm ..... revolutions per minute
RT ..... reverse transcription
SD ..... standard deviation
SE ..... standard error
Stat1 ..... signal transducer and activator of transcription 1
Stk40 ..... serine/threonine kinase 40
TFBS ..... transcription factor binding site
Tyk2 ..... tyrosine kinase 2
Ube2d2 ..... ubiquitin-conjugating enzyme E2D 2
WT ..... wild type

INTRODUCTION

The immune system

In order to provide effective defence against invading pathogens, jawed vertebrates have developed a sophisticated immune system consisting of two complementary parts. The adaptive immune system mediates highly specific responses against virtually any pathogen. Genetic rearrangements and somatic hypermutation of antigen-receptor genes allow for the detection and consequently the elimination of potential antigenic components. Moreover the adaptive immune system is able to remember a pathogen once encountered and will fight it immediately next time meeting a known insult. However, launching this kind of immune response for the first time takes about one week, which would be far too long to cope with an immediate threat. The innate immune system is able to react immediately to invading pathogens. From the evolutionary point of view the innate immune system is quite old, as it is found in invertebrates and vertebrates as well as in plants. It relies on germline encoded receptors, so-called pattern recognition receptors (PRRs) that recognise structures conserved amongst pathogens, but not present in the host, such as bacterial proteins, cell wall components, or nucleic acids of bacterial or viral origin (Carpenter and O'Neill, 2007). PRRs also recognise endogenous components, danger signals, such as degradation products of macromolecules or extracellular breakdown products, that are generated upon tissue damage. On the one hand PRR-mediated signalling in response to endogenous ligands is necessary for the initiation of tissue regeneration processes. On the other hand it is critically involved in the pathogenesis of autoimmune diseases such as systemic lupus erythematosus (Zhang and Schluesener, 2006).

The interferon system

Interferons (IFNs) were found more than 50 years ago as secreted molecules that interfere with viral replication. Intensive research over the last decades has revealed that IFNs are pleiotropic cytokines that exhibit antiviral, antiproliferative and immunomodulatory effects. IFNs inhibit initial infection and virus replication and thus limit virus spread until the adaptive immune system has launched an effective cell-mediated and humoral response to the infection. Without IFNs, an organism would succumb to viral, as well as bacterial infection, which was shown in mice lacking IFN or components of the downstream signalling pathways. IFNs also have a pronounced anti-proliferative effect as they are able to induce apoptosis in a number of documented malignancies including herpesvirus-associated lymphomas, acute promyelotic leukemia, non-small-cell lung cancer, non-melanoma skin cancer and glioma. Moreover, IFNs exhibit an immunomodulatory role as they can mediate the activation and recruitment of the adaptive immune response (Barber, 2001; Schroder *et al.*, 2004; Krause and Pestka, 2007).

IFNs are grouped into three classes, i.e. the type I, II and III IFNs, based on structural similarities and receptor usage. Members of the type I IFNs, their induction and effects will be described in detail below.

There is only one type II IFN, which is IFNγ. This cytokine is mainly produced by natural killer (NK) cells during the early immune response, and by activated T-cells in the course of the adaptive immune response. IFNγ plays a prominent role in macrophage activation, as it induces direct antimicrobial and antitumor mechanisms, antigen processing and presentation pathways. Moreover, IFNγ mediates leukocyte attraction and directs growth, maturation, and differentiation of many cell types. It enhances NK-cell activity and regulates B-cell functions such as immunoglobulin (Ig) production and class switching (Schroder *et al.*, 2004).

Only recently the class of type III IFNs has been established. IFNλ1 (or IL-29), IFNλ2 (IL-28A) and IFNλ3 (IL-28B) are in many ways similar to type I IFNs. Although they differ from type I IFNs in their structure as well as in their cognate receptor, they signal *via* the same pathway, induce expression of similar (or the same) target genes and thus lead to similar effects (Ank *et al.*, 2006). The IFNλ receptor consists of two subunits, namely IL10R2, which is ubiquitously expressed, and IL28RA, which is expressed only on a limited number of cell types. This cell type specific expression of the IFNλ receptor constitutes the major difference between the type I and type III IFN systems (Uzé and Monneron).

Type I IFNs

The class of type I IFNs contains the multi-gene family of IFNαs (IFNα-1 through -14), and the single copy genes IFNβ, IFNε, IFNκ, IFNω and IFNζ/limitin, all of which are encoded by intron-less genes and are clustered on mouse chromosome 4. They bind to a common receptor, the IFNα/β receptor consisting of the two subunits Ifnar1 and Ifnar2 (Krause and Pestka, 2007).

Induction of type I IFNs

In line with their essential role in innate immunity, type I IFNs (especially IFNα/β) can be produced by almost all cell types. Large amounts are rapidly and transiently induced upon recognition of viral or other microbial infections *via* PRRs. So far two major receptor families of PRRs have been shown to function in the innate immune system and induce type I IFNs in response to ligand recognition: ***(i)*** the membrane bound Toll-like receptors (TLRs), and ***(ii)*** the retinoic acid-inducible gene I (RIG-I)-like helicases (RLHs), which are found in the cytosol (Carpenter and O'Neill, 2007). In addition and only discovered recently, cytosolic DNA sensors are also able to induce IFNα/β (Vilaysane and Muruve, 2009).

Induction of type I IFNs through TLR signalling

The family of TLR receptors is highly conserved throughout evolution and homologues have been found in *Drosophila melanogaster* as well as in *Caenorhabditis elegans*. So far 13 mammalian TLRs have been identified (table 1). Together with the interleukin (IL)-1 receptors, the TLRs form a receptor superfamily (IL-1/TLR superfamily), which is characterised by the common cytosolic Toll-IL-1-receptor (TIR)-domain. In contrast to the IL-1 receptors, which have an immunoglobulin-like structured extracellular domain, the extracellular domains of TLRs contain leucine rich repeats. Each TLR, alone or in combination with another TLR or an accessory protein, is specific for a certain set of ligands (Akira *et al.*, 2006).

Table 1: Mammalian TLRs and their ligands, adapted from (Akira *et al.*, 2006).

TLR	Ligand	Organisms
TLR1	Triacyl-lipopeptides	Bacteria
TLR2	Peptidoglycan, lipoprotein, lipopeptides, atypical LPS	Bacteria
	Zymosan, phospholipomannan	Fungi
	GPI anchor	Protozoa
	VV (Barbalat *et al.*, 2009)	Virus
TLR3	Poly(I:C), dsRNA	Viruses
	mRNA (Karikó *et al.*, 2004)	endogenous
TLR4	Lipopolysaccharide (LPS)	Bacteria
	Mannan, glucuronoxylomannan	Fungi
	Glycoinositolphospholipids	Protozoa
	RSV fusion protein MMTV envelope protein (Lee and Kim, 2007) VSV G protein (Krishnan *et al.*, 2007)	Viruses
	heat shock proteins, fibronectin, hyaluronan (Krishnan *et al.*, 2007)	endogenous
TLR5	Flagellin	Bacteria
TLR6	Diacyl-lipopeptides Lipoteichoic acids (Lee and Kim, 2007)	Bacteria
	Zymosan (Lee and Kim, 2007)	Fungi
TLR7/TLR8	Synthetic imidazoquinoline-like molecules, ssRNA	Viruses
TLR9	CpG DNA	Batceria, Protozoa, Viruses
	DNA sugar backbone (Haas *et al.*, 2008)	all
	Hemozoin	Protozoa
TLR10[1]	unknown (Hasan *et al.*, 2005)	
TLR11	component of uropathogenic bacteria	Bacteria
	Profilin-like molecule	Protozoa
TLR12[2]	unknown (Krishnan *et al.*, 2007)	
TLR13[2]	unknown (Krishnan *et al.*, 2007)	

VV: Vaccinia virus, RSV: respiratory syncytial virus, MMTV: mouse mammary tumor virus, VSV: vesicular stomatitis virus

[1] TLR10 is not functional in mice due to disruption by retroviral insertion; [2] TLR12, 13 are not found in humans

TLRs are membrane bound, whereby TLR1, TLR2, TLR5, TLR6, TLR10, TLR11, TLR12 and TLR13 are located in the plasma membrane, TLR3, TLR7, TLR8 and TLR9 are found in the membrane of the endosomal compartment (Akira *et al.*, 2006; Kawai and Akira, 2008). TLR4 is found in the cytoplasmic as well as in the endosomal membrane (Kagan *et al.*, 2008). Similarly, TLR2 after internalisation and endosomal/lysosomal localisation mediates type I IFN induction in response to VV infection (Barbalat *et al.*, 2009). All TLRs, except for TLR3, activate a signalling pathway that involves the adaptor molecule MyD88, resulting in the activation of the transcription factors NFκB and AP-1. Upon activation they induce the expression of proinflammatory genes, such as TNFα, IL-6, IL-1β and IL-12 (Figure 1). A subset of TLRs, basically those that locate to the endosomal compartment, initiate signalling cascades leading to the induction of IFNβ. The induction of IFNβ in response to the ligands of TLR3 and TLR4, is mediated *via* the activation of IFN regulatory factor 3 (Irf3) in a MyD88-independent, but TRIF-dependent manner (Figure 1) (Uematsu and Akira, 2007).

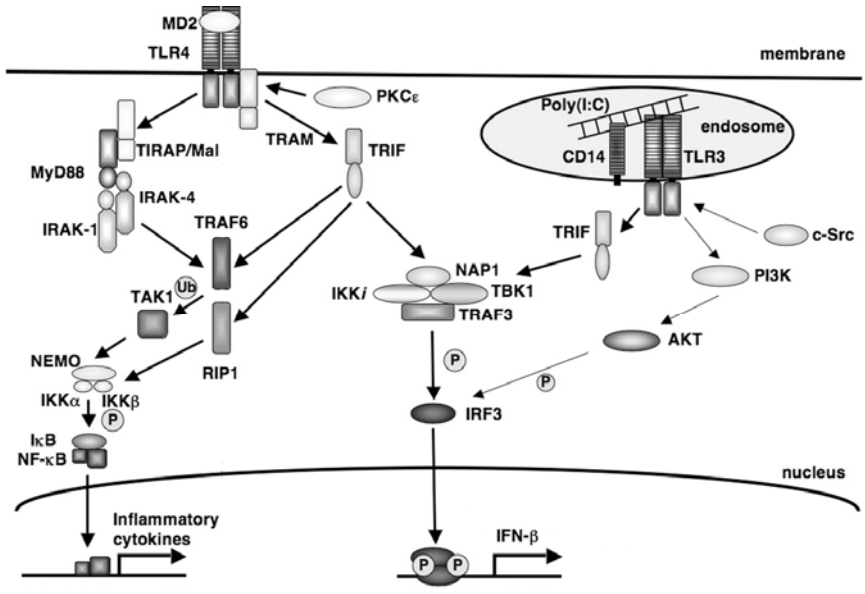

Figure 1. TLR3- and TLR4-mediated signalling pathways (adapted from Uematsu and Akira, 2007)**.** TLR signalling pathways originate from the cytoplasmic TIR domain. Upon ligand binding the adapter protein MyD88 (myeloid differentiation primary response gene 88) associates with the TLRs and recruits IRAKs (interleukin-1 receptor-associated kinases) to the receptor. IRAKs then activate TRAF6 (TNF-receptor-associated factor 6), leading to the activation of TAK1 (transforming growth factor-β-activated kinase). TAK1 activates the IKK (inhibitor of NFκB kinase) complex consisting of IKKα, IKKβ, and NEMO/IKKγ. The IKK complex phosphorylates IκB (inhibitor of NFκB), which is degraded resulting in nuclear translocation of NFκB (nuclear factor-κB), which induces expression of proinflammatory cytokines. Another adapter, TRIF (TIR domain-containing adapter protein inducing IFNβ), is responsible for TLR3- and TLR4-mediated Irf3 activation. Additionally, TLR4 also requires yet another adapter, TRAM (TRIF-related adaptor molecule), for Irf3 activation. TRIF interacts with NAP1 (NAK-associated protein 1; in complex with TANK (TRAF-family member associated NF-κB activator)/SINTBAD (similar to NAP1 TBK1 adaptor); complemented from Nakhaei *et al.*, 2009) TBK1 (TANK-binding kinase 1), IKKι, RIP1 (receptor-interacting protein-1), and TRAF6. Irf3 is activated by TBK1 and IKKι, which mediate Irf3 phosphorylation and stimulate its nuclear translocation, DNA-binding and induction of IFNβ, IP-10 and Rantes expression.

Induction of type I IFNs through RLH signalling

The existence of cytoplasmic RNA receptors had been postulated based on the fact that cells deficient for TLR3 could still respond to intracellular poly(I:C) and induce IFNβ to wild type levels. The RNA helicases, RIG-I and Mda5 (melanoma differentiation associated protein-5) were shown to bind to viral RNA and poly(I:C), although with different specificity, and induce a signalling cascade resulting in the induction of IFNβ and inflammatory cytokines. In addition to a DExD/H-box RNA-helicase domain, Rig-I and Mda5 harbour two caspase recruiting domain (CARD)-like domains, which are necessary for downstream signalling. Another member of the family is Lgp2 RIG-I-like receptor Lgp2), which lacks these CARD-like domains and is supposed to interfere with RIG-I signalling by competing for the ligand. In contrast, Lgp2 is needed for full induction of type I IFNs in the case of Mda-5 signalling (Figure 2) (Takeuchi and Akira, 2007; Kawai and Akira, 2008; Nakhaei *et al.*, 2009).

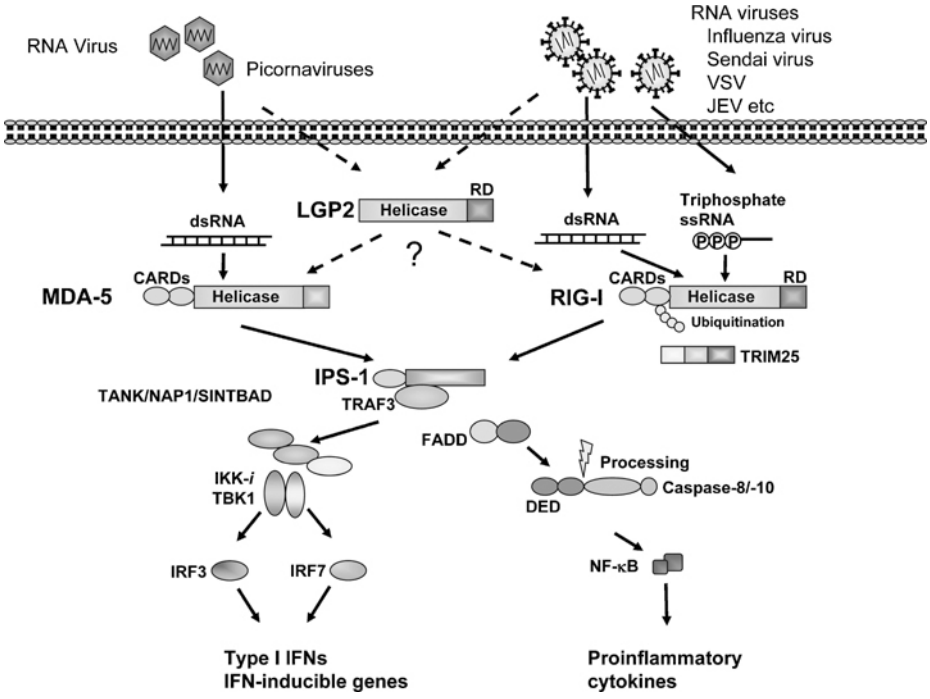

Figure 2: Signalling pathways downstream of RLHs (adapted from Takeuchi and Akira, 2007)**.** Following ligand binding, RIG-I or MDA-5 associate with the adapter IPS-1 *via* the CARD-like domains. IPS-1 (IFNβ promoter stimulator 1) is located to mitochondria and initiates two signalling pathways leading to activation of Irf3 or NFκB, and finally to the expression of IFNβ or proinflammatory cytokines, respectively. A complex consisting of TRADD (TNF receptor 1 associated signal transducer), TRAF6, TRAF2, and RIP1 (not depicted, complemented from Nakhaei *et al.*, 2009) signals from IPS-1 to a FADD (Fas-associated via death domain), caspase-8, and caspase-10 conatining complex which leads to NFκB activation. IPS-1 signals *via* TRAF3 and a complex of TANK, NEMO (complemented from Nakhaei *et al.*, 2009), NAP1, SINTBAD, TBK1 and IKKι to activate Irf3 and Irf7. Ddx3x (DEAD/H (Asp-Glu-Ala-Asp/His) box polypeptide 3, X-linked) is also activated by TBK1 and is necessary for full induction of IFNβ (not depicted, complemented from (Soulat *et al.*, 2008; Schröder *et al.*, 2008)).

Induction of type I IFNs through cytosolic DNA sensors

The fact that cytosolic DNA induces expression of IFNβ independent of TLR and RLH signalling, argues for the existence of (a) cytoplasmic sensor(s). DAI (DNA dependent activator of Irfs; or Zbp1 for Z-DNA-binding protein 1) was reported to be involved in IFNβ induction in response to Z-DNA, B-DNA and herpes simplex virus (HSV) infection. The induction was shown to be mediated by a TBK1 dependent activation of Irf3 (Vilaysane and Muruve, 2009). Only recently, Zbp1, Irf3 and Ddx3x were shown to be involved in induction of type I IFNs after human cytomegalovirus (HCMV) infection (Defilippis *et al.*, 2009). However, cytosolic DNA induced IFNβ was only partially reduced upon knockdown of DAI (Vilaysane and Muruve, 2009). Moreover, DNA-mediated activation of immune responses was observed to be almost normally in DAI-deficient mice (Ishii *et al.*, 2008). This argues for the presence of at least one other cytosolic DNA receptor. Very recently, the DNA dependent RNA polymerase III (PolIII) has been shown to recognise cytosolic AT-rich dsDNA and transcribe it into AU-rich dsRNA containing a 5'triphosphate (Chiu *et al.*, 2009). This RNA in turn is recognised by Rig-I which induces a signalling cascade resulting in the induction of IFNβ, as described above (Figure 2). AIM2 has been found to also bind to cytosolic dsDNA and, by activation of the inflammasome, leads to processing and secretion of IL-1β but not to the induction of type I IFNs (Vilaysane and Muruve, 2009).

Transcriptional regulation of IFNβ

The enhancer of the IFNβ gene is located -102 to -47 bp upstream of the transcription start and has been subdivided into four so-called positive regulatory domains (PRD I through IV). Coordinate activation and binding of the transcription factors Irf3 and/or Irf7, ATF-2/c-Jun and NFκB (p50/p65) to this enhancer element are crucial for the expression of IFNβ. Together with the architectural protein HMG-I(Y) they form a complex known as the enhanceosome (Figure 3) (Honda *et al.*, 2006; Panne, 2008).

Especially Irf3 and the highly homologous Irf7 are key regulators of type I IFN expression. Irf3 is constitutively expressed in most cell types and localises to the cytoplasm as long as it is in the latent, non-activated state. Upon activation by phosphorylation, Irf3 dimerises and translocates to the nucleus. In contrast, Irf7 is expressed only at rather low levels in most cell types, but the levels are rapidly increased in response to type I IFN signalling. Similar to Irf3, Irf7 also requires phosphorylation for its activation, dimerisation (either homodimers, or heterodimers with Irf3) and nuclear translocation (Honda *et al.*, 2006; Génin *et al.*, 2009).

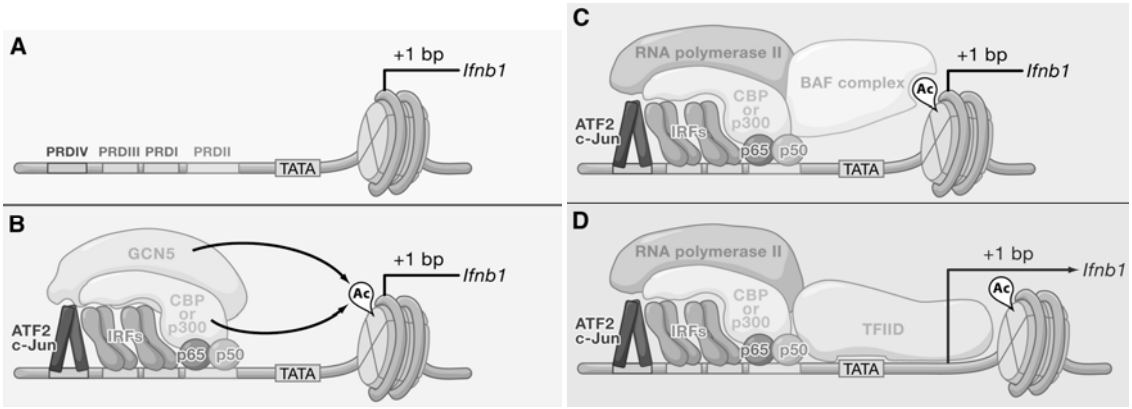

Figure 3: Assembly of the IFNβ enhanceosome and IFNβ gene induction (adapted from Honda *et al.*, 2006)**. (A)** In the steady state, the transcription start site of the IFNβ gene is covered by a positioned nucleosome. **(B)** PRD I-IV direct the assembly of ATF-2/c-Jun, Irfs, NFκB, and HMG-I(Y). The enhanceosome recruits histone acetyltransferases, such as GCN5 and CBP/p300, which acetylate (Ac) a subset of lysine residues of histones in the nucleosome. **(C)** Next, the RNA polymerase II holoenzyme (lacking the transcription factor TFIID) is recruited to the promoter. Chromatin-remodeling complexes such as BAF complexes are then recruited by contacting the acetylated histone. **(D)** BAF complexes induce nucleosome displacement from the transcription start site, making it accessible to TFIID for the induction of IFNβ expression.

Type I IFN signalling

The canonical Jak/Stat pathway

All type I IFNs bind to a common receptor, the IFNα/β receptor (Ifnar) consisting of two subunits, namely Ifnar1 and Ifnar2. Members of the Janus protein tyrosine kinases (Jaks) are constitutively associated with the cytoplasmic domains of the receptor chains, which lack intrinsic kinase activities. Tyk2 and Jak1 are associated with Ifnar1 and Ifnar2, respectively. Upon ligand binding the receptor complex undergoes conformational changes which results in the activation of the associated kinases. Jak1 and Tyk2 undergo auto- and cross-phosphorylation, and phosphorylate the receptor chains. This allows binding of preformed, but inactive, dimers of signal transducers and activators of transcription (Stats) to phosphorylated tyrosine residues of the receptor. Stats get phosphorylated, undergo conformational changes and translocate to the nucleus, where they initiate transcritpion of IFN-stimulated genes (ISGs; Figure 4) (Schindler *et al.*, 2007). In response to type I IFN mainly Stat1/Stat2 heterodimers are formed, which associate with another transcription factor, Irf9. Together they form the transcription factor complex IFN-stimulated gene factor 3 (ISGF3), which binds to promoters containing an interferon stimulated response element (ISRE; GATTTC$(N)_2$TTTCNY; Decker *et al.*, 1997). To a lesser extent also Stat1 homodimers are activated, which induce the expression of genes containing a IFNγ activated site (GAS; TTC$(N)_{2\text{-}4}$GAA; Decker *et al.*, 1997) in their promoter (Horvath, 2000; Takaoka and Yanai, 2006).

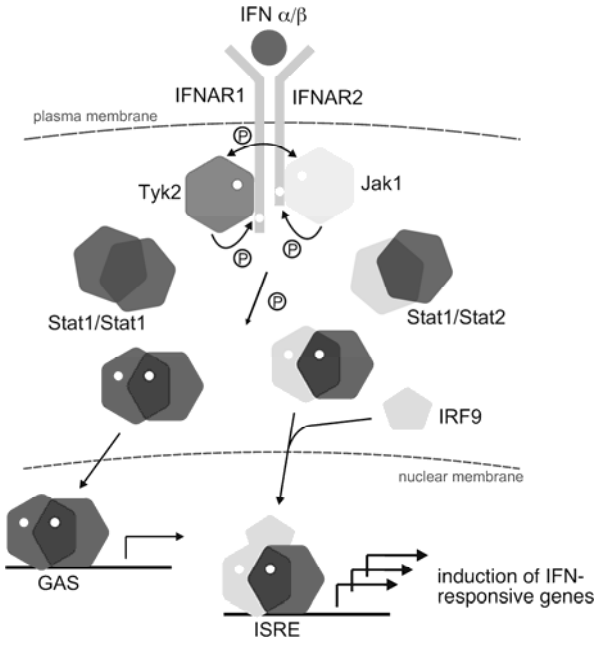

Figure 4: Jak/Stat signalling pathway downstream of type I IFNs (www.jak-stat.at)**.** Ligand-binding initiates a phosphorylation cascade mediated by the Jaks, Jak1 and Tyk2. Activated Stat1/Stat2 and to a lesser extent Stat1/Stat1 dimers translocate to the nucleus and induce the transcription of IFN-responsive genes.

Apart from Stat1 and Stat2 other Stats can be activated in response to type I IFNs. Actually, type I IFNs seem to be unique amongst all cytokines in that they are able to activate all seven Stats, which seems to be largely dependent on the cell type and the activation status of the cells (van Boxel-Dezaire *et al.*, 2006).

Pathways additionally activated by type I IFNs

In addition to the canonical Jak/Stat pathway, type I IFNs activate other pathways involving various kinases and transcription factors, which altogether mediate the complex responses to type I IFNs (Figure 5) (Stark, 2007). Activation of the phosphatidylinositol-3'-kinase (PI3-kinase) and its downstream signalling has been shown to play an important role in mediating effects of type I IFN, i.e. regulation of gene induction and initiation of translation (Kaur *et al.*, 2005). Another pathway critically involved in mediating the pleiotropic effects of type I IFN signalling is the mitogen-activated protein (MAP) kinase pathway. Three major MAP kinase pathways, namely the p38 MAP kinase, the extracellular signal-regulated kinase (ERK) and the c-Jun NH_2-terminal kinase (JNK) pathway, are activated in response to type I IFN signalling (Katsoulidis *et al.*, 2005).

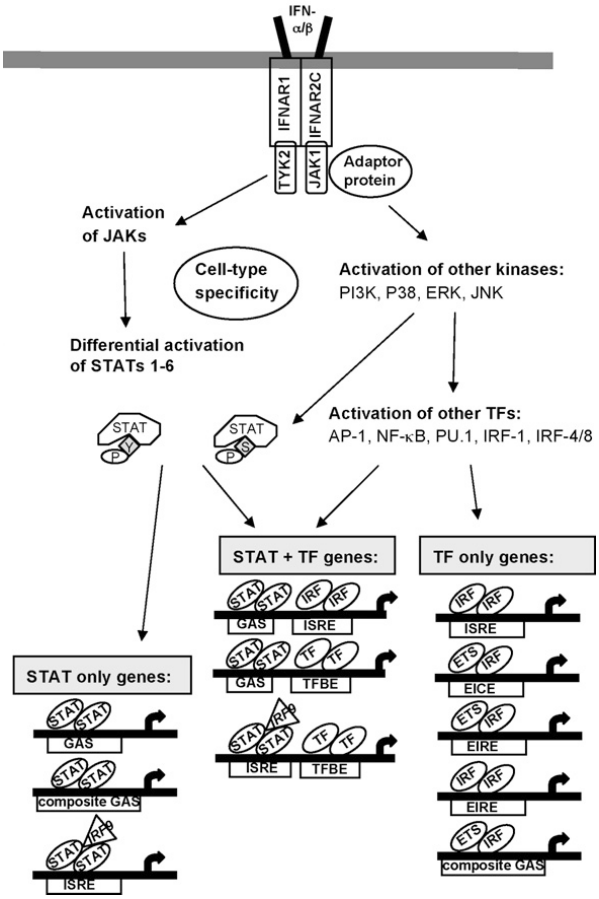

Figure 5: Complexity of the responses to type I IFNs (adapted from Stark, 2007)**.** In addition to the activation of Jaks and Stats, type I IFNs activate other kinases and transcription factors (TFs), as indicated in detail in the figure. The patterns of Stat, TF and kinase activation in response to each specific IFN are likely to be dependent on the cell type. Some genes respond only to activated Stats, some only to activated TFs, such as activated Irfs and/or the Ets-family member PU.1 (EIRE: Ets/Irf responsive element; EICE: Ets/Irf composite element), and some genes require binding of Stats together with other TFs.

Biological effects of type I IFNs

IFN treatment results in the induction of hundreds of IFN-stimulated genes (ISGs) (Der *et al.*, 1998). Direct antiviral activities have been attributed to only a few of these gene products, e.g. Myxovirus resistance gene 1 and 2 (Mx1, Mx2), 2',5'-oligoadenylate synthetases (Oas), ribonuclease L (RNaseL), dsRNA-dependent, protein kinase R (Pkr) and IFN-stimulated protein of 15 kDa (Isg15). Other ISGs encode PRRs (e.g. Rig-I, TLR3; de Veer *et al.*, 2001; Ifi200 class of genes: e.g. AIM2) or transcription factors (e.g. Irf7, Stat1; Der *et al.*, 1998), which are involved in feed forward loops, leading to an amplification of type I IFN production and thus resulting in further protection from virus spread and disease (Sadler and Williams, 2008).

Two tetratriocopeptide motif containing proteins, ISG54 and ISG56, have been shown to be implicated in inhibition of translation (Terenzi *et al.*, 2006). Members of the IFI200-family are involved in regulation of cell growth and differentiation (Asefa *et al.*, 2004). Type I IFNs initiate pathways leading to apoptosis, e.g. by inducing TNF-related apoptosis inducing ligand, Fas antigen, or caspases 4 and 8 (de Veer *et al.*, 2001). The growth arrest/cell death induced by type I IFNs contributes to the anitiviral effect, as viral replication is dependent on cellular replication and cell survival. Antiproliferative effects of type I IFNs are also exploited for treating several types of cancer, e.g. hairy cell leukemia, chronic myeloid leukemia, myeloma and B- and T-cell lymphomas. A number of solid tumors have also been shown to be responsive to IFN, including melanoma, renal cell carcinoma, and midgut carcinoids. Moreover, premalignant virally induced neoplasms, such as human papillomavirus related papillomas are also responsive to IFN treatment (Pokrovskaja *et al.*, 2005). Type I IFNs exert multiple functions on cells of the innate as well as the adaptive immune system, e.g. macrophages, dendritic cells, NK-cells, T-cell subsets and B-cells. The reported effects of type I IFNs are highly dependent on the overall context of the immune response investigated, i.e. on the amount of type I IFN, the diverse subtypes of type I IFNs, the stimulus, additional cytokines and the cell types involved (Bogdan *et al.*, 2004).

The POU-family of transcription factors

Members of the Pit-Oct-Unc- (POU-) family of transcription factors are involved in a variety of cellular processes, ranging from house-keeping gene function (Oct-1) and programming of embryonic stem cells (Oct-4), to the development of the immune system (Oct-1 and Oct-2), the pituitary gland (Pit-1) or the nervous system (Brn-1 through -4 and Oct-6) (Ryan and Rosenfeld, 1997; Phillips and Luisi, 2000). The transcription factors are characterised by the highly conserved structure of their DNA-binding domain, the POU-domain. This domain consists of 150-160 amino acids and is named after the first four transcription factors found to contain this conserved domain, namely the mammalian proteins Pit-1, Oct-1 and Oct-2, and the *Caenorhabditis elegans* protein Unc86. The POU-domain itself is a bipartite domain, divided into the N-terminal POU-specific domain, which is unique to the transcription factors of this family, and the C-terminal POU-homeodomain. The latter is related to the domain found in members of the homeobox-transcription factor family, which is involved in various developmental processes. The POU-specific domain and the POU-homeodomain are separated by a variable linker region of 15 to 56 amino acids (Figure 6) (Herr and Cleary, 1995; Phillips and Luisi, 2000).

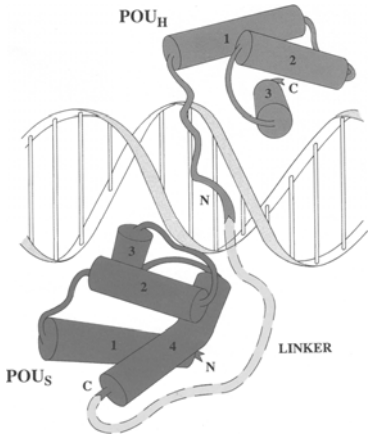

Figure 6: The conserved DNA-binding domain of POU-transcription factors.. The POU-domain consists of two sub-domains, i.e. the POU-specific domain (POU_S) and the POU-homeodomain (POU_H). These are connected by a flexible linker, which shows high variability among the different classes of POU-proteins (adapted from Herr and Cleary, 1995).

The members of the POU-family of proteins are divided into six classes according to amino acid sequence similarities of the POU-domain and to the conservation of the variable linker region. For example, the ubiquitously expressed Oct-1 and the tissue specific Oct-2, which has been found in B-cells (Shivdasani and Orkin, 1996), in peripheral-blood monocytes (PBMCs) and macrophages (Neumann *et al.*, 2000), belong to the second class and have been renamed to Pou2f1 and Pou2f2, respectively. The embryonic stem cell-specific Oct-4 was assigned to the fifth class and is now called Pou5f1. Oct-6 (Pou3f1), Brn-2 (Pou3f2), Brn-1 (Pou3f3) and Brn-4 (Pou3f4), all of which are mainly involved in processes of nervous system development, constitute the third class of POU-proteins (table 2) (Ryan and Rosenfeld, 1997; Phillips and Luisi, 2000; Holland *et al.*, 2007).

Table 2: The POU-family of transcription factors (adapted from Ryan and Rosenfeld, 1997 and Holland *et al.*, 2007)**.**

Class	Name	also known as	**expressed in** (according to current literature)
I	Pou1f1	Pit-1	pituitary gland
II	Pou2f1	Oct-1, Otf1	ubiquitously
	Pou2f2	Oct-2, Otf2	B-cells, macrophages, PBMCs
	Pou2f3	Oct-11, Skn-1a	squamous epithelia, keratinocytes
III	Pou3f1	Oct-6, Tst-1, SCIP	Schwann cells, neuronal subpopulations, keratinocytes
	Pou3f2	Brn-2, Oct-7, Otf7	central nervous system, oligodendrocytes, Schwann cells
	Pou3f3	Brn-1, Otf8	central nervous system
	Pou3f4	Brn-4, Otf9, Dfn3	neuronal cells
IV	Pou4f1	Brn-3a	sensory nervous system, B- and T-cells
	Pou4f2	Brn-3b, Brn3.2	retina, subpopulation of ganglion cells
	Pou4f3	Brn-3c, Dfna15	ear sensory epithelial cells
V	Pou5f1	Oct-4, Oct-3	embryonic stem cells
	Pou5f2	Sprm-1	male germ cells
VI	Pou6f1	Brn-5, Tcfb1	nervous system, Schwann cells
	Pou6f2	Wt5, Wtsl, Rpf-1	retinal ganglion, kidney

DNA-binding of the POU-transcription factors

POU-domain transcription factors recognise a sequence known as the octamer consensus motif (ATGCAAAT/A) or variants thereof. One variant is the "palindromic Oct-factor recognition element" (PORE; ATTTGAAATGCAAAT), which was first identified as an Oct-4 responsive DNA element in the first intron of the osteopontin gene. Another variant is the consensus sequence "more of PORE" (MORE; ATGCATATGCAT) element of the immunoglobulin heavy chain enhancers, which are regulated by Oct-1 and Oct-2 (Reményi *et al.*, 2002). Other members of the POU-family also recognise and bind to the consensus octamer sequence, but this might not be their highest affinity binding site. POU-proteins, however, have diverged sufficiently, so that their specifically preferred binding sites differ from the consensus sequence (Herr and Cleary, 1995). For example, the consensus recognition sequence for members of the third class of POU-proteins, including Oct-6, is $CAT(N)_{0\text{-}3}T/AAAT$ (Figure 7B). Oct-1 and Pit-1 have been most intensively studied with respect to their crystal structure and DNA-binding properties. The POU-specific domain and the POU-homeodomain were shown to bind independently to distinct regions of the recognised element, the linker region is enforcing the cooperative binding. POU-proteins were shown to be highly flexible in

terms of orientation of the two DNA-binding subdomains when bound to DNA. In general, the arrangement of the POU domain on the DNA, and thereby its DNA-binding affinity, and sequence specificity seems to be dependent on the linker region, the surrounding DNA sequence, and potential binding partners (Figure 7) (Herr and Cleary, 1995; Phillips and Luisi, 2000; Reményi *et al.*, 2002).

(A)

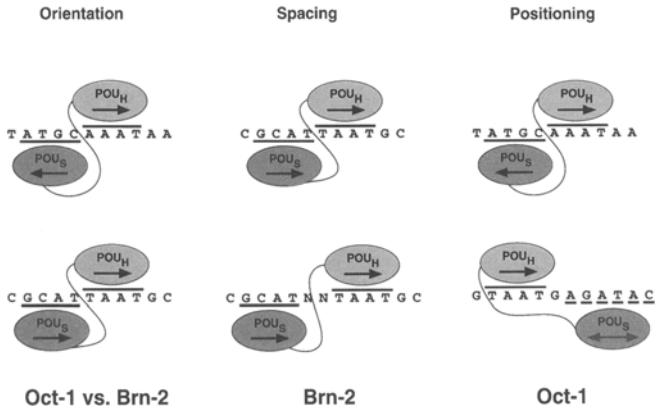

(B)

POU-subclass	Spacing	Consensus	Gene regulated	Sequence	POU-factor
III	0	CATT/AAAT	Ddc	**CATAAAT**	vvl (*D.m.*)
	2	CATN$_2$T/AAAT	Mpz	**CAT***TC***TAAT**	Oct-6 (*M.m.*)
	3	CATN$_3$T/AAAT	Crh	**CAT***AAA***TAAT**	Brn-2 (*R.n.*)

Figure 7: Flexibility of POU-proteins in their arrangement on DNA. (A) Based on the example of Oct-1 and Brn-2, the scheme shows, how the arrangements on the DNA differ in the relative orientation of the two subdomains, on the spacing between the POU-specific- (POU_S) and the POU-homeodomain (POU_H), and on the positioning of the two subdomains. POU_S and POU_H domain-binding sites are underlined and overlined, respectively (Herr and Cleary, 1995). **(B)** Summary of the identified DNA recognition elements for members of POU-III class according to their spacing preferences (modified from (Li *et al.*, 1993); Ddc, dopa decarboxylase; vvl, ventral veins lacking (drifter); *D.m.*, *Drosophila melanogaster*; Mpz, Myelin protein zero; *M.m.*, *Mus musculus*; Crh, corticotropin releasing hormone; *R.n.*, *Rattus norvegicus*).

POU-proteins show varying binding preferences, as they can act as monomers, homodimers, or form heterodimers with other POU-family members (Herr and Cleary, 1995). Additionally, POU-proteins display a high flexibility in cooperating with heterologous, non-POU transcription factors of cellular or even viral origin. Members of the high mobility-group (HMG) domain family are known to interact with homeodomain containing proteins in general. Especially, members of a subfamily, the Sry-box containing (Sox) proteins, were shown to specifically interact with members of the POU-family (Dailey and Basilico, 2001). Moreover, viral proteins, for example VP16 of Herpes simplex virus and T-antigen of JC virus (a human polyomavirus causing progressive multifocal leukoencephalopathy), were found to interact with the POU-proteins Oct-1 and Oct-6, respectively (Latchman, 1999). Oct-1 binding to an octamer motif in the viral promoter of the immediate early genes and subsequent association of VP16 with Oct-1 are necessary to initiate lytic infection. Similarly, Oct-6 binds to the promoter of JC virus early and late genes and in coorperation with JC virus T-antigen activates viral gene transcription resulting in the glial-cell tropism of JC virus.

Oct-6 (Pou3f1, SCIP, Tst-1)

Octamer-binding factor 6 (Oct-6), also known as suppressed cAMP-inducible POU protein (SCIP, (Monuki *et al.*, 1989)), or Testes-1 (He *et al.*, 1989) is encoded by an intronless gene on mouse chromosome 4, which shows all characteristics of a retroposed pseudogene (Kuhn *et al.*, 1991). The 45 kDa Oct-6 protein consists of 449 amino acids, the N-terminal third encoding a glycine- and alanine-rich transcriptional effector domain, followed by the DNA-binding POU-domain and a proline-rich sequence of so far unknown function (Meijer *et al.*, 1992; Monuki *et al.*, 1993).

Expression and regulation of Oct-6

Oct-6 belongs to the third class of POU domain transcription factors and plays an essential role in the terminal differentiation of myelinating Schwann cells and squamous epithelia (Jaegle *et al.*, 1996; Faus *et al.*, 1994; Andersen *et al.*, 1997). Expression of Oct-6 was also observed in undifferentiated embryonic carcinoma cells (P19 EC; Meijer *et al.*, 1990), during early embryogenesis, in developing neural and glial cells (Monuki *et al.*, 1989), in cells of neonatal testes (He *et al.*, 1989) and pancreatic β-cells (Baumeister and Meyerhof, 2000).

Expression of Oct-6 is tightly controlled, although the mechanisms, the cis-acting elements, and the signalling pathways leading to its expression are largely unknown. Proximal promoter elements, the transcription start site, the TATA box and a CCAAT motif have been identified, but are suggested to be responsible only for maintaining a basal expression of Oct-6 (Kuhn *et al.*, 1991). Tissue-specific and time-dependent expression of Oct-6 is regulated by distal enhancer elements. For example ~5 kb upstream of the transcription start a sequence element responsive to estrogen has been identified (Renner *et al.*, 1996). Another enhancer element ~12 kb downstream of the transcription start site was identified, which was shown to be responsible for Schwann cell-specific expression of Oct-6 (SCE for Schwann cell specific enhancer; Mandemakers *et al.*, 2000).

Oct-6 contains a nuclear localisation signal (NLS; Figure 8) within the POU-homeodomain, which is conserved in other POU-family members. Accordingly, Oct-6 protein is found mainly in the nucleus. Since Oct-6 shows potential phosphorylation sites near the NLS, it was suggested that the nuclear import of Oct-6 might be influenced/controlled by phosphorylation, but phosphorylated Oct-6 has not been detected yet. A nuclear export signal (NES; Figure 8) is located in the POU-homeodomain of Oct-6, which also seems to be conserved among all POU-family members. Regulation of nuclear import/export might be one means of regulating the activity of Oct-6 as a transcription factor, as similar mechanisms have already been shown for Oct-1 in *Xenopus* and Brn-2 in murine development (Baranek *et al.*, 2005 and references therein).

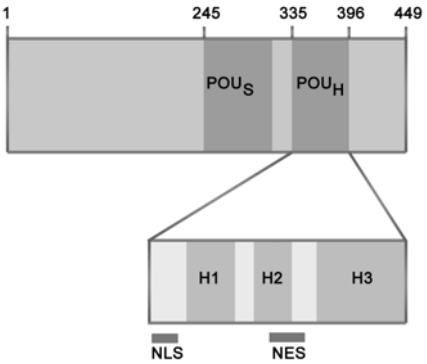

Figure 8: Schematic representation of the murine Oct-6 protein (adapted from Baranek *et al.*, 2005). The POU-specific domain (POU_S) and the POU-homeodomain (POU_H), the latter consisting of three helices (H1, H2 and H3), are indicated, as are the locations of the NLS and the NES within the POU-homeodomain.

The Role of Oct-6 in Schwann cell development

Oct-6 has been analysed mainly with respect to its role in Schwann cell development. Schwann cells are the glial cells of the peripheral nervous system. They originate from cells of the neural crest, a transient group of cells of the dorsal part of the neural tube, which also gives rise to melanocytes and neuronal precursors. Schwann cell precursors develop into immature Schwann cells which finally differentiate into myelinating and non-myelinating Schwann cells. While myelinating Schwann cells build up the myelin sheath, which is necessary for fast conduction velocity (saltatory conduction) along the axon, non-myelinating Schwann cells are crucial for neuronal survival. A myelinating phenotype is first defined by a Schwann cell forming an one-to-one association with an axon. This promyelinating Schwann cell then forms the myelin sheath within a few days. Myelin is a multi-lamellar structure formed by spiral wrapping of the cell membrane, which contains mainly the structural proteins myelin protein zero (Mpz, P0), myelin basic protein (Mbp), peripheral myelin protein 22 (Pmp22) and myelin-associated glycoprotein (Mag) (Mirsky *et al.*, 2001).

By postnatal day 30 (P30) the onset of myelination is complete and all Schwann cells show either a myelinating or non-myelinating phenotype. The maintenance of the myelinating phenotype is dependent on axonal contact, in developing as well as in regenerating nerves (Scherer *et al.*, 1994). Only recently, a G-protein coupled receptor family member, Gpr126, was found to be involved in elevating cAMP levels and leading to induction of Oct-6 and initiating myelination in zebrafish (Monk *et al.*, 2009). However, the axonal ligand has not been identified yet, and involvement of other receptors cannot be excluded. Signalling involves cAMP second messenger, and drugs such as forskolin inducing cAMP also induce Oct-6 expression (Svaren and Meijer, 2008; Meijer, 2009). Protein kinase A (PKA) is activated by cAMP signalling and further phosphorylates/activates cAMP response element binding protein and NFκB, both of which are involved in Oct-6 expression. Moreover, type III neuregulin 1 (Nrg1) mediated activation of PI3K/Akt and Ras/MAPK pathways

leading to Schwann cell proliferation and survival might also be involved in the regulation of Oct-6 expression (Svaren and Meijer, 2008; Birchmeier and Nave, 2008).

Oct-6 (Jaegle *et al.*, 1996; Bermingham *et al.*, 1996; Ghazvini *et al.*, 2002) and Egr2 (Krox20; Topilko *et al.*, 1994) are the two main transcription factors responsible for the correct development of myelinating Schwann cells, as deleting either factor leads to a block in myelination. Expression of Oct-6 is transiently upregulated in proliferating, promyelinating Schwann cells with expression levels peaking between P1 and P10. As myelination progresses Oct-6 expression decreases sharply (Arroyo *et al.*, 1998). Oct-6-deficient animals die soon after birth from a breathing insufficiency, caused by defective migration and differentiation of certain neurons in the brainstem. Only 2 to 4% of homozygous Oct-6-deficient mice have been reported to survive (Jaegle *et al.*, 1996; Bermingham *et al.*, 1996). Studies in those survivors and in mice with a Schwann cell specific knockout of Oct-6 (ΔSCE; Ghazvini *et al.*, 2002) reported severe defects in peripheral myelination and Schwann cells are arrested in the promyelinating stage. Thus, Oct-6 seems to be essential for terminal differentiation of myelinating Schwann cells (Figure 9). However, in the absence of Oct-6 the myelination is not completely blocked but only considerably delayed (by 10 to 15 days; Jaegle *et al.*, 1996; Bermingham *et al.*, 1996; Ghazvini *et al.*, 2002). In contrast, deleting Egr2 leads to a continuous block of myelination. Egr2 was shown to be a target gene of Oct-6, as in the absence of Oct-6 the expression of Egr2 is reduced (Ghislain *et al.*, 2002).

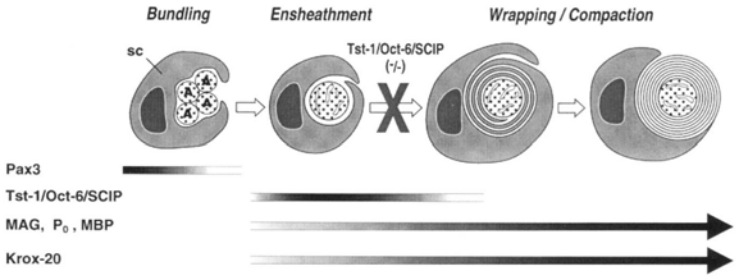

Figure 9: Arrest of Oct-6-deficient Schwann cells at the ensheathment stage (adapted from Bermingham *et al.*, 1996)**.** Oct-6 expression is transient and precedes the peak of Krox-20 (Egr2), Mag, Mbp, and Mpz expression. Pax3 expression declines prior to the onset of myelination (SC: Schwann cell; A: axon).

The closely related proteins Brn-1 and Brn-2, which belong to the same class (class III) of POU-proteins as Oct-6, are able to compensate for the loss of Oct-6. Brn-1, which is usually not expressed in Schwann cells, can fully replace Oct-6, when manipulated to be expressed instead of Oct-6 (Brn-1 knockin; Friedrich *et al.*, 2005). Brn-2 is expressed in Schwann cells at the same time as Oct-6, but has only partially overlapping functions. One reason for this might be that Oct-6 and Brn-2 require different co-factors, members of the Sry-box containing transcription factors, Sox10 and Sox11, respectively, for full transcriptional activity (Jaegle *et al.*, 2003).

Both, activating as well as repressing transcriptional effects, have been attributed to Oct-6 in the course of Schwann cell development. In Oct-6-deficient animals, expression of Egr2 and of the myelin genes (Mpz and Mbp) was reduced. The effect on the latter two might be indirect, since both genes are also dependent on Egr2. Conditional transgenic mice that constitutively express Oct-6 specifically in Schwann cells (condPou3f1:Mpz(Cre); Ryu *et al.*, 2007) show a persistent block in myelination. These mice have normal levels of Egr2, but the levels of Mpz, Mbp, and Pmp22 are significantly reduced. Taken together the results argue for the following scenario: Oct-6 exerts activating (Egr2) as well as repressing (Mpz, Mbp, Pmp22) functions during myelination. Correctly timed expression of Oct-6 is crucial for the terminal differentiation of myelinating Schwann cells.

Other roles of Oct-6

Apart from its crucial role in Schwann cell development, Oct-6 is involved in the terminal differentiation of keratinocytes. Together with another POU-family member, Skn1a (Pou2f3, Oct-11), Oct-6 exerts repressive effects on the expression of keratin K14 (Andersen *et al.*, 1997; Sugihara *et al.*, 2001) and matrix metalloprotease 19 (Beck *et al.*, 2007). Moreover, Oct-6 is also expressed in pancreatic β-cells, where it activates the expression of Sst1, a gene encoding somatostatin receptor 1 (Baumeister and Meyerhof, 2000).

POU-proteins in the immune system

Some POU-proteins play a role in the immune system. For example, Oct-2 and in a redundant way Oct-1, regulate immunoglobuline gene expression in B-cells (Phillips and Luisi, 2000). Oct-1 binding sites have been identified within the promoters of several IFNα subtypes and in Oct-1-deficient murine embryonic fibroblasts IFNα expression was enhanced (Mesplède *et al.*, 2005). Similarly, a functional Oct-1 binding site has been reported within the human IFNβ promoter, and IFNβ expression can be repressed by Oct-1 (Haggarty *et al.*, 1991). Several POU-transcription factors (Oct-1, Oct-2, Brn3a and Brn3b) have activating effects on inducible nitric oxide synthase (iNOS). In addition to the NFκB, C/EBPβ, ISRE and Irf1 sites, an octamer consensus motif is located approximately 60 bp upstream of the iNOS transcription start site (Goldring *et al.*, 1996; Kleinert *et al.*, 2004). A role for Oct-6 in the context of immunity has not been described so far.

AIMS

The first aim of the thesis is to elucidate the role of Tyk2 during LPS responses in macrophages using transcriptional-profiling approach. In a whole genome microarray experiment the transcriptional responses of WT and Tyk2-deficient peritoneal macrophages to LPS will be compared. Expression levels of genes found to be differentially regulated in the absence of Tyk2 will be further analysed using RT-qPCR.

The second aim is based on previous findings that Oct-6 is induced in response to IFNβ treatment in a Tyk2-dependent manner. Oct-6 expression patterns in response to IFNs, other cytokines and in the course of viral infections will be analysed in detail on mRNA as well as on protein level. Moreover, the molecular requirements for Oct-6 induction, i.e. signalling molecules, transcription factors and *cis*-regulatory elements, will be analysed. Finally, the question, whether Oct-6 is involved in transcriptional regulation in the context of innate immunity, will be addressed in gain- and loss-of-function experiments.

MATERIALS and METHODS

Mice

Wild type mice (C57BL/6) and mice deficient for Ifnar1 (Muller *et al.*, 1994), Tyk2 (Karaghiosoff *et al.*, 2000), Stat1 (Durbin *et al.*,1996), Irf1 (Reis *et al.*, 1994) and IFNβ (Erlandsson *et al.*, 1998) (all C57BL/6 background) were housed under specific pathogen-free conditions. Oct-6 heterozygous mice (mixed background) were a kind gift of Dies Meijer (Department of Cell Biology and Genetics, Erasmus University Medical Center Rotterdam, Netherlands; Jaegle *et al.*, 1996), the heterozygous breeding was done under conventional housing. Genotyping of Oct-6-/- mice and cells was done by 2 PCRs, one for Oct-6 (across the inserted Neo-cassette) and one for the Neo-cassette (Figure 10). The PCRs were run in a final volume of 25 µl containing 300 nM primer (gtOct6-F: CCAACCTGG-ACAAGATCG, gtOct6-R: CGCATAAACGTCGTCCAT, gtNeo-F: TTTTGTCAAGACCGACCTG, gtNeo-R: TGATGGATACTTTCTCGGC), 200 µM dNTP mix, 1x Biotaq buffer, 1U/reaction Biotaq DNA polymerase. $MgCl_2$ was used at a final concentration of 2 mM and 1.5 mM for the Oct-6- and the Neo-PCR, respectively. For the Oct-6 amplification 5% of DMSO was added. The Oct-6 PCR was run under the following conditions: 5 min initial denaturation at 95°C, 40 cycles of 95°C for 30 sec, 54°C for 30 sec and 72°C for 30 sec. The PCR for the Neo-cassette was run under following conditions: 5 min initial denaturation at 95°C, 40 cycles of 95°C for 30 sec, 55°C for 20 sec and 72°C for 30 sec.

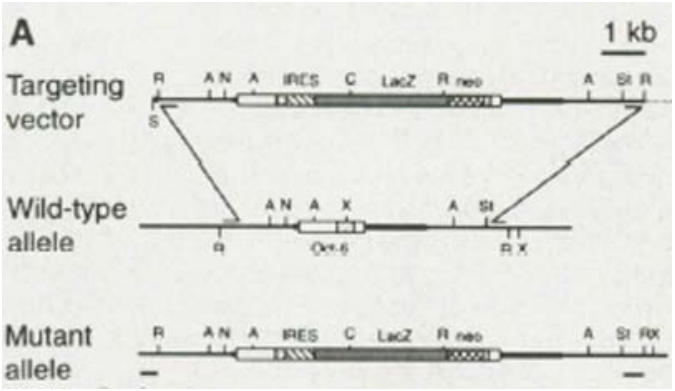

Figure 10: Targeted disruption of Oct-6 (adapted from Jaegle *et al.*, 1996). The thick black line indicates the transcribed part of the Oct-6 locus, which is encoded by a single exon on mouse chromosome 4. The open box represents the open reading frame, the hatched box shows the part of the POU-domain. A β-galactosidase-neomycin (lacZ-Neo) fusion gene under the control of an internal ribosome entry site (IRES) was inserted into the XhoI site of the Oct-6 gene, thereby disrupting the DNA-binding domain of the Oct-6 protein. From the mutant allele a 6.9 kb bicistronic mRNA is expressed, no full-length Oct-6 protein can be produced from this mRNA.

Cell culture

Bone marrow-derived macrophages (BMMs) were grown by culturing bone marrow cells in DMEM (high glucose; Invitrogen) supplemented with 15% L929 cell line conditioned medium (Baccarini *et al.*, 1985), 10% fetal calf serum (FCS; Invitrogen), 2 mM L-glutamin (L-Glu; Invitrogen), 100 µg/ml penicillin and 100 U/ml streptomycin (Pen/Strep; Invitrogen) and 50 µM β-mercaptoethanol (β-ME; Invitrogen). Fully differentiated macrophages were used for experiments on day 7 after isolation. Fetal liver-derived macrophages (FLMs) were derived by culturing suspensions of fetal livers (d 13.5-14.5) under the same conditions like BMMs. FLMs were used for experiments on d 6 after isolation. For peritoneal macrophages (PMs, Bogdan *et al.*, 1997), mice were injected with 2 ml of 4% thioglycollate intra-peritoneally four days prior to isolation. PMs were prepared by peritoneal lavage and cultivated for 1 day prior to the experiment in DMEM containing 5% FCS, L-Glu, Pen/Strep and β-ME. Primary murine embryonic fibroblasts (pMEFs) were derived by homogenisation of decapitated fetuses (d 13.5-14.5) after removal of the liver. Primary MEFs were grown in DMEM supplemented with 10% FCS, L-Glu, Pen/Strep and β-ME. For cultivation of MEF cell lines the same medium but without β-ME was used. SW10 cells, a murine, SV40 large T-antigen-immortalised Schwann cell line (purchased from ATCC®; Catalog No. CRL-2766; Hai *et al.*, 2002), were grown in DMEM supplemented with 10% FCS, L-Glu, and Pen/Strep at the permissive temperature of 33°C. For experiments, cells were shifted to 37°C and/or 39°C in order to inactivate the temperature-sensitive SV40 large T-antigen.

Treatments and infections

Cells were treated for the indicated time points with indicated amounts of IFNα, IFNβ, IFNγ or IL-6 (all purchased from Calbiochem), with polyinosinic-polycytidylic acid (poly(I:C), GE Healthcare) or lipopolysaccharide (LPS, *E. coli* serotype O55:B5, Sigma). Primary MEFs were transfected with poly(I:C) according to the manufacturer's protocols (MEF1 nucleofector kit, AMAXA transfection system). For infection of cells with murine cytomegalovirus (MCMV) a standard multiplicity of infection (MOI) of 1 was used. For optimal infection efficiency, cells were centrifuged at 3000 rpm (Beckman GH3.8A rotor; equals 1462 rcf on average, or 2056 rcf on maximum) for 30 min.

Plaque assays

Supernatants of infected cells were collected at indicated times and titrated onto a Stat1-deficient MEF cell line. Therefore, 2.5 x 10^5 MEFs per well were plated into 24-well plates and covered with serial 10-fold dilutions of the supernatant. Cells were incubated at 37°C for 1 to 2 hours with gently rocking the plates every 15 minutes. Virus containing medium was removed and replaced by fresh medium containing 1% agarose. Cells were incubated until plaques could be counted, usually 4 to 5 days after infection.

Plasmids and overexpression

Expression plasmids (CMV-enhancer driven based on pEVRF0 plasmid; Meijer *et al.*, 1992 and references therein) of Oct-6, Brn-1 and Brn-2 were kindly provided by Dies Meijer (Department of Cell Biology and Genetics, Erasmus University Medical Center Rotterdam). Additionally, we cloned the sense as well as the antisense sequence of the Oct-6 cDNA, and the sense sequence of Oct-1 cDNA, into the EF1α-promoter driven expression vector pEFZeo (kind gift of Pavel Kovarik, MFPL University, Vienna). Oct-6 coding sequence (cds) was PCR-amplified from genomic DNA with primers containing restriction sites for BamHI (underlined) at the 5'ends of the forward (Oct6_BamHI-F: TACGGATCCCGCAGACGGAGCGAGGCG) and reverse (Oct6_BamHI-R: TAGGGATCCGAACCCAGTCCGCAGGGTCAC) primer under the following conditions: in 50 µl final volume 300 nM primer (Invitrogen), 5% DMSO (Sigma), 200 µM dNTPs, 5 U/reaction Pfu DNA polymerase, 1x Pfu buffer incl. $MgSO_4$ (2 mM final concentration; all MBI Fermentas) were used, running following PCR program: 95°C for 3 min, 35 cycles of 95°C for 30 sec, 67°C for 30 sec, 72°C for 2 min, and a final extension step of 72°C for 7 min. The pEFZeo plasmid was digested with EcoRV and the 1.4kb column purified insert was blunt-ligated into the vector. Sense and antisense insertion was checked by XhoI digestion.

For Oct-1 cds amplification, cDNA was prepared using the iScript Select first strand cDNA synthesis kit with oligo$(dT)_{20}$ priming (Biorad). PCR for Oct-1 cds with primers containing restriction sites for BamHI and XbaI at the 5'ends of the forward (Oct1_BamHI-F: TACGGATCCAGCAGCAGA-CTCAAGAATGAA) and reverse (Oct1_XbaI-R: TAGTCTAGAGTAGTGAGGAAAGCCTGTGGC) primer, respectively, was done under following conditions: 300 nM primer (Invitrogen), 200 µM dNTPs, 5 U/reaction Pfu DNA polymerase, 1x Pfu buffer incl. $MgSO_4$ (2 mM final concentration; all MBI Fermentas), running following PCR program: 95°C for 3 min, 5 cycles of 95°C for 30 sec, 55°C for 30 sec, 72°C for 3 min, followed by 35 cycles of 95°C for 30 sec, 65°C for 30 sec, 72°C for 3 min and a final extension step of 72°C for 7 min. The 2.3kb fragment was cut and purified from the gel as described above. The pEFZeo plasmid was double digested with BamHI and XbaI (MBI Fermentas), dephosphorylated (CIAP; MBI Fermentas) and column-purified (Qiaquick protocol; Qiagen). The PCR product was also double digested and column-purified and ligated into the pEFZeo plasmid. Insertion was checked by BamHI/XbaI double digestion. The enhanced GFP expression plasmid (GFP) was supplied with the transfection kit (AMAXA Lonza) as a positive control.

For amplification plasmids were transfected into $CaCl_2$-competent *E. coli* XL-1 blue following a heatshock transformation protocol. Amplified plasmids were purified using the Jetstar Plasmid Midiprep 2.0 Kit (Genomed). Plasmid transfection into pMEFs (10 µg DNA/$2x10^6$ cells) was performed using the AMAXA nucleofector system (MEF1 nucleofector kit) according to the manufacturer's instructions.

Whole-cell extracts, SDS-polyacrylamid-gelelectrophoresis and western blot

Cells were lysed in a buffer containing 50 mM Tris.HCl pH8, 150 mM NaCl, 0.5% Nonidet P-40, 10% glycerol, 2 mM DTT, 0.1 mM EDTA, 0.2 mM Na_3VO_4, 25 mM NaF, 1 µg/ml aprotinin, 1 µg/ml leupeptin and 1 mM PMSF. In order to remove cell debris, samples were centrifuged at 20.800 x g for 8 minutes at 4°C. Whole-cell lysates were mixed 1:1 with 2x Lämmli sample buffer (126 mM Tris.HCl pH6.8, 4% SDS, 20% glycerol, 0.02% bromphenolblue, 200 mM DTT), denaturated at 96°C for 10 minutes and separated on 6.5%, or 8% polyacrylamide-gels, containing 0.01% SDS (10x electrode buffer without SDS: 1L contains 144 g glycin and 30 g Tris.base; 1 x buffer contains 0.01% SDS). The gels were blotted (1x transfer buffer: 25 mM Tris.base, 150 mM glycine, 20% methanol) onto nitrocelullose membranes (GE Healthcare) which were then blocked in a 5% milk powder solution (ressolved in 1x PY-TBST: 100 mM Tris.HCl pH 7.4, 750 mM NaCl, 1 mM EDTA, 0.1% Tween-20). The membranes were probed with the indicated primary antibodies. For detection α-rabbit-IgG, or α-mouse-IgG horse-radish peroxidase conjugated secondary antibodies were used (table 3). Target bands were visualised by a chemiluminescence reaction using the ECL™-detection system (GE Healthcare) according to the manufacturer's instructions.

Table 3: Antibodies for western blot (WB), supershift (SS), immunoprecipitation (IP), and immunofluorescence (IF)

Antibody	origin	Application (dilution)	from	Cat. number
primary antibodies				
α-Oct-6 (N-terminal)	rabbit	WB (1:1000)	Dies Meijer[1]	-
α-Oct-6 (C-terminal)	goat	IF (1:50); SS, IP	Santa Cruz	sc-11661
α-Oct-1 (12F11) X	mouse	SS	Santa Cruz	sc-8024 X
α-Oct-2 (C-20) X	rabbit	SS	Santa Cruz	sc-233 X
α-Stat1-C	rabbit	IP	Pavel Kovarik[2]	-
α-phospho-NFκB p65 (Ser536)	mouse	1:1000	Cell Signaling Technology	3036
α-NFκB p65	rabbit	WB (1:1000)	Upstate Cell Signaling solutions	06-418
α-phospho-p38 MAPK (Thr180/Tyr182)	rabbit	WB (1:1000)	Cell Signaling Technology	9211
α-p38 MAPK	rabbit	WB (1:1000)	Cell Signaling Technology	sc-535
α-pan-Erk	mouse	WB (1:2000)	BD Biosciences	612641
secondary antibodies				
α-rabbit IgG	donkey	WB (1:2000)	GE Healthcare	NA9340
α-mouse IgG	sheep	WB (1:2000)	GE Healthcare	NA9310

Antibody	origin	Application (dilution)	from	Cat. number
α-goat IgG	donkey	WB (1:20000)	Jackson ImmunoResearch Labs	705-035-003
α-goat IgG-Fluor488	rabbit	IF (1:200)	Alexa	a-21222

Primary antibodies for WB were diluted in 1% BSA, 0.01% azide (in PY-TBST).
Secondary antibodies for WB diluted in 1% milk (in PY-TBST).
[1] (Zwart *et al.*, 1996), [2] (Kovarik *et al.*, 1998)

Immunoprecipitation

Whole cell lysates (1 mg/ml protein in the lysis buffer described above) were incubated with 2 µg antibody (table 3) rotating at 4°C overnight. Protein-A sepharose CL-4B (Pharmacia Biotech; in case the antibody origin was rabbit) or Protein-G PLUS-agarose (Santa Cruz; in case the antibody origin was goat) was added (50 µl of 50% slurry) and samples were incubated rotating for another 2 hours at 4°C. After washing, beads were resuspended in 50 µl 2x Lämmli sample buffer and submitted to western blot analysis as described above.

Electrophoretic mobility shift assays (EMSAs, bandshifts)

The sense oligonucletide (200 ng; OCT-probe: GAGAGGA*ATTTGCAT*TTCCACCGACCTTCC, Invitrogen; c-abl; Jaegle *et al.*, 2003) was radioactively labelled at the 5'end using a T4 polynucleotide kinase reaction (MBI Fermentas) according to the manufacturer's instructions. Labelled sense and the antisense oligonucleotide were annealed by adding 250 ng of the antisense oligonucleotide to the labelling reaction mix, inreasing the NaCl concentration (by adding 1.5 µl of an 1.5 M NaCl solution), heating the mixture to 95°C for 5 min and slowly cooling to room temperature. The radioactive dsDNA oligonucleotide was purified *via* NAP^{TM}-5 G25 sepharose columns (area: 0.9 x 2.8 cm; Pharmacia) and 10 fractions à 100 µl were collected. The fraction containing the dsDNA oligonucleotide (usually fraction 5-6) was used for bandshift experiments. Whole-cell extracts (10 to 15 µg/15µl) were incubated with 2 µl poly(dI:dC) (62.5 U/ml; Amersham) for 5 min at room temperature. A probe mix (for 20 samples including 10% volume for pipet lost) was prepared containing 100 µl WBB (1x; Wu-Binding-Buffer: 10 mM HEPES, 1.5 mM MgCl2, 0.1 mM EGTA, 5% glycerol, 100 nM NaCl), 100 µl Ficoll (10% in 1x WBB), 10 µl BSA (50 µg/µl; fraction V, Sigma), 10 µl tRNA (10 µg/µl; from baker's yeast, Sigma) and radioactively labelled dsDNA probe (8 µl). After incubation with poly(dI:dC) 10 µl of probemix were added and samples were incubated at room temperature for 20 min. 25 µl/sample were separated on a 6% polyacrylamide gel (in 0.5x Tris-borate-EDTA buffer) under native conditions for 3 hours with 200 V. Bandshifts were detected by autoradiography. Supershifts were done by incubating the cell extracts with 1 µl of the respective antibody (α-Oct-6, α-Oct-1, α-Oct-2; all Santa Cruz, table 3) prior to separation.

Immunofluorescence

Cells (7.5 x 10^5 FLMs, BMMs) were grown and stimulated on glass slides, and fixed with 4% formaldehyde for 15 minutes (Histofix, Roth). Formaldehyde was quenched by glycine (100 mM, 15 minutes), cells were permeabilised by methanol treatment (-20°C, 5 minutes). Slides were blocked with 1% BSA in PBS for 1 hour. Oct-6 was detected incubating the slides with α-Oct-6 primary antibody (Santa Cruz; 1:50 in blocking solution from a 0.2 mg/ml stock solution; 4°C overnight) and a fluorescently labelled α-goat IgG secondary antibody (Fluor 488; Alexa; 1:200 in PBS; 1 hour at room temperature in the dark). In order to control for unspecific signals, goat IgG (Invitrogen Cat. No. 02-6202; 1:50 in blocking solution from 0.5 µg/ml solution) was used as an isotype control instead of the specific primary antibody.

Chromatin immunoprecipitation (ChIP)

ChIP for Stat1 (α-Stat1-C) was performed as described earlier (Nissen and Yamamoto, 2000; Sadzak *et al.*, 2008) with minor modifications. Sonication (Sonopuls HD70, MS72 sonotrode; Bandelin) was initially performed at 50% power and only 30% duty cycle in order to avoid foaming, for 10 times 15 sec with 1 min break between the pulses. This procedure was then repeated with the duty cycle increased to 90%. Equal amounts of lysate were used for Stat1 immunopreciptation (4 µl α-Stat1-C antibody/500 µl lysate; the antibody was a kind gift of Pavel Kovarik, MFPL University, Vienna) and a control reaction using unspecific rabbit serum. DNA was isolated following a phenol:chloroform extraction protocol and subjected to PCR analysis. PCRs were run in a final volume of 25 µl containing 300 nM primer (ChIP_Oct6-F: GTCTCTGCTCGGAACCCGA, ChIP_Oct6_S-R: CCCACGTTCCACACAAGCT, ChIP_Oct6_L-R: GCCCGCGTACACATTCAC; ChIP_Irf1-F: GCACAGCTGCCTTGTACT-TCC, ChIP_Irf1-R: TCGGCCTCATCATTTCGG), 2 mM $MgCl_2$, 200 µM dNTP mix, 1x Biotaq buffer, 2 U/reaction Biotaq DNA polymerase under these cycling conditions: 5 min at 95°C for initial denaturation, followed by 35 cycles of 95°C for 30 sec and 61°C for 1 min. PCRs were done from all samples of the α-Stat1 IP, the control IP (unspecific rabbit serum; Sigma) and from an aliquot of the initial sample input prior to the IP (input DNA).

RNA isolation and reverse transcription

Total RNA was isolated following the TRiZOL (Invitrogen) protocol. RNA concentration and purity was assessed by photometric analysis, measuring the absorption (A) at 260 nm and 280 nm for nucleic acids and protein contamination, respectively. RNA was considered to be pure when the ratio of A_{260}/A_{280} was about 2.0. RNA integrity was further analysed by gel electrophoresis under non-denaturing conditions. Prior to cDNA synthesis the RNA was treated with 1 U/µg RNA RQ1 DNase I (Promega) in order to digest contaminating genomic DNA. Then cDNA was prepared from 1 µg total

RNA using the iScript First Strand cDNA synthesis kit (Biorad), always including controls for DNA contamination, that were prepared lacking the reverse transcriptase (RT- controls).

Real-time quantitative PCR (qPCR) analysis of gene expression

Target gene expression was assessed by qPCR with Ube2d2 as endogenous control gene. Taqman® probes labelled with 6-carboxyfluorescein (FAM) at the 5'end, and a black-hole-quencher (BHQ1) at the 3'end were used to quantify IFNβ and Ube2d2 (table 4). For the quantification of IL17-A and IL17-F, ready-to-use Taqman® assays were purchased from Applied Biosystems (IL17-A: Mm00439619_m1, IL17-F: Mm00521423_m1). The dsDNA-binding dye EvaGreen (Biotium) was chosen to detect Oct-6, Egr2, Pmp22 and the genes that were to be validated from the microarray (Dapp1, Dyrk1b, E4f1, Lsm10, Map3k5, Map3k12, Nox1, Stk40, and Zdhhc3; table 5).

Table 4: qPCR assays using Taqman® probes (continued on the following page**).**

gene	oligo-name	oligo-sequence
Ube2d2 Ubiquitin conjugating enzyme E2D 2	Ube2d2-F	AGGTCCTGTTGGAGATGATATGTT
	Ube2d2-R	TTGGGAAATGAATTGTCAAGAAA
	Ube2d2-FAM	CCAAATGACAGCCCCTATCAGGGTGG
IFNβ Interferon beta 1, fibroblast	IFNβ-F	ATGAGTGGTGGTTGCAGGC
	IFNβ-R	TGACCTTTCAAATGCAGTAGATTCA
	IFNβ-FAM	AAGCATCAGAGGCGGACTCTGGGA
panIFNα Interferon alpha 1-14	panIFNα-F	CCACAGGATCACTGTGT(A/T)CCTGAGA
	panIFNα-R	CTGATCACCTCCCAGGCACAG
	panIFNα-FAM[1]	AG+AA+GAA+A+C+AC+AG+CC
iNOS Inducible nitric oxide synthase	iNOS-F	TGGTCCGCAAGAGAGTGCT
	iNOS-R	CCTCATTGGCCAGCTGCTT
	iNOS-FAM	CCCGGCAAACCCAAGGTCTACGTTC

[1] Locked nucleic acids (LNAs) containing probe: LNA monomers are indicated by the "+" in front of the respective bases (Letertre *et al.*, 2003).

Table 5: qPCR assays using a dsDNA-binding dye (EvaGreen).

gene	oligo-name	oligo-sequence
Oct-6 POU domain, class 3, transcription factor 1	Oct-6-F	AGGTCCTGTTGGAGATGATATGTT
	Oct-6-R	TTGGGAAATGAATTGTCAAGAAA
Egr2 early growth response 2	Egr2-F	GGTGACCATCTTCCCCAATG
	Egr2-R	TTGATCATGCCATCTCCCG
Pmp22 peripheral myelin protein 22	Pmp22-F	CCGGTTTTACATCACTGGATTCT
	Pmp22-R	TGTAGATGGCCGCTGCACT

gene	oligo-name	oligo-sequence
Dapp1 dual adaptor for phospho-tyrosine and 3-phospho-inositides 1	Dapp1-F	AAAGAAGGCTATCTCACCAAGCA
	Dapp1-R	AGGTCTAGGATCCGAATTGGTTC
Dyrk1b dual-specificity tyrosine-(Y)-phosphorylation regulated kinase 1b	Dyrk1b-F	CCATTGACATGTGGTCCCTG
	Dyrk1b-R	TGCCCAACACCTCCACAATA
E4f1 E4F transcription factor 1	E4f1-F	GTGGAGTTCTCGTCTGTGGTAGCT
	E4f1-R	CAATGATCTCGGTGGCTTCA
Lsm10 U7 snRNP-specific Sm-like protein LSM10	Lsm10-F	CCTCCAAAAGGCCATGAGACT
	Lsm10-R	CGGGAGTTGGCTCAGAACAC
Map3k5 mitogen-activated protein kinase kinase kinase 5	Map3k5-F	TCCGATTCACTCCAGTCCCT
	Map3k5-R	TCACAGCAGTAGACCTTGTTGTGT
Map3k12 mitogen-activated protein kinase kinase kinase 12	Map3k12-F	GTCTGGACAATGATTGGCAAAG
	Map3k12-R	GAAGCGTCCCAGGAAAACAG
Nox1 NADPH oxidase 1	Nox1-F	GGGAGACCAATGTGGGACAA
	Nox1-R	CTCGAGTATCGCTGACAGCG
Stk40 serine/threonine kinase 40	Stk40-F	CTCTCAGTGCCATCATTGCATC
	Stk40-R	CACCTTTGCCTCCTGGGA
Zdhhc3 zinc finger, DHHC domain containing 3	Zdhhc3-F	TCCTTGCACGCCCTCATC
	Zdhhc3-R	GGCGAGAAGGAGCTGCACT

Taqman qPCR assays were run in a final volume of 25 µl containing 300 nM primer (Invitrogen), 100 nM probe (Sigma or Metabion), 200 µM dNTP mix (Fermentas), 4 mM $MgCl_2$, 1x HotFire buffer B, and 1U/reaction HotFire DNA polymerase (all Solis BioDyne). The conditions were basically the same for the EvaGreen assays except for the use of 0.2x EvaGreen dye instead of the probe in the presence of only 2.5 mM $MgCl_2$. All qPCRs were run on a Mastercycler® ep Realplex (Eppendorf) applying following cycling conditions: 15 min at 95°C for initial denaturation, then 40 to 45 cycles of 95°C for 20 sec and 60°C for 1 min. In case of the EvaGreen-assays, the PCR was followed by a melting curve analysis in order to confirm assay specificity.

Data were analysed using the realplex software (Eppendorf) and relative target gene expression levels (i.e. n-fold expression levels) were calculated following the standard curve method (Giulietti *et al.*, 2001; Karaghiosoff *et al.*, 2003), or following the ΔΔCt method, assuming an amplification efficiency of 100% (Bustin, 2000).

Gene expression profiling using Taqman® Custom Arrays

Taqman® Custom Arrays (Applied Biosystems) were used to analyse the expression of 240 genes in PMs upon LPS treatment. These medium-throughput arrays are 384-well micro fluidic cards and available in several conformations. We used 1 array in the 48-genes-format allowing the analysis of 48

genes for 4 samples in duplicates in one run. Two more arrays in the 96-genes-format were run, analysing 96 genes for 4 samples in unicates per run (table 6). RNA (50 ng/µl) was reverse transcribed using the iScript First Strand cDNA Synthesis Kit (Biorad). For qPCR a 100 µl mastermix was loaded per sample-loading port including 250 ng cDNA (assumed to equal RNA input). The mastermix further contained 200 µM of each dNTP (MBI Fermentas), 1 x ROX reference dye (Invitrogen), 5 mM $MgCl_2$, 1 x reaction buffer B and 4 U HotFire DNA polymerase (all Solis Biodyne). The arrays were processed as described by the manufacturer's protocol. QPCR was performed on the ABI PRISM 7900 HT (Applied Biosystems) running the following cycling conditions: initial denaturation at 95 °C for 12 min, 40 cycles of 95 °C for 15 sec and 60 °C for 1 min. Data were analysed using the SDS 2.2 software (Applied Biosystems).

Table 6: Gene list for the Taqman® low density arrays (continued on the following pages**).**

	gene symbol	**gene name [commonly known *alias*]**	**assay ID**
Taqman® array – "BS-2" (n = 48 genes in duplicate)	Rn18s	18S rRNA	4342379
	Cpd	carboxypeptidase D	Mm00483956_m1
	Csf3	colony stimulating factor 3 (granulocyte)	Mm00438334_m1
	Csnk1g1	casein kinase 1, gamma 1	Mm00557447_m1
	Ddx58	DEAD (Asp-Glu-Ala-Asp) box polypeptide 58 [Rig-I]	Mm00554529_m1
	Ddx6	DEAD (Asp-Glu-Ala-Asp) box polypeptide 6	Mm00619326_m1
	Dhx29	DEAH (Asp-Glu-Ala-His) box polypeptide 29	Mm00553691_m1
	Dhx9	DEAH (Asp-Glu-Ala-His) box polypeptide 9	Mm00456021_m1
	Dnmt1	DNA methyltransferase (cytosine-5) 1	Mm00599763_m1
	Eda2r	ectodysplasin A2 isoform receptor	Mm00723601_m1
	Eef1a2	eukaryotic translation elongation factor 1 alpha 2	Mm00514649_m1
	Efnb2	ephrin B2	Mm00438670_m1
	Eif2c1	eukaryotic translation initiation factor 2C, 1	Mm00462977_m1
	Myof (Fer1l3)	myoferlin	Mm00621780_m1
	Fmr1	fragile X mental retardation syndrome 1 homolog	Mm00484415_m1
	Gbp2	guanylate binding protein 2	Mm00494575_m1
	Grb10	growth factor receptor bound protein 10	Mm00494735_m1
	Hipk2	homeodomain interacting protein kinase 2	Mm00439329_m1
	Hmbs	hydroxymethylbilane synthase	Mm00660262_g1
	Hprt1	hypoxanthine guanine phosphoribosyl transferase 1	Mm00446968_m1
	Ifi203	interferon activated gene 203	Mm00492597_m1
	Ifit1	interferon-induced protein with tetratricopeptide repeats 1 [Ifi56]	Mm00515153_m1
	Ifit2	interferon-induced protein with tetratricopeptide repeats 2 [Ifi54]	Mm00492606_m1
	Iqgap1	IQ motif containing GTPase activating protein 1	Mm00443860_m1
	Irf1	interferon regulatory factor 1	Mm00515191_m1
	Irf7	interferon regulatory factor 7	Mm00516788_m1
	Jak1	Janus kinase 1	Mm00600614_m1
	Mx1	myxovirus (influenza virus) resistance 1	Mm00487796_m1
	Notch3	Notch gene homolog 3 (Drosophila)	Mm00435270_m1
	Oas1b	2'-5' oligoadenylate synthetase 1B	Mm00449297_m1
	Pftk1	PFTAIRE protein kinase 1	Mm00448111_m1
	R3hdm1	R3H domain 1 (binds single-stranded nucleic acids)	Mm00725197_m1
	Rhpn1	rhophilin, Rho GTPase binding protein 1	Mm00492435_m1
	Polr1a (Rpo14)	polymerase (RNA) I polypeptide A	Mm00485835_m1
	Rqcd1	rcd1 (required for cell differentiation) homolog 1 (S. pombe)	Mm00457967_m1
	Sfrp1	secreted frizzled-related protein 1	Mm00489161_m1
	Skiv2l	superkiller viralicidic activity 2-like (S. cerevisiae)	Mm00451675_m1
	Smad3	MAD homolog 3 (Drosophila)	Mm00489637_m1
	Smarcc1	SWI/SNF related, matrix associated, actin dependent regulator of chromatin, subfamily c, member 1	Mm00486224_m1
	Smc1a	structural maintenance of chromosomes 1A	Mm00490624_m1

	Socs1	suppressor of cytokine signaling 1	Mm00782550_s1
	Srrm1	serine/arginine repetitive matrix 1	Mm00489728_m1
	Stat1	signal transducer and activator of transcription 1	Mm00439518_m1
	Sulf1	sulfatase 1	Mm00552283_m1
	Trim37	tripartite motif-containing 37	Mm00816034_s1
	Ube2d2	ubiquitin-conjugating enzyme E2D 2	Mm00785931_s1
	Ubtf	upstream binding transcription factor, RNA polymerase I	Mm00456972_m1
	Usp45	ubiquitin specific petidase 45	Mm00507696_m1

	gene symbol	**gene name [commonly known *alias*]**	**assay ID**
Taqman® array – "BS-3" (n = 96 genes in unicate)	Rn18s	18S rRNA	4342379
	A2m	alpha-2-macroglobulin	Mm00558642_m1
	Als2	amyotrophic lateral sclerosis 2 (juvenile) homolog (human)	Mm00511865_m1
	Arap3	ArfGAP with RhoGAP domain, ankyrin repeat and PH domain 3	Mm00551866_m1
	Arhgef2	rho/rac guanine nucleotide exchange factor (GEF) 2	Mm00434757_m1
	As3mt	arsenic (+3 oxidation state) methyltransferase	Mm00491075_m1
	Bhmt2	betaine-homocysteine methyltransferase 2	Mm00517726_m1
	Xiap (Birc4)	X-linked inhibitor of apoptosis	Mm00776505_m1
	Casp2	caspase 2	Mm00432314_m1
	Cd3d	CD3 antigen, delta polypeptide	Mm00442746_m1
	Cd79a	CD79A antigen (immunoglobulin-associated alpha)	Mm00432423_m1
	Cd84	CD84 antigen	Mm00488934_m1
	Cdkn1b	cyclin-dependent kinase inhibitor 1B	Mm00438168_m1
	Cidea	cell death-inducing DNA fragmentation factor, alpha subunit-like effector A	Mm00432554_m1
	Cpd	carboxypeptidase D	Mm00483956_m1
	Csnk1a1	casein kinase 1, alpha 1	Mm00521599_m1
	Dab2	disabled homolog 2 (Drosophila)	Mm00517751_m1
	Dclre1a	DNA cross-link repair 1A, PSO2 homolog (S. cerevisiae)	Mm00457569_m1
	Dlx5	distal-less homeobox 5	Mm00438430_m1
	Dvl3	dishevelled 3, dsh homolog (Drosophila)	Mm00432914_m1
	Dyrk1b	dual-specificity tyrosine-(Y)-phosphorylation regulated kinase 1b	Mm00599813_m1
	Ebf2	early B-cell factor 2	Mm00438622_m1
	Eef1e1	eukaryotic translation elongation factor 1 epsilon 1	Mm00470535_m1
	Egr3	early growth response 3	Mm00516979_m1
	Epha4	Eph receptor A4	Mm00433056_m1
	Ercc4	excision repair cross-complementing rodent repair deficiency, complementation group 4	Mm00516619_m1
	Ercc5	excision repair cross-complementing rodent repair deficiency, complementation group 5	Mm00468968_m1
	Esm1	endothelial cell-specific molecule 1	Mm00469953_m1
	Ets1	E26 avian leukemia oncogene 1, 5' domain	Mm00468970_m1
	Evi2b	ecotropic viral integration site 2b	Mm00524622_m1
	Fgf1	fibroblast growth factor 1	Mm00438906_m1
	Fgf17	fibroblast growth factor 17	Mm00433282_m1
	Gabpb2	GA repeat binding protein, beta 2	Mm00552940_m1
	Gnao1	guanine nucleotide binding protein, alpha O	Mm00494677_m1
	Gnaz	guanine nucleotide binding protein, alpha z subunit	Mm00726444_s1
	Hmbs	hydroxymethylbilane synthase	Mm00660262_g1
	Hoxc5	homeo box C5	Mm00433971_m1
	Hprt1	hypoxanthine guanine phosphoribosyl transferase 1	Mm00446968_m1
	Htr2a	5-hydroxytryptamine (serotonin) receptor 2A	Mm00555764_m1
	Icam5	intercellular adhesion molecule 5, telencephalin	Mm00492566_m1
	Ifna2	interferon alpha 2	Mm00833961_s1
	Il17c	interleukin 17C	Mm00521397_m1
	Il7	interleukin 7	Mm00434291_m1
	Jak2	Janus kinase 2	Mm00434561_m1
	Klf2	Kruppel-like factor 2 (lung)	Mm00500486_g1
	Lbp	lipopolysaccharide binding protein	Mm00493139_m1
	Lect1	leukocyte cell derived chemotaxin 1	Mm00495291_m1
	Lefty2	left-right determination factor 2	Mm00774547_m1

	gene symbol	gene name [commonly known *alias*]	assay ID
Taqman® array – "BS-3" (n = 96 genes in unicate)	Lpin2	lipin 2	Mm00522390_m1
	Muc13 (Ly64)	mucin 13, epithelial transmembrane	Mm00495397_m1
	Masp1	mannan-binding lectin serine peptidase 1	Mm00434830_m1
	Mcpt1	mast cell protease 1	Mm00656886_g1
	Mcpt2	mast cell protease 2	Mm00484932_m1
	Mcpt8	mast cell protease 8	Mm00484935_g1
	Mdm4	transformed mouse 3T3 cell double minute 4	Mm00484944_m1
	Mds1	myelodysplasia syndrome 1 homolog (human)	Mm00491303_m1
	Mga	MAX gene associated	Mm00465485_m1
	Foxo4 (Mllt7)	forkhead box O4	Mm00840140_g1
	Mmp13	matrix metallopeptidase 13	Mm00439491_m1
	Mybl1	myeloblastosis oncogene-like 1	Mm00485327_m1
	Nat1	N-acetyltransferase 1 (arylamine N-acetyltransferase)	Mm00500740_s1
	Nedd4	neural precursor cell expressed, developmentally down-regulated 4	Mm00456829_m1
	Nog	noggin	Mm00476456_s1
	Nrarp	Notch-regulated ankyrin repeat protein	Mm00482529_s1
	NULL	unknown	Mm00498572_m1
	Orm2	orosomucoid 2	Mm00440570_g1
	Padi4	peptidyl arginine deiminase, type IV	Mm00478087_m1
	Pax3	paired box gene 3	Mm00435491_m1
	Pcsk2	proprotein convertase subtilisin/kexin type 2	Mm00500981_m1
	Pdcd1	programmed cell death 1	Mm00435532_m1
	Pou1f1 (Pit1)	POU domain, class 1, transcription factor 1 (Pit1, growth hormone factor 1)	Mm00476852_m1
	Pou3f1	POU domain, class 3, transcription factor 1 (Oct-6)	Mm00843534_s1
	Ppp1r16b	protein phosphatase 1, regulatory (inhibitor) subunit 16B	Mm00462096_m1
	Ppp1r1b	protein phosphatase 1, regulatory (inhibitor) subunit 1B	Mm00454892_m1
	Prkce	protein kinase C, epsilon	Mm00440894_m1
	Prkcq	protein kinase C, theta	Mm00435796_m1
	Klk6 (Prss18)	kallikrein related-peptidase 6	Mm00478322_m1
	Ptpn14	protein tyrosine phosphatase, non-receptor type 14	Mm00501215_m1
	Ptprm	protein tyrosine phosphatase, receptor type, M	Mm00436095_m1
	Ptprs	protein tyrosine phosphatase, receptor type, S	Mm00465158_m1
	Rb1	retinoblastoma 1	Mm00485586_m1
	Reck	reversion-inducing-cysteine-rich protein with kazal motifs	Mm00443829_m1
	Rgs6	regulator of G-protein signaling 6	Mm00658736_m1
	Runx2	runt related transcription factor 2	Mm00501578_m1
	Sf3a1	splicing factor 3a, subunit 1	Mm00660438_m1
	Slfn8	schlafen 8	Mm00824405_m1
	Socs2	suppressor of cytokine signaling 2	Mm00850544_g1
	Styxl1	serine/threonine/tyrosine interacting-like 1	Mm00472555_m1
	Supt6h	suppressor of Ty 6 homolog (S. cerevisiae)	Mm00486479_m1
	Tal1	T-cell acute lymphocytic leukemia 1	Mm00441665_m1
	Tbx4	T-box 4	Mm00550370_m1
	Tcea2	transcription elongation factor A (SII), 2	Mm00447447_m1
	Tcl1b5	T-cell leukemia/lymphoma 1B, 5	Mm00834432_g1
	Tnfsf10	tumor necrosis factor (ligand) superfamily, member 10 [Trail]	Mm00437174_m1
	Traf1	TNF receptor-associated factor 1	Mm00493827_m1
	Ube2d2	ubiquitin-conjugating enzyme E2D 2	Mm00785931_s1

	gene symbol	gene name [commonly known *alias*]	assay ID
Taqman® array – "BS-4" (n = 96 genes in unicate)	Rn18s	18S rRNA	4342379
	4932417H02Rik	RIKEN cDNA 4932417H02 gene [Raptor]	Mm00712676_m1
	Adipoq (Acdc)	adiponectin, C1Q and collagen domain containing	Mm00456425_m1
	Aif1	allograft inflammatory factor 1	Mm00479862_g1
	Aqp9	aquaporin 9	Mm00508094_m1
	Arg2	arginase type II	Mm00477592_m1
	Bcar3	breast cancer anti-estrogen resistance 3	Mm00600213_m1
	Naip2 (Birc1b)	NLR family, apoptosis inhibitory protein 2	Mm00440446_m1
	Nod2 (Card15)	nucleotide-binding oligomerization domain containing 2	Mm00467543_m1
	Ccl5	chemokine (C-C motif) ligand 5 [RANTES]	Mm01302428_m1
	Ccnb1	cyclin B1	Mm00838401_g1
	Nlrp3 (Cias1)	NLR family, pyrin domain containing 3	Mm00840904_m1
	Cxcl9	chemokine (C-X-C motif) ligand 9 [Mig]	Mm00434946_m1
	Cyp2c37	cytochrome P450, family 2. subfamily c, polypeptide 37	Mm00833845_m1
	Ddx50	DEAD (Asp-Glu-Ala-Asp) box polypeptide 50	Mm00459758_m1
	Defb6	defensin beta 6	Mm00651498_m1
	Defa4 (Defcr4)	defensin, alpha, 4	Mm00651736_g1
	Defa5 (Defcr5)	defensin, alpha, 5	Mm00651548_g1
	Diras1	DIRAS family, GTP-binding RAS-like 1	Mm00507471_s1
	Dmrta1	doublesex and mab-3 related transcription factor like family A1	Mm00558696_m1
	Dok5	docking protein 5	Mm00499684_m1
	Dusp16	dual specificity phosphatase 16	Mm00459935_m1
	Ebi3	Epstein-Barr virus induced gene 3	Mm00469294_m1
	Faim2	Fas apoptotic inhibitory molecule 2	Mm00511461_m1
	Fgfr3	fibroblast growth factor receptor 3	Mm00433294_m1
	Fgr	Gardner-Rasheed feline sarcoma viral (Fgr) oncogene homolog [Mus musculus]	Mm00438949_m1
	Fosb	FBJ osteosarcoma oncogene B	Mm00500401_m1
	Foxf1a	forkhead box F1a	Mm00487497_m1
	Foxj2	forkhead box J2	Mm00491502_m1
	Foxp3	forkhead box P3	Mm00475156_m1
	Gdf5	growth differentiation factor 5	Mm00433564_m1
	Gfi1	growth factor independent 1	Mm00515853_m1
	Ghrl	ghrelin	Mm00445450_m1
	Gimap9	GTPase, IMAP family member 9	Mm00558102_m1
	Gnas	GNAS (guanine nucleotide binding protein, alpha stimulating) complex locus	Mm00456660_m1
	Gnmt	glycine N-methyltransferase	Mm00494689_m1
	Prokr2 (Gpr73l1)	prokineticin receptor 2	Mm00769571_m1
	Hhex	hematopoietically expressed homeobox	Mm00433954_m1
	Hist1h1e	histone cluster 1, H1e	Mm00469312_s1
	Hmbs	hydroxymethylbilane synthase	Mm00660262_g1
	Hprt1	hypoxanthine guanine phosphoribosyl transferase 1	Mm00446968_m1
	Icam2	intercellular adhesion molecule 2	Mm00494862_m1
	Icam4	intercellular adhesion molecule 4, Landsteiner-Wiener blood group	Mm00470225_g1
	Irf8 (Icsbp1)	interferon regulatory factor 8	Mm00492567_m1
	Ifna4	interferon alpha 4	Mm00833969_s1
	Igsf9	immunoglobulin superfamily, member 9	Mm00459672_m1
	Il16	interleukin 16	Mm00516039_m1
	Il17b	interleukin 17B	Mm00444686_m1

	gene symbol	gene name [commonly known *alias*]	assay ID
Taqman® array – "BS-4" (n = 96 genes in unicate)	Il17f	interleukin 17F	Mm00521423_m1
	Il2ra	interleukin 2 receptor, alpha chain	Mm00434261_m1
	Il9	interleukin 9	Mm00434305_m1
	Itgb3	integrin beta 3	Mm00443980_m1
	Khdrbs1	KH domain containing, RNA binding, signal transduction associated 1	Mm00516130_m1
	Lag3	lymphocyte-activation gene 3	Mm00493071_m1
	Lhx5	LIM homeobox protein 5	Mm00521778_m1
	Madd	MAP-kinase activating death domain	Mm00523709_m1
	Map3k6	mitogen-activated protein kinase kinase kinase 6	Mm00522222_m1
	Map3k8	mitogen-activated protein kinase kinase kinase 8	Mm00432637_m1
	Mitf	microphthalmia-associated transcription factor	Mm00434954_m1
	Msh2	mutS homolog 2 (E. coli)	Mm00500563_m1
	Nfe2l3	nuclear factor, erythroid derived 2, like 3	Mm00477788_m1
	Nfkbib	nuclear factor of kappa light polypeptide gene enhancer in B-cells inhibitor, beta	Mm00456849_m1
	Nr2f6	nuclear receptor subfamily 2, group F, member 6	Mm00438762_m1
	Nxf2	nuclear RNA export factor 2	Mm00453239_m1
	Palm2	paralemmin 2	Mm00556267_m1
	Pdcd1lg2	programmed cell death 1 ligand 2	Mm00451734_m1
	Phkg1	phosphorylase kinase gamma 1	Mm00440767_m1
	Pla2g10	phospholipase A2, group X	Mm00449530_m1
	Plunc	palate, lung, and nasal epithelium associated	Mm00465064_m1
	Pou2f3	POU domain, class 2, transcription factor 3 [Skn-1a, Oct-11]	Mm00478284_m1
	Pramel1	preferentially expressed antigen in melanoma-like 1	Mm00473193_m1
	Prdx4	peroxiredoxin 4	Mm00450261_m1
	Prdx6	peroxiredoxin 6	Mm00725435_s1
	Prss33	protease, serine, 33	Mm00617657_m1
	Prss34	protease, serine, 34	Mm00617666_g1
	Ptpn4	protein tyrosine phosphatase, non-receptor type 4	Mm00480178_m1
	Pycard	PYD and CARD domain containing	Mm00445747_g1
	Rab23	RAB23, member RAS oncogene family	Mm00436209_m1
	Rac2	RAS-related C3 botulinum substrate 2	Mm00485472_m1
	Ralgps1	Ral GEF with PH domain and SH3 binding motif 1	Mm00613690_m1
	Raly	hnRNP-associated with lethal yellow	Mm00499167_m1
	Rbpjl (Rbpsuhl)	recombination signal binding protein for immunoglobulin kappa J region-like	Mm00485631_m1
	Rem1	rad and gem related GTP binding protein 1	Mm00485674_m1
	Rnf24	ring finger protein 24	Mm00724270_m1
	Rnf32	ring finger protein 32	Mm00502428_m1
	Satb1	special AT-rich sequence binding protein 1	Mm00485916_m1
	Aimp1 (Scye1)	ARS inducible multifunctional protein 1	Mm00433034_m1
	Serpina6	serine (or cysteine) peptidase inhibitor, clade A, member 6	Mm00432327_m1
	Serpinb9e	serine (or cysteine) peptidase inhibitor, clade B, member 9e	Mm00660208_m1
	Stab2	stabilin 2	Mm00454684_m1
	Tll2	tolloid-like 2	Mm00449432_m1
	Tlr5	toll-like receptor 5	Mm00546288_s1
	Tnfrsf26	tumor necrosis factor receptor superfamily, member 26	Mm00558700_m1
	Ubd	ubiquitin D	Mm00499179_m1
	Ube2d2	ubiquitin-conjugating enzyme E2D 2	Mm00785931_s1
	Scaper (Zfp291)	S phase cyclin A-associated protein in the ER	Mm00615854_m1

The n-fold expression levels were calculated by the ΔΔCt method. In addition to the "default"-endogenous control gene (18S rRNA), we included another 3 endogenous control genes, namely Hmbs, Hprt and Ube2d2. Endogenous control genes should meet the following criteria: ***(i)*** they must not be regulated by any of the experimental parameters (treatment and genotype; Bustin, 2000), ***(ii)*** they should not vary more than 5-fold between the samples (Dheda *et al.*, 2004) and ***(iii)*** the Ct values should be approximately in the same range like the Ct values of the target genes (Bustin, 2002). The Ct values for the 18SrRNA were rather low (between 9 and 11) compared to the Ct values of the target genes (between 20 and 35) and varied considerably (Figure 11). Hmbs even turned out to be regulated not only by LPS treatment, but also in a Tyk2-dependent fashion (see results). Since Ct value differences of Hprt and Ube2d2 did not exceed 2.3, i.e. 5-fold differences assuming 100% PCR efficiency, they met the criteria for endogenous control genes. Therefore the target-gene data were normalised to a mean of Hprt andUbe2d2 (for "R" statistics), or to Ube2d2 alone (for all other calculations). Usually, normalised data were calibrated to the untreated WT of the first experiment (1WT_0h = 1).

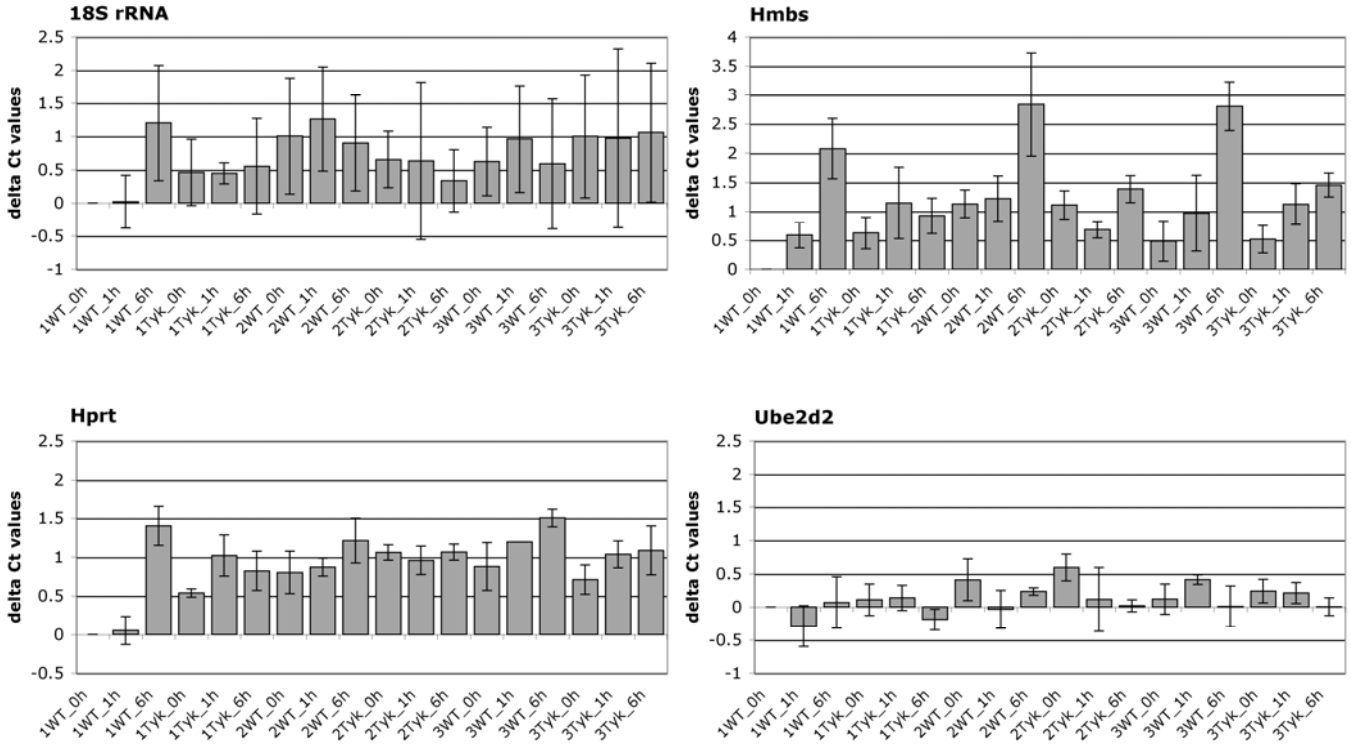

Figure 11: Average Ct value differences for the endogenous controls. Ct values were calibrated to the first untreated WT sample (1WT_0h = 0), then averages and standard deviations from the 3 Taqman® arrays were calculated.

Statistics for qPCR data

For the statistical analysis of qPCR-data in general a linear model for one dependent variable was run in the program SPSS Statistics 17.0. In order to provide linearity of the data log-transformed data were used for the statistical analysis. Normalised ΔCt values which are per definition log(2) or the normalised log(10) transformed values derived from the standard curve method were submitted to statistical analysis. Mean values ± SE of independent experiments were calculated. To calculate the significances of the "genotype effect" the samples of the genotype in question were compared to their corresponding samples of the WT, e.g. Tyk2-/- at time point 6 hours compared to the WT at time point 6 hours. Similarly, the significances of the "treatment effect" were calculated by comparing the treated to the untreated samples of the different genotypes, e.g. WT at time point 6 hours compared to WT at 0 h, and Tyk2-/- at time point 6h compared to Tyk2-/- at 0 hours. The independent experiments were considered as random factor in this statistical analysis.

The results of the Taqman® Custom arrays were statistically "pre-screened" in order to filter for genes that differ significantly between WT and Tyk2-deficient cells. The qPCR results were analysed with the "R" statistical package (Many: The R-project. http://www.r-project.org/, February 2007). In general, results proved highly variable and thus unreliable for low expression levels. Therefore genes that had Ct values beyond 30 were excluded from further analysis. Out of 240 genes 106 genes were further analysed. The target-gene data were normalised to a mean of the 2 endogenous control genes Hprt and Ube2d2. These ΔCt values were standardised to the same means and variances for each genotype and treatment. Subsequently, a linear model with the effects of genotype, i.e., WT *vs.* Tyk2-/-, of time, i.e., before and after 1 hours and 6 hours LPS treatment, was computed for each gene separately. The distribution of standard deviations from this model was used to compute moderated t-statistics (Smyth, 2004). This procedure ensured approximately t-distributed differences in gene expression values centered around a mean of about 0. Deviations from this mean were considered to be significant and highly significant if they exceeded the level of 2.14 and 2.96, i.e., the one-sided 0.05- and 0.01-limit for the t-test, respectively. SPSS statistical analysis was performed for the genes found by the "R"-screen to be differentially regulated between WT and Tyk2-deficient PMs.

Microarray analysis

Two whole genome microarray studies were performed. In the first study, WT and Tyk2-/- PMs were treated with 100 ng/ml LPS for 6 hours in 3 independent experiments. For this experiment CodeLink™ mouse whole genome microarrays were processed according to the manufacturer's instructions (www.appliedmicroarrays.com; February 2007). Analysis is described in detail in the submitted manuscript Vogl *et al*., 2010. In the second study WT and Oct-6-/- FLMs were treated with 50 µg/ml poly(I:C) for 8 hours in 3 independent experiments. This study was done with the ABI1700 gene expression profiling system (Applied Biosystems).

For both studies, total RNA was isolated according to the TRiZOL protocol. The RNA for the microarray analysis fulfilled highest quality requirements. All RNAs showed high and uniform RNA integrity as assessed by capillary electrophoresis (Agilent Technologies; Figure 12) and absorption ratios 260 nm/280 nm of 2.1 as determined by photometry.

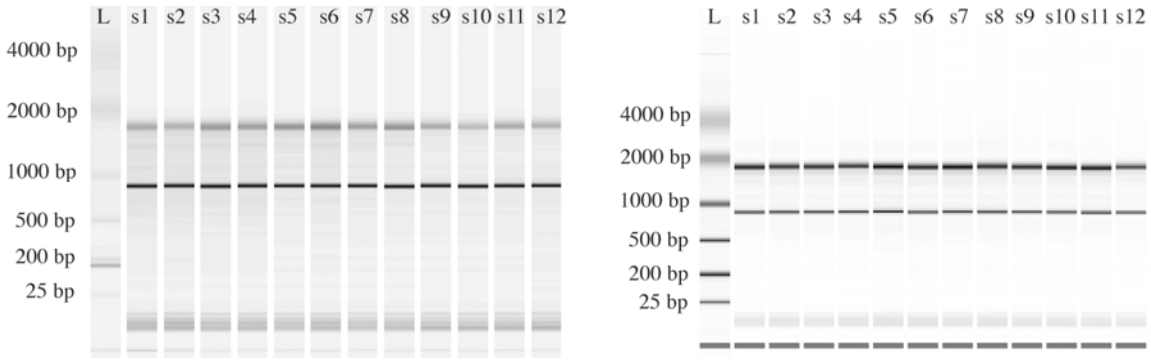

Figure 12: Check of RNA quality by capillary electrophoresis. (A) LPS experiment in WT and Tyk2-/- PMs; **(B)** poly(I:C) experiment in WT and Oct-6 deficient FLMs. Total, TRiZOL isolated RNA was heated to 65°C for 3 minutes, loaded onto a mammalian total RNA Nano Chip (Agilent Technologies) and processed according to manufacturer's instructions.

ABI1700 whole genome arrays

For the further analysis the RNA was handed over to an external institution, i.e. the Core Facility of Molecular Biology at the Centre for Medical Research of the Medical University of Graz, headed by Dr. Christian Gülly (Mouse whole genome arrays of the ABI1700 gene expression profiling system, Applied Biosystems).

For normalisation and further calculation values less than 10 were set to 10. Each of the 12 chips was normalised to the 50th percentile, each gene was normalised to the median of all chips. A boxplot diagram of the normalised fluorescence values showed uniform distribution among the samples (Figure 13), therefore all 12 chips were included in the calculation.

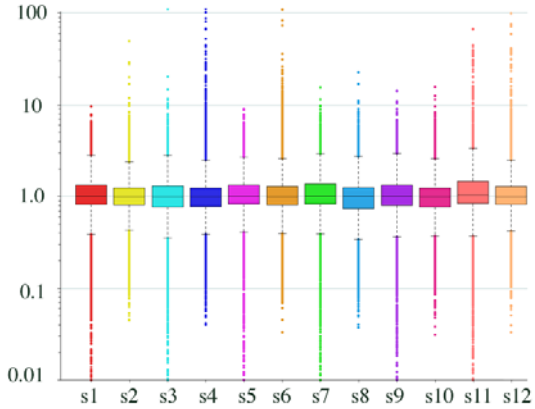

Figure 13: Normalised fluorescence data plotted for the 12 samples (s).

For statistical analysis (GeneSpring Expression Analysis 7.3.1 tool, Agilent Technologies) the data were filtered based on the signal to noise ratio. Samples were grouped according to the biological replicates (3x WT_0; 3x WT_poly(I:C); 3x Oct6_0; 3x Oct6_poly(I:C), and only genes that gave a signal to noise ratio above 2 in 3 out of 3 samples per group (i.e. all samples within at least 1 group), were included in the analyses. Under these conditions 12,220 out of 32,000 genes were further processed. The data were analysed for significant differences either between treated and untreated WT cells (treatment effect) or between treated Oct-6-deficient and treated WT cells (genotype effect after poly(I:C)). A 1-way ANOVA analysis was applied, using a parametric test, variances were not assumed equal (Welch t-test), and the cut off was set to $p<0.05$. Expression differences of at least 2-fold were considered relevant. Not fully annotated probes, i.e. probes that did not correspond to an NCBI RefSeq, EST or RIKEN cDNA, were excluded.

RESULTS I

Gene expression profiling in peritoneal macrophages in response to LPS treatment: role of Tyk2

Tyk2 has a detrimental effect in lipopolysaccharide (LPS)-induced shock, as Tyk2-deficient, in contrast to wild type (WT) mice, are able to survive the endotoxic shock (Karaghiosoff *et al.*, 2003). Peritoneal macrophages (PMs) from Tyk2-deficient mice showed reduced expression of the type I interferons (IFNs), IFNβ and IFNα□4, as well as of the IFN regulatory factors (Irfs) Irf1 and Irf7 in response to LPS treatment. In order to more globally characterise the effect of Tyk2 deficiency on LPS responses of macrophages, whole mouse genome microarray analysis was performed comparing Tyk2-/- and WT PMs with or without LPS treatment. On the one hand, extensive bioinformatic analyses of differentially regulated genes/clusters were performed to identify correlations with ***(i)*** 5' and 3' regulatory elements (e.g. transcription factor binding sites and miRNA cognate sequences) and ***(ii)*** functional categories (Fuhrmann B. Diploma thesis; Vogl *et al.*, 2010; accepted manuscript). On the other hand, and part of this thesis, gene expression patterns of selected genes were validated for the above study and analysed in more detail by RT-qPCR. We analysed gene expression patterns of 240 genes (table 6 in the material and methods section) in a medium-throughput format using Taqman® Custom Arrays (Applied Biosystems). These genes included known IFN-regulated genes and genes for which we had indications from a previous microarray screen to be differentially regulated in the absence of Tyk2 after IFNβ treatment (C. Gausterer, unpublished).

WT and Tyk2-deficient PMs were treated with LPS for 1 and 6 hours, or were left untreated. IFNβ expression levels were tested prior to microarray and Taqman® Array analysis in order to control for the stimulation and genotype effects, as reduced expression levels of IFNβ in the absence of Tyk2 had already been demonstrated. In WT PMs, the expression of IFNβ peaked at 1 hour and declined again after 6 hours of LPS treatment. As expected, the expression of IFNβ was significantly reduced in the absence of Tyk2 (see table 7 for statistical analysis). This was observed for basal expression levels, i.e. expression levels in untreated PMs, as well as for expression levels after LPS treatment (Figure 14).

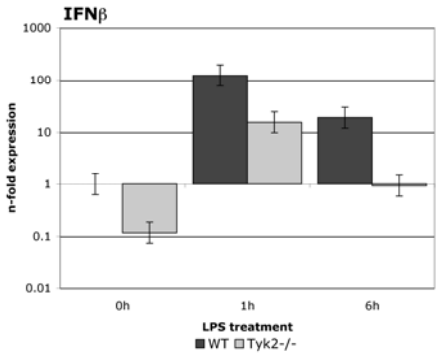

Figure 14: Expression levels of IFNβ are reduced in the absence of Tyk2. WT and Tyk2-/- PMs were treated with LPS (100 ng/ml; 1 h, 6 h), or left untreated (0 h). Expression levels of IFNβ were determined by RT-qPCR using the standard curve method for calculation of the n-fold expression levels and normalising the data to Ube2d2. N-fold expression levels are depicted as relative mean values of 3 experiments ± SE in a log-scaled diagram.

Of the 240 genes analysed, 22 genes were induced/reduced in response to LPS-treatment and showed altered expression levels in the absence of Tyk2. Most of them are known ISGs, namely Mx1, Irf1, Irf7, Gbp2, Ifit1, Ifit2, Ifi203, Oas1b, Stat1, Socs1, Socs2, Ccl5, Cxcl9, Tnfsf10, Ddx58 and Slfn8 (Figure 15). Differences between the genotypes above 2-fold were considered as relevant (Figures 15-17, table 7; genes with a significant, but only 1.5- to 2-fold differential expression are summarised in table 8). Most of the ISGs showed similar expression patterns (Figure 15), with expression levels in WT unchanged after 1 hour and increased after 6 hours of LPS treatment. In the absence of Tyk2, the expression levels were significantly reduced at all time points. Different patterns were only observed for Irf1, Socs1 and Socs2. The expression of Irf1 peaked after 1 hour of LPS treatment, and levels were again declining after 6 hours. However, significant reduction of Irf1 expression in the absence of Tyk2 was observed for all time points. In the case of Socs1, only the basal expression level was significantly reduced in the absence of Tyk2, whereas expression levels were comparable to those of WT cells after LPS treatment. In contrast, increased basal expression in the absence of Tyk2 was observed for Socs2. In addition, although Socs2 was induced upon LPS treatment in WT cells, its expression level after 6 hours was still significantly below that of Tyk2-deficient cells.

Figure 15 – continued on the following pages

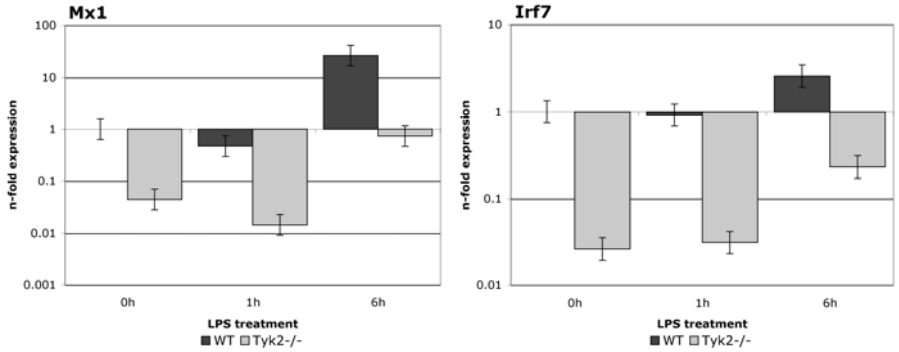

Figure 15 – continued on the following pages

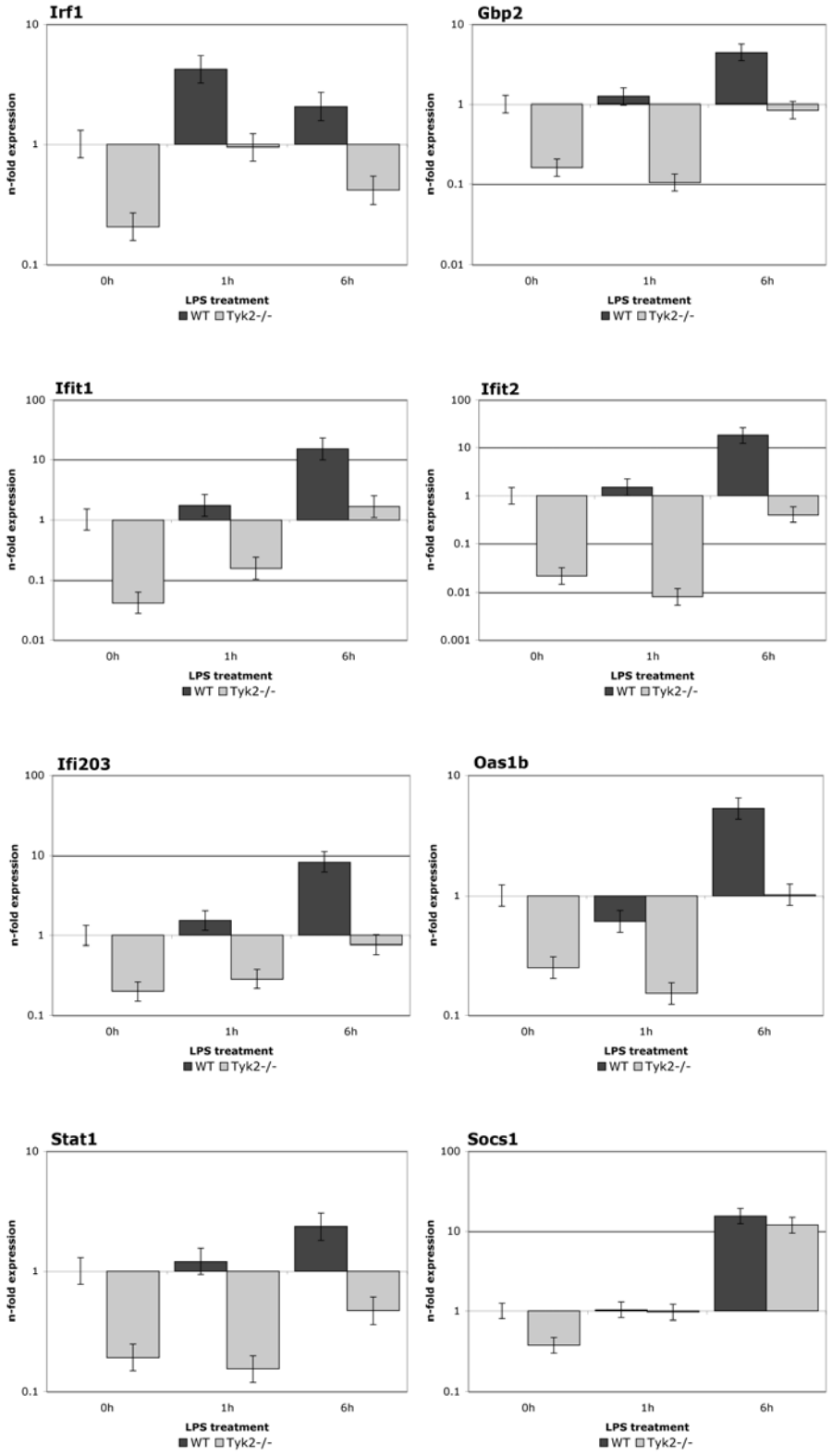

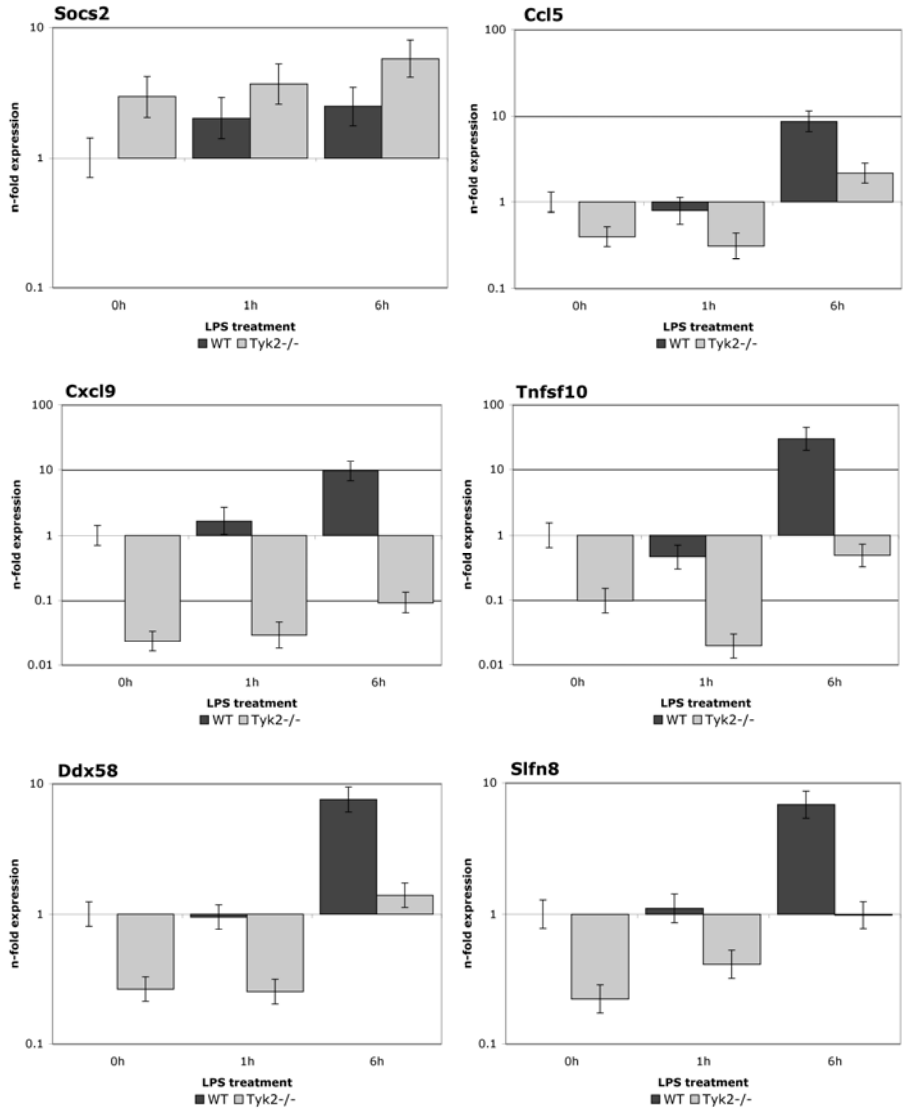

Figure 15: ISGs are differentially expressed in WT and Tyk2-deficient PMs after LPS treatment. WT and Tyk2-/- PMs were treated with LPS (100 ng/ml; 1 h, 6 h), or left untreated (0 h). The n-fold expression levels were determined by RT-qPCR in the Taqman® array format, using the ΔΔCt method. The target gene data were normalised to Ube2d2 as endogenous control, the samples were calibrated to the untreated WT (i.e. WT_0h = 1). N-fold expression levels are depicted as relative mean values of 3 experiments ± SE in a log-scaled diagram (see table 7 for the statistical analysis).

Six genes that so far have not been reported to be regulated by LPS treatment or to be dependent on Tyk2, namely Pou3f1, IL-17F, Fgr, Hmbs, Aif1 and Cd79a, were found to be expressed differentially between WT and Tyk2-deficient PMs (Figure 16). So far, they have not been reported to be induced in PMs, upon IFN-treatment, and/or to be dependent on Tyk2.

The pattern of Oct-6 (Pou3f1) expression was comparable to that of most ISGs, with expression levels in WT cells being unchanged after 1 hour and increased after 6 hours of LPS treatment, and with largely reduced expression levels in the absence of Tyk2 at all time points (Figure 16A).

IL-17F was hardly detectable at basal levels (Ct > 35). The expression was increased already after 1 hour and further increased after 6 hours of treatment. Significantly lower levels of IL-17F were found in the absence of Tyk2 after LPS treatment (Figure 16B). Since IL-17 has obtained quite some attention as being the signature cytokine of the Th17 subset of T-cells, expression of IL-17F and of the closely related, more prominent IL-17A was further analysed in separate qPCR assays. This improved the sensitivity so that also basal levels could be reliably detected. The results for IL-17F from the Taqman® Array could be confirmed and IL-17A showed similar expression patterns. In the absence of Tyk2, expression levels of IL-17F and IL-17A were significantly reduced at all time points (Figure 17).

Basal expression level of Aif1 and Cd79a (Figure 16C and 16D) were also reduced in the absence Tyk2. However, those genes were not significantly regulated in response to LPS in WT cells. Aif1 expression was significantly downregulated upon LPS treatment in Tyk2-deficient cells.

Expression levels of Fgr and Hmbs (Figure 16E and 16F) were downregulated after LPS treatment in a Tyk2-dependent manner.

Figure 16 – continued on the following pages

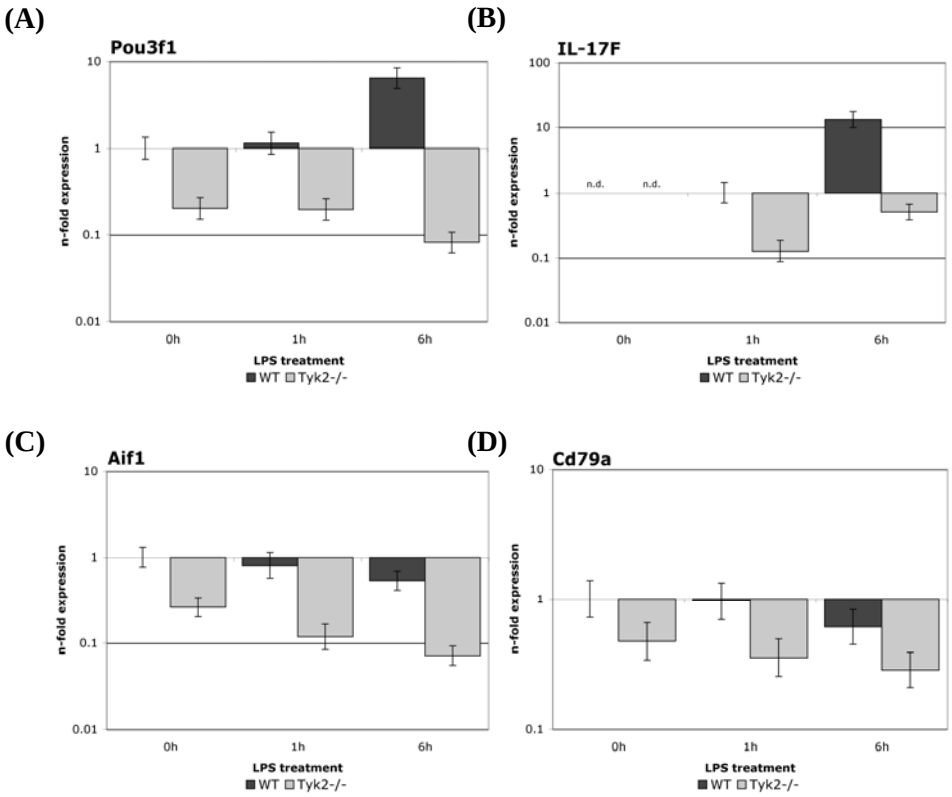

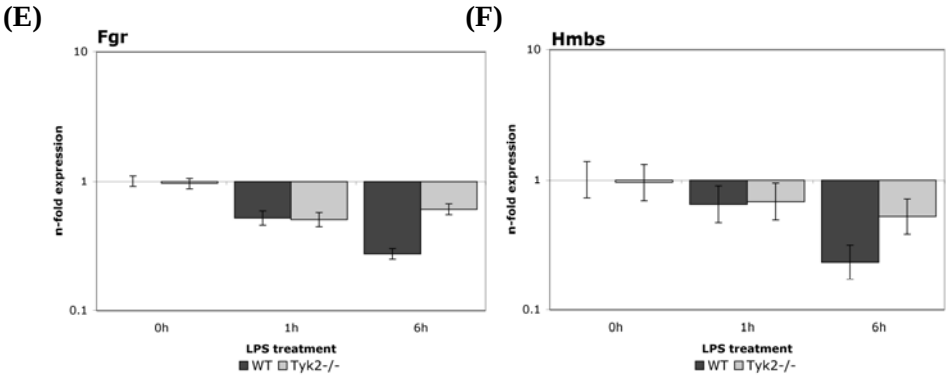

Figure 16: Further genes showing altered expression patterns in the absence of Tyk2. WT and Tyk2-/- PMs were treated with LPS (100 ng/ml; 1 h, 6 h), or left untreated (0 h). N-fold expression levels were calculated as described above for Figure 15.

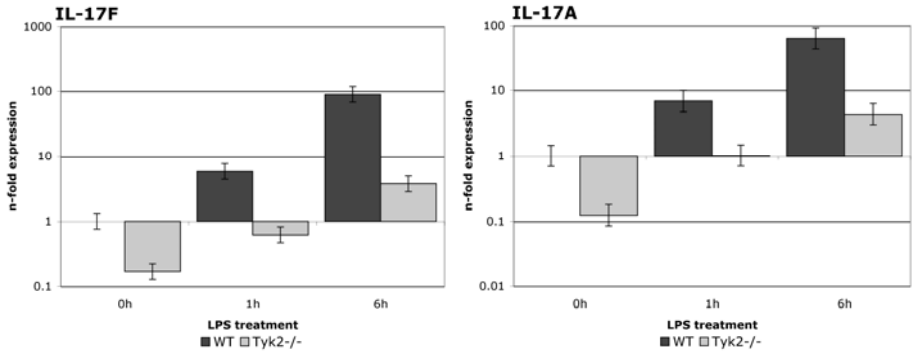

Figure 17: Expression of IL-17F and IL-17A is induced in PMs after LPS treatment in a Tyk2-dependent manner. In 3 independent experiments, WT and Tyk2-/- PMs were treated with LPS (100 ng/ml; 1 h, 6 h), or left untreated (0 h). N-fold expression levels for IL-17F and IL-17A were determined as described above in Figure 14.

Table 7: Significances of treatment and genotype effects for genes showing at least 2-fold differential expression between WT and Tyk2-/- PMs upon LPS treatment (ad Figures 14-17, table continued on the following page**).**

gene	treated *versus* untreated				Tyk2-/- *versus* WT		
	WT_1h	WT_6h	Tyk2-/-_1h	Tyk2-/-_6h	0h	1h	6h
IFNβ [1]	**	**	**	**	**	**	**
Irf1	**		**		**	**	**
Irf7		*		**	**	**	**
Mx1		**		**	**	**	**
Gbp2		**		**	**	**	**
Ifit1		**	*	**	**	**	**
Ifit2		**		**	**	**	**

gene	treated *versus* untreated				Tyk2-/- *versus* WT		
	WT_1h	WT_6h	Tyk2-/-_1h	Tyk2-/-_6h	0h	1h	6h
Ifi203		**		**	**	**	**
Oas1b		**		**	**	**	**
Stat1		*		*	**	**	**
Socs1		**	**	**	**		
Socs2		*			*		*
Ccl5		**		**	*	*	**
Cxcl9		**		**	**	**	**
Tnfsf10		**	*	**	**	**	**
Ddx58		**		**	**	**	**
Slfn8		**	**	**	**	**	**
Pou3f1		**		*	**	**	**
IL-17F	**	**		*		**	**
IL-17F [1]	**	**	**	**	**	**	**
IL-17A [1]	**	**	**	**	**	**	**
Fgr	**	**	**	**			**
Hmbs	*	**		**			**
Aif1			*	**	**	**	**
Cd79a						*	

The normalised ΔCt values or the, normalised log(10) transformed (in case of the genes analysed separately) values were submitted to statistical analysis in SPSS.17.0 applying an univariate linear model. The results for the selected genes shown in figures 14-17 are summarised with ** indicating $p<0.01$, and * $p<0.05$, empty fields identify non-significant differences. ISGs are indicated by the shaded boxes.

Table 8: Genes showing a significant 1.5- to 2-fold differential expression between WT and Tyk2-/- PMs after LPS treatment (table continued on the following page**).**

gene	treated *versus* untreated		Tyk2-/- *versus* WT		
	WT_1h	WT_6h	0h	1h	6h
As3mt		0.40 (**)			1.86 (**)
Birc4			1.58 (**)		
Casp2	0.53 (**)				0.55 (**)
Cias1 [1]	-	10.3 (**)	0.66 (*)	-	
Ebi3 [1]	-			-	1.80 (**)
Efnb2				1.96 (**)	
Eif2c1					1.62 (**)

gene	treated *versus* untreated		Tyk2-/- *versus* WT		
	WT_1h	WT_6h	0h	1h	6h
Fmr1		2.25 (**)			0.51 (**)
Gimap9[1]	-	4.46 (**)		-	0.56 (**)
Hipk2				1.72 (**)	
Icam2[1]	-			-	0.54 (**)
Lbp				0.52 (**)	
Mga		0.59 (**)			1.69 (**)
Mitf[1]	-		1.60 (**)	-	
Mmp13	1.53 (**)	10.6 (**)			0.52 (*)
Nedd4		0.62 (**)		1.76 (**)	1.62 (**)
Nr2f6[1]	-	0.40 (**)		-	1.98 (**)
Padi4		0.55 (**)	0.61 (*)	0.53 (**)	
Prdx6[1]	-		1.67 (**)	-	1.92 (**)
Prkce		2.42 (**)			0.62 (**)
Ptprm			1.55 (**)	1.66 (**)	
Rnf24[1]	-	4.48 (**)		-	0.52 (**)

WT and Tyk2-/- PMs were treated with LPS (100 ng/ml; 1h, 6h), or left untreated (0h). The n-fold expression levels were determined by RT-qPCR in the Taqman® array format, using the ΔΔCt method, normalising the gene-of-interest data to the mean of Ube2d2 and Hprt as endogenous controls. Genes giving Ct values of 30 and above were excluded from the analysis. The normalised ΔCt values were submitted to statistical analysis in "R" applying an univariate linear model (** indicate $p<0.01$, and * $p<0.05$, empty fields identify non-significant changes). For certain genes ([1]) 1 of the 3 replicates was missing for the 1 hour time point. That is why no statistical analysis could be performed for these genes for this time point (-).

In summary, absence of Tyk2 had a profound effect on the expression of the ISGs analysed in this study. Following expression patterns in the absence of Tyk2 compared to WT were observed: ***(i)*** reduced expression at basal levels and after treatment with LPS (most ISGs), ***(ii)*** reduced basal expression, but similar to WT after LPS treatment (Socs1), ***(iii)*** enhanced expression at basal levels and after LPS treatment (Socs2). Six, novel Tyk2-dependent genes (displaying at least 2-fold differential expression as compared to WT) were identified and following patterns were found: ***(i)*** comparable to the expression pattern of most ISGs (Pou3f1, IL-17A, IL-17F), ***(ii)*** reduced expression at basal levels and after LPS treatment, whereby expression levels in WT were unchanged in response to treatment (Aif1, Cd79a), ***(iii)*** no difference at basal levels and enhanced expression after LPS treatment in comparison to WT (Fgr, Hmbs).

RESULTS II

Oct-6 is an interferon stimulated gene (ISG)

Oct-6 expression after IFNβ treatment in fibroblasts

In a whole genome microarray study (C. Gausterer unpublished), octamer-binding-factor 6 (Oct-6; also known as Pou3f1, SCIP, Tst-1) was found to be induced in response to IFNβ treatment in murine embryonic fibroblast (MEF) cell lines. Expression of Oct-6 mRNA was reduced in the absence of Tyk2. Oct-6 belongs to the group of POU-domain containing transcription factors and is involved in terminal differentiation of myelinating Schwann cells and keratinocytes. Oct-6 has never been shown before to be expressed outside the neuroendocrine system and keratinocytes or to play a role in the context of type I IFN responses or in immunity in general.

In the course of validation by reverse-transcription real-time quantitative PCR (RT-qPCR), microarray results were confirmed in MEF cell lines treated with IFNβ (Figure 18A). Corresponding experiments were performed in primary MEFs (pMEFs; Figure 18B). In both cell types, Oct-6 mRNA expression levels were induced about 40- to 60-fold after 6 hours of IFNβ treatment in wild type (WT) cells and only about 7- to 20-fold in the absence of Tyk2.

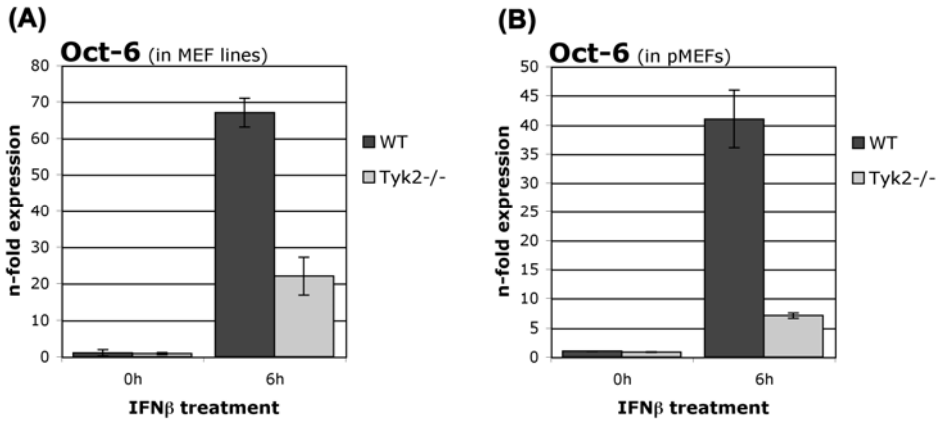

Figure 18: Oct-6 mRNA expression is induced in MEF cell lines and pMEFs after IFNβ treatment and is partially dependent on Tyk2. Cells were treated with IFNβ (500 U/ml) for 6 hours. **(A)** N-fold expression levels relative to untreated WT cells were determined by RT-qPCR in the Taqman® Custom Array format using the ΔΔCt method. Data were normalised to a mean of 3 endogenous control genes (Hprt, Hmbs and Ube2d2). N-fold expression levels are depicted as mean values of 3 experiments ± standard deviation (SD; data in collaboration with C. Gausterer). **(B)** N-fold expression levels relative to untreated WT cells were determined by RT-qPCR using the standard curve method, using Ube2d2 for normalisation. Data are shown as mean values of technical duplicates ± SD for 1 representative out of 2 independent experiments.

We were not able to reliably detect Oct-6 protein by western blot, since a strong background dominated over a weak specific signal. Therefore we analysed Oct-6 protein expression and DNA-binding activity by bandshift assays using an oligonucleotide containing the octamer consensus motif.

Oct-6 DNA-binding was observed after treating WT pMEFs with IFNβ, whereas it was not detected in untreated cells (Figure 19). Since other members of the POU-family of proteins also bind to this oligonucleotide, identity of Oct-6 was confirmed by supershift assays with an Oct-6-specific antibody and by the absence of the signal in Oct-6-deficient cells (Figure 19A). A slower migrating protein or complex, which was present in all samples irrespective of treatment was identified as Oct-1, which is known to be ubiquitously expressed (Ryan and Rosenfeld, 1997). Another protein/complex, migrating between Oct-1 and Oct-6 (weak in Fig. 19A, better visible in Fig. 19B) was detected, but could not be assigned to a specific octamer-binding protein. Reduced IFNβ-induced Oct-6 expression in the absence of Tyk2 could also be confirmed by bandshift assays in MEF cell lines (data not shown) as well as in pMEFs (Figure 19B).

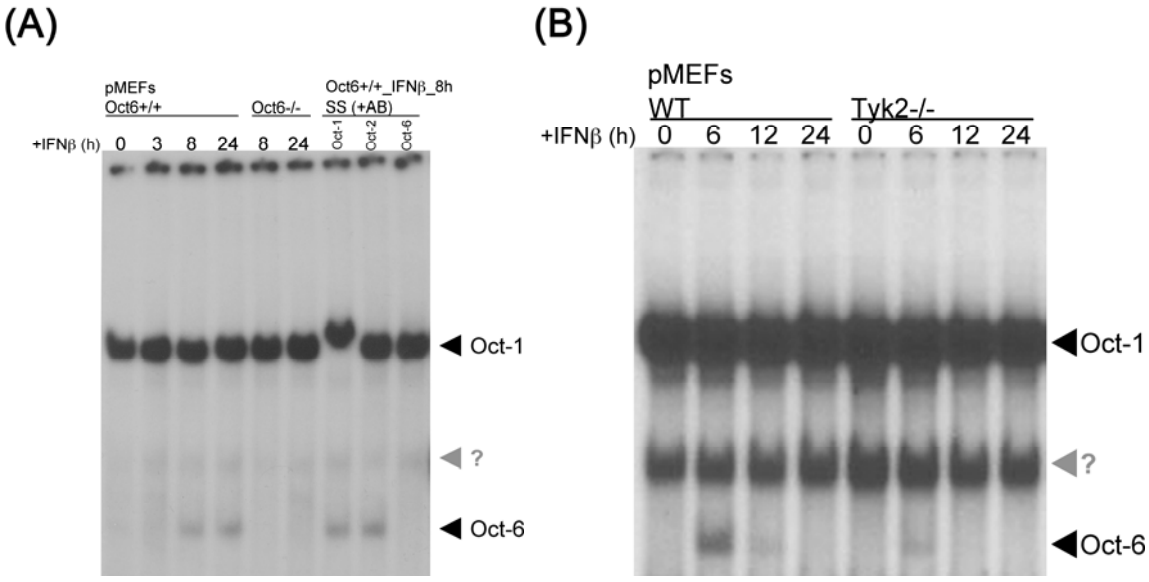

Figure 19: Oct-6 protein is expressed in pMEFs in response to IFNβ treatment, and expression is partially dependent on Tyk2. (A) Oct-6+/+ and Oct-6-/- pMEFs were treated with IFNβ (1000 U/ml) for the indicated times. Whole cell extracts were analysed by bandshift assays with an octamer motif-containing probe (SS: supershifts with the respective antibodies (+AB); "?" unidentified octamer-binding complex). **(B)** WT and Tyk2-/- pMEFs were treated with IFNβ (1000 U/ml) for the indicated times. Bandshifts were performed as described in (A).

Oct-6 induction after IFNβ treatment in macrophages

Macrophages play a major role in immunity, and therefore the expression of Oct-6 in bone marrow-derived macrophages (BMMs) upon IFNβ treatment was analysed. In general, Oct-6 DNA-binding activity was much higher induced in BMMs than in MEFs. Oct-6 protein was readily detected after 3 hours and reached the maximum between 6 to 12 hours of IFNβ treatment (Figure 20A, B). As in MEFs, Oct-6 binding was not observed in untreated macrophages. Again, Oct-6 was identified by supershift with the respective antibody. Furthermore, Oct-6 overexpressed in a MEF cell line showed

the same migration in the bandshift gel (Figure 20A). Apart from Oct-6 and the ubiquitously expressed Oct-1, a third complex was observed in BMMs. This complex migrated between Oct-1 and Oct-6 and could be supershifted with an α-Oct-2 antibody, which is in line with previous publications demonstrating Oct-2 expression in various macrophage populations (Dunn *et al.*, 1996 and references therein).

(A) **(B)**

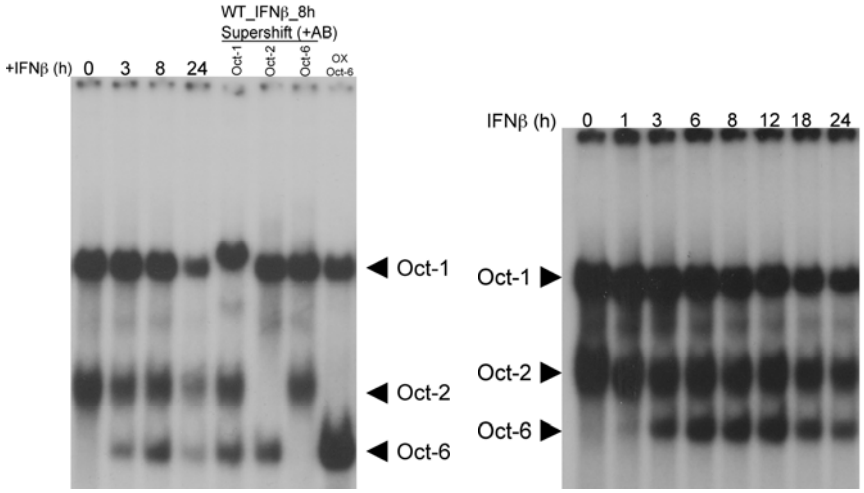

Figure 20: Oct-6 is expressed in BMMs in response to IFNβ treatment. (A, B) WT BMMs were treated with IFNβ (1000 U/ml) for the indicated times. Whole cell extracts were analysed by bandshift assays with an oligonucleotide containing the octamer consensus motif. **(A)** +AB: supershifts with Oct-1, Oct-2 and Oct-6 specific antibodies; OX: transient overexpression of Oct-6 in a MEF cell line.

In order to elucidate the molecular requirements for the induction of Oct-6, BMMs deficient for components of the signalling pathway mediating IFNβ responses, namely Tyk2, Stat1, Ifnar1 and Irf1, were analysed by bandshift assays. In Tyk2-deficient macrophages, the binding of Oct-6 was clearly reduced (Figure 21), which is similar to the results obtained in pMEFs. In the absence of Stat1, Oct-6 expression was nearly absent, and only very weakly detectable after 24 hours of IFNβ treatment. Irf1-deficient cells were included in the analysis in order to test whether expression Oct-6 is directly dependent on Stat1, or whether Irf1 is required as an intermediate step, but absence of Irf1 did not affect Oct-6 induction. As expected, Oct-6 protein after IFNβ treatment was not detected in Ifnar1-deficient BMMs, thus confirming that the effect on Oct-6 expression is mediated by IFNβ and not by any other component that might be present in the IFNβ solution.

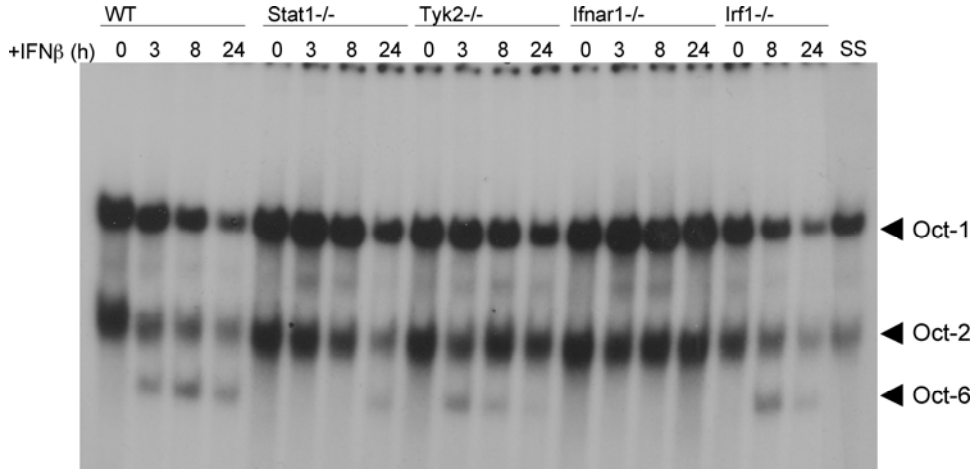

Figure 21: Expression of Oct-6 in response to IFNβ is largely dependent on Jak/Stat signalling. WT, Stat1-/-, Tyk2-/-, Ifnar1-/- or Irf1-/- BMMs were treated with IFNβ (1000 U/ml) for the indicated times. Whole cell extracts were analysed by a bandshift assay with an oligonucleotide containing the octamer consensus motif (SS: Supershift of WT_8h lysates with an α-Oct-6 antibody).

Oct-6 induction in response to other cytokines

In order to test whether Oct-6 is also induced in response to other cytokines, BMMs were treated with IFNγ or IL-6, respectively. IFNγ also signals through Stat1, but in contrast to type I IFNs, which activate Stat1/Stat2 heterodimers, IFNγ activates mainly Stat1/Stat1 homodimers. IL-6 employs Jak/Stat signalling, but activates mainly Stat3. IFNγ induced detectable amounts of Oct-6 DNA-binding activity, but slightly less and with a different kinetic than IFNβ (Figure 22). In contrast Oct-6 protein was not detected in response to IL-6 treatment.

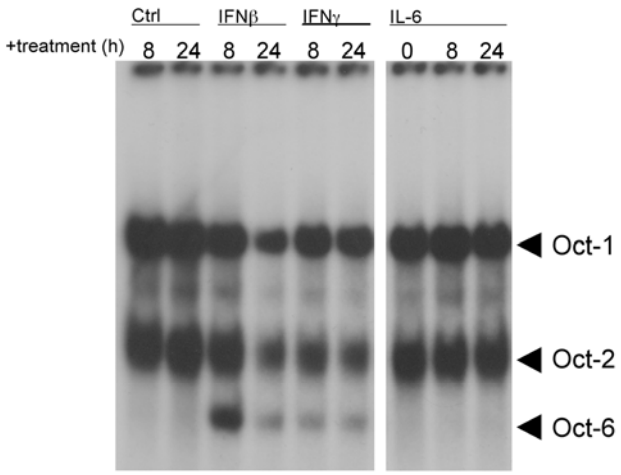

Figure 22: Oct-6 expression is induced in response to IFNγ but not to IL-6. BMMs were treated with IFNβ (1000 U/ml), IFNγ (1000 U/ml), IL-6 (125 ng/ml), or were left untreated (Ctrl). Whole cell extracts were analysed by a bandshift assay with an oligonucleotide containing the octamer consensus motif.

Oct-6 induction in response to poly(I:C) and virus infection

We next wanted to test, if Oct-6 is only induced in response to high levels of exogenous IFNβ, or also by endogenously produced type I IFNs. BMMs were infected with murine cytomegalovirus (MCMV) or stimulated with poly(I:C), a dsRNA analogon mimicking viral infection. Both stimuli strongly induced Oct-6 DNA-binding activity (Figure 23). The induction of Oct-6 in response to poly(I:C) treatment (Figure 23A) and MCMV infection (Figure 23B) was clearly dependent on type I IFN signalling, since Oct-6 protein could not be detected in Ifnar1-deficient BMMs. Consistent with the prominent role of IFNβ in viral infections, Oct-6 DNA-binding activity was hardly detectable after both stimuli in the absence of IFNβ. Thus, other type I IFNs can also induce Oct-6. In Tyk2-deficient BMMs reduced Oct-6 expression was observed upon both stimuli. In the absence of Stat1, poly(I:C) failed to induce detectable amounts of Oct-6 protein. In contrast, a very weak signal of Oct-6 DNA-binding activity in Stat1-/- BMMs was detected after 24 hours of MCMV infection, which is similar to the results obtained after long IFNβ treatment.

Figure 23 – continued on the following page

(A)

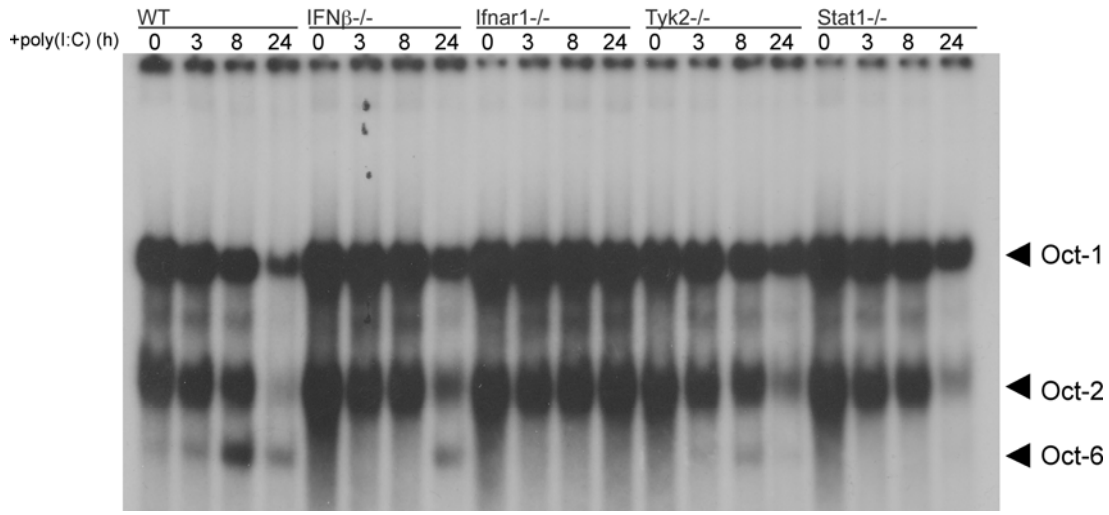

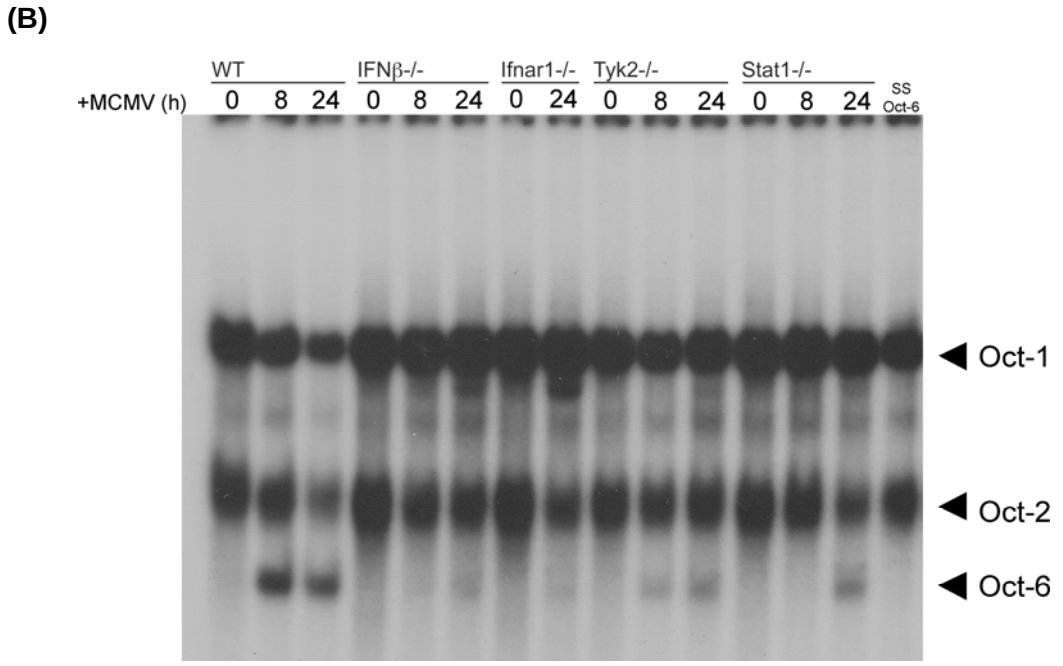

Figure 23: Expression of Oct-6 in response to poly(I:C) and during MCMV infection is largely dependent on type I IFN and Jak/Stat signalling. WT, IFNβ-/-, Ifnar1-/-, Stat1-/-, or Tyk2-/- BMMs were **(A)** treated with poly(I:C) (50 µg/ml) or **(B)** infected with MCMV (MOI = 1) for the indicated times. Whole cell extracts were analysed by bandshift assays with an oligonucleotide containing the octamer consensus motif (SS: Supershift of WT_8h lysates with an α-Oct-6 antibody).

Analysis of the Oct-6 promoter region

Based on the fact that Oct-6 is induced in a largely Stat1-dependent manner after IFNβ treatment, the promoter region of Oct-6 was searched for potential IFN-stimulated response elements (ISREs) and IFNγ activated sites (GASs). Therefore a genomic region 10 kb upstream of the transcription start site was analysed. Assuming that only conserved sequence elements would be of interest regarding the functionality of a predicted transcription factor binding site (TFBS), the murine sequence was aligned to the corresponding human and rat sequences (Blast 2 sequences: http://blast.ncbi.nlm.nih.gov/bl2seq/wblast2.cgi; March 2008). Whereas the 2 rodent sequences showed a high degree of homology, only a few homologous regions were found for murine and human sequences. These sequence parts, i.e. -7691 to -8047, -4367 to -4500, -1598 to -3233, and -161 to -637 (base counts correlate to the murine sequence), were submitted to TFBS analysis using "Patch" (http://www.gene-regulation.com/pub/programs.html; August 2008), a publicly available program scanning input sequences for potential TFBSs based on the Transfac database. A number of Stat1- and ISGF3-binding sites were predicted for each sequence part (data not shown). We decided to concentrate on the homolgous sequence part nearest to the transcription start site (-161 to -637) of Oct-6, based on a report showing that the regions 500 bp upstream of the transcription start site of

IFN-inducible genes are enriched in predicted binding sites for Stat1, ISGF3, Irf1 and NFκB (Ananko *et al.*, 2007). One GAS (-477 to -468) and one ISRE (-412 to -409) were predicted. Another GAS (-402 to -392) located in close proximity to the predicted ISRE was found by checking the sequences next to the predicted sites manually. The GAS elements (Figure 24) show only one mismatch each compared to the consensus sequence ($TTC(N)_{2\text{-}4}GAA$; Decker *et al.*, 1997). The predicted ISRE (-412 to -409) seems rather imperfect when compared to the published consensus motif ($GATTTC(N)_2TTTCNY$; Decker *et al.*, 1997), but is identical in comparison to the Transfac annotated ISGF3 motif (GGAAA; accession number in Transfac database: HS$IFI616_01).

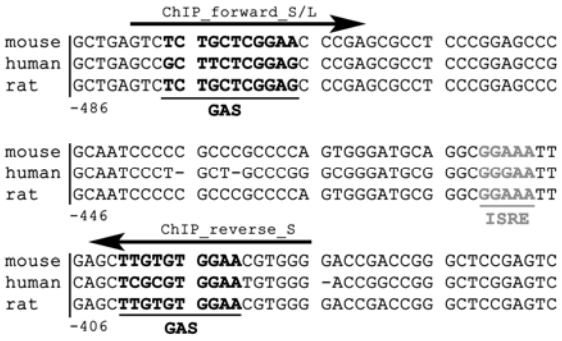

Figure 24: Two GAS and one ISRE elements are predicted in the region 500 bp upstream of the Oct-6 transcription start site. The homologous sequence part containing the predicted Stat1 binding sites, i.e. 2 GAS (black bold letters) and one ISRE (grey bold letters), is shown (base counts correlate to the murine sequence). The primer set for the short Oct-6-ChIP-PCR (Oct-6_S; -481 to -387; results in Figure 25A) is indicated by arrows. For the long Oct-6-ChIP-PCR (Oct-6_L; -481 to -243; results in Figure 25B), the same forward primer as for the short PCR was used. The corresponding reverse primer is located 150 bases downstream of the reverse primer of the short PCR and is not shown in this figure.

Stat1 binding to the Oct-6 promoter

In order to test Stat1 binding to the potential GAS and ISRE sites in the Oct-6 promoter a chromatin immunoprecipitation (ChIP) approach was used. Two PCRs covering the predicted sites were designed to analyse whether Stat1 binds to this region after IFN treatment (Figure 25). As a control, Stat1 binding to the GAS within the Irf1 promoter (Sadzak *et al.*, 2008) was included in the analysis.

Both PCRs for the Oct-6 promoter (Figure 25A, B) clearly show that IFNβ as well as IFNγ treatment induce Stat1 binding to the respective region. The signals for the untreated samples correlate to background (unspecific AB controls). As expected, Stat1 binding to the Irf1 promoter could be demonstrated in response to IFNβ and IFNγ treatment (Figure 25C).

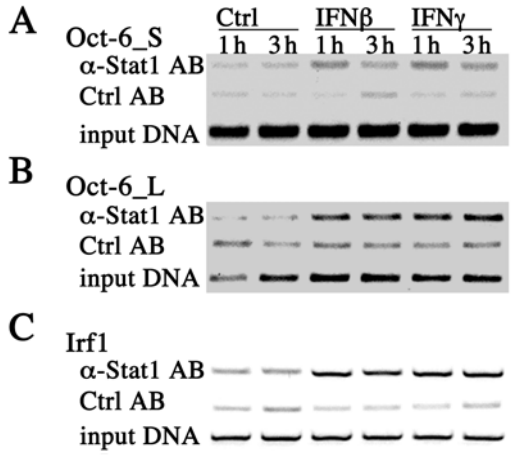

Figure 25: Upon IFN treatment Stat1 binds to a region in the Oct-6 promoter containing potential GAS and/or ISRE motifs. BMMs were treated with IFNβ (500 U/ml) or IFNγ (200 U/ml) for the indicated times, or were left untreated (Ctrl). ChIP assays for Stat1 (α-Stat1 AB) were performed, followed by PCRs: **(A)** Oct-6_S, **(B)** Oct-6_L (Figure 24), **(C)** PCR for a region in the Irf1 promoter known to contain GAS elements. Rabbit serum was used as an unspecific antibody control (Ctrl AB), input DNA was amplified to control for DNA amount/loading prior to the immunoprecipitation step.

Subcellular localisation of Oct-6 protein

So far, no postranslational modifications required for full transcriptional activity of Oct-6 have been described. The transcriptional activity of Oct-6 seems to be regulated by its expression and possibly by its subcellular localisation (Baranek *et al.*, 2005). In order to investigate if IFN treatment results in nuclear accumulation of Oct-6, an indirect immunofluorescence approach was followed. Since Oct-6 is stronger induced in macrophages than in MEFs and Oct-6-deficient mice die perinatally, fetal liver-derived macrophages (FLMs) were used in these experiments. Similar induction of Oct-6 in FLMs as compared to BMMs was confirmed by bandshift assays (Figure App. 2). FLMs were treated with IFNβ or poly(I:C) and subcellular localisation was analysed. As shown in Figure 26, Oct-6 is prominently detected in the nucleus in response to both stimuli. No Oct-6 staining was observed in untreated (Figure 26) and in Oct-6-deficient cells (data not shown).

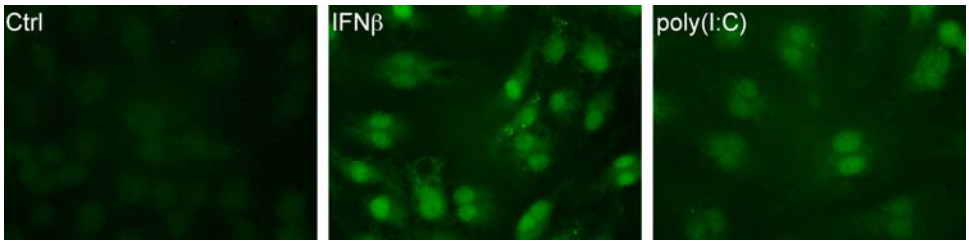

Figure 26: Oct-6 is located in the nucleus after IFNβ or poly(I:C) treatment. FLMs were grown on glass slides, treated with IFNβ (1000 U/ml) or poly(I:C) (50 µg/ml) for 8 hours, or were left untreated (Ctrl). Oct-6 was detected by immunofluorescence with an α-Oct-6 primary antibody and a fluorescently labeled secondary antibody.

Oct-6 expression in the murine Schwann cell line SW10

Expression and function of Oct-6 have been mainly described in the context of Schwann cell development. Therefore the murine Schwann cell line SW10 was analysed for the expression of Oct-6 in response to IFNβ treatment. This cell line was immortalised with a temperature sensitive variant of the SV40 large T-antigen (Hai *et al.*, 2002). Cells were kept at 33°C (permissive temperature), 37°C and 39°C (non-permissive temperatures), and stimulated with IFNβ. Oct-6 mRNA was clearly induced independent of the culture conditions (Figure 27A). Interestingly, basal expression levels of Oct-6 mRNA were enhanced with increasing temperature, i.e. more than 10-fold at 39°C as compared to 33°C. Consistently, Oct-6 DNA-binding activity was detectable in response to IFNβ treatment in a temperature dependent manner. However, Oct-6 DNA-binding activity was rather weak (Figure 27B) as compared to MEFs and macrophages.

(A)

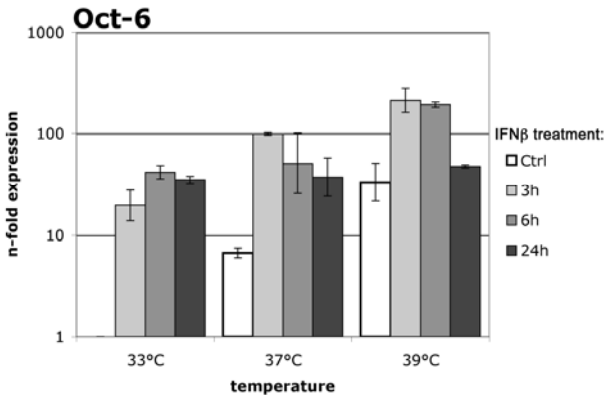

(B)

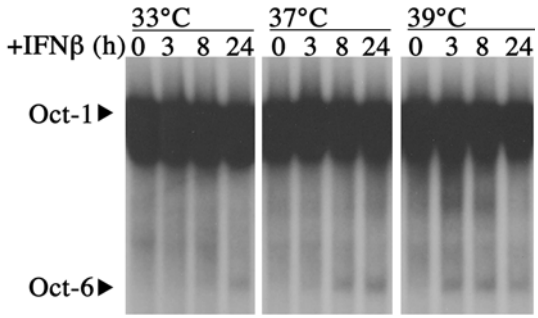

Figure 27: Oct-6 is expressed in the murine Schwann cell line SW10 after IFNβ treatment. Cells were kept at the 3 different temperatures for three days (33°C, 37°C and 39°C) and were treated with IFNβ (1000 U/ml, for the indicated times) or left untreated (Ctrl). **(A)** Oct-6 mRNA expression was analysed by RT-qPCR applying the standard curve method with Ube2d2 as endogenous control (mean values of technical duplicates ± SD from 1 representative out of 2 independent experiments are shown). **(B)** Whole cell extracts were analysed by a bandshift assay with an octamer motif-containing oligonucleotide, 1 representative out of 2 experiments is shown.

In summary, we found that Oct-6 was expressed in fibroblasts, macrophages and the murine Schwann cell line SW10 after stimulation with IFNβ. More detailed analyses in macrophages showed that IFNγ also induces Oct-6 expression. Furthermore, Oct-6 was induced in response to poly(I:C) treatment and during viral infections, in both cases in a strictly type I IFN-dependent manner. The expression of Oct-6 was largely dependent on Stat1, and we could demonstrate Stat1 binding to a region in the Oct-6 promoter in response to IFNβ or IFNγ treatment. Moreover, we showed that Oct-6 localised to the nucleus after IFNβ or poly(I:C) treatment.

The role of Oct-6 in innate immunity

In order to analyse the biological function of Oct-6 in the setting of innate immunity two complementary approaches were followed. On the one hand, gain-of-function experiments were performed by overexpressing Oct-6 in primary fibroblasts (pMEFs). On the other hand, pMEFs and fetal-liver derived macrophages (FLMs) deficient for Oct-6 were analysed in loss-of-function experiments. Since Oct-6 is a transcription factor, we mainly focussed on the analysis of candidate target gene expression using RT-qPCR. Egr2 and Pmp22 were analysed, because both genes are known to be regulated by Oct-6 in the course of Schwann cell development (Ghislain *et al.*, 2002; Ryu *et al.*, 2007). Furthermore, expression levels of IFNαs (all subtypes collectively, panIFNα), IFNβ and iNOS, all of which contain functional octamer motifs in their promoters (Mesplède *et al.*, 2005; Haggarty *et al.*, 1991; Kleinert *et al.*, 2004), were analysed. Moreover, a microarray experiment was performed in search for the role of Oct-6 in regulation of the transcriptional responses to poly(I:C) in macrophages.

Candidate target gene expression upon Oct-6 overexpression

For overexpression of Oct-6 the respective coding sequence was cloned into an expression plasmid under the control of the constitutively active EF1α-promoter (pEFZeo; Oct6_sense1). In order to control for unspecific effects, the antisense sequence of Oct-6 (Oct6_anti) was also cloned. Additionally, a CMV-promoter driven Oct-6 expression plasmid was used (Oct6_sense2). Oct-1 was cloned into pEFZeo (Oct1_sense), as a positive control, as effects of Oct-1 on IFNα expression have already been described (Mesplède *et al.*, 2005). To control for transfection efficiency and for unspecific transfection effects an enhanced-GFP expression plasmid (GFP) and the empty pEFZeo plasmid were included in these experiments. Primary MEFs were transiently transfected with the different plasmids and gene expression of candidate target genes was analysed 24, 36 and 48 hours after transfection.

As expected, transient induction of IFNβ was observed in response to transfection of the control plasmids, i.e. the empty vector, the GFP-plasmid and the Oct-6 antisense plasmid (Figure 28A). However, expression levels of IFNβ and also of panIFNα (Figure 28B) were significantly higher when Oct-6 (or Oct-1) was overexpressed. Expression levels of IFNβ 48 hours after transfection were approximately 10- to 100-fold higher upon overexpression of Oct-6 than after transfection of the control plasmids (Figure 28A). Thus, we conclude that in addition to the PRR-mediated induction of type I IFNs, which is also observed with the control plasmids, an Oct-6- (also Oct-1-) specific effect leads to the continued high-level expression of type I IFNs.

No differences between transfection of Oct-6/Oct-1 overexpression and control plasmids were observed for Egr2 and Pmp22 expression 36 and 48 hours after transfection (Figures 28C, D). Egr2 expression levels were slightly (about 2-fold) reduced 24 hours after transfection. However, the effects

of transfection observed were independent of Oct-6. Expression levels of iNOS could not be determined, because the respective mRNA could not be reliably detected in pMEFs (all Ct>33).

Figure 28 – continued on the following page.

(A)

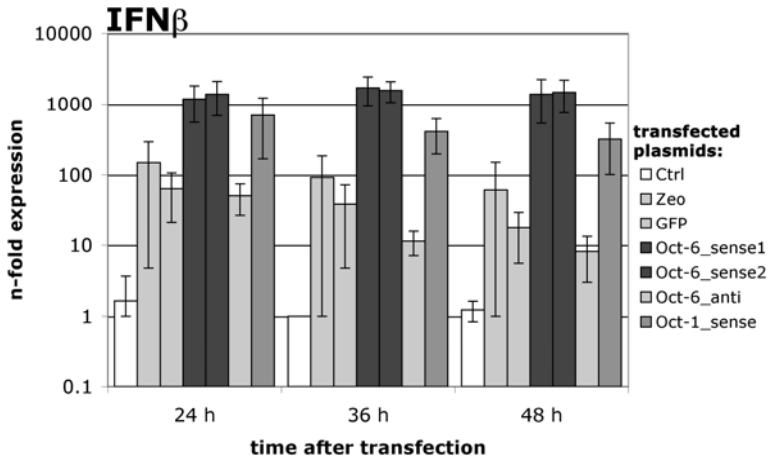

(B)

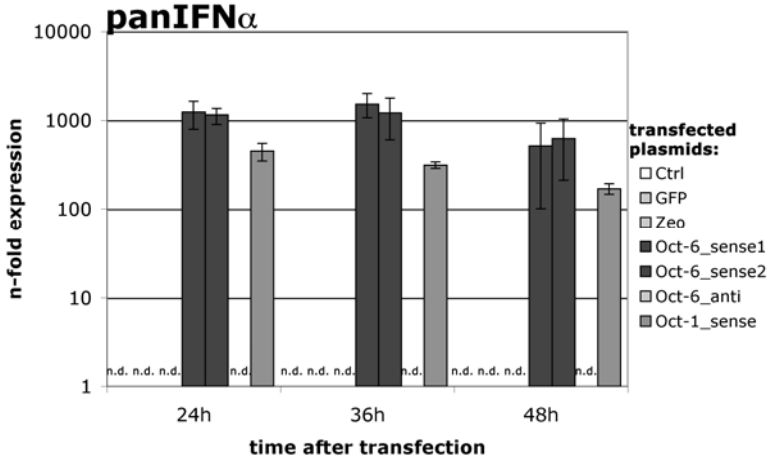

(C)

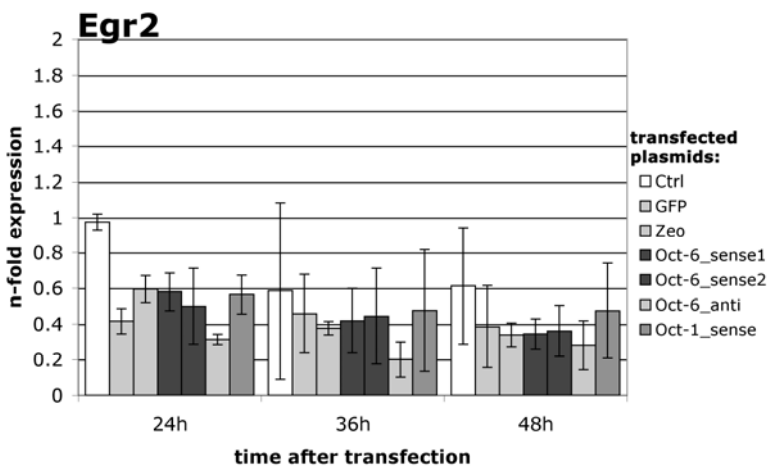

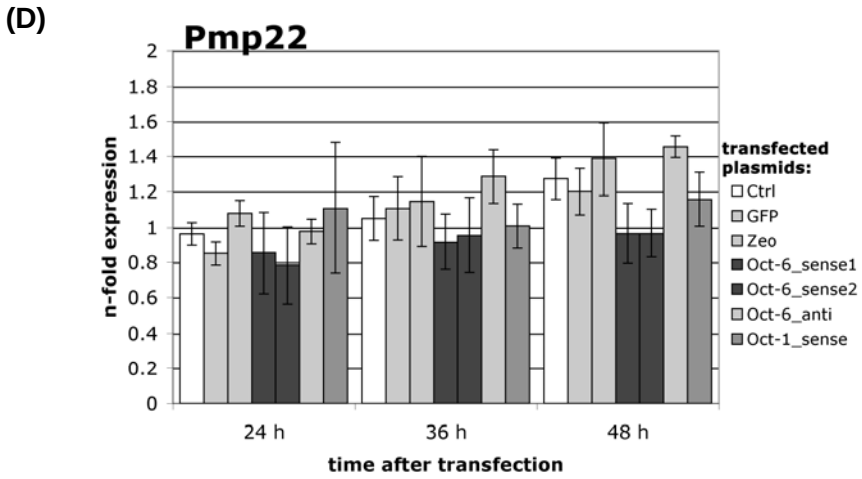

Figure 28: Expression levels of IFNβ and panIFNα but not of Egr2 and Pmp22 are strongly enhanced by the overexpression of Oct-6. WT pMEFs were transfected with empty vector (pEFZeo), enhanced-GFP expression vector (GFP), 2 different plasmids for Oct-6 expression (Oct6_sense1/2), a plasmid containing Oct-6 cDNA in antisense direction (Oct6_anti), and a plasmid for Oct-1 expression (Oct1_sense). As a control untransfected cells (Ctrl) were analysed. mRNA levels of **(A)** IFNβ, **(B)** panIFNα, **(C)** Egr2 and **(D)** Pmp22 were determined by RT-qPCR at 24, 36, and 48 h after transfection. N-fold expression values were calculated relative to the untransfected control (Ctrl_24h=1) using the standard curve method with Ube2d2 as endogenous control. PanIFNα could not be detected in untransfected cells, therefore the n-fold expression levels were just normalised to the endogenous control, thus reflecting panIFNα mRNA levels in relation to the endogenous control gene (mean values ± SD from 3 independent experiments).

Candidate target gene expression in Oct-6-deficient fibroblasts after DNA transfection

In order to analyse the impact of endogenous Oct-6 on candidate target gene expression, WT and Oct-6-deficient pMEFs were transfected with the GFP-plasmid and gene expression was analysed 3, 8 and 24 hours after transfection. As expected, expression of IFNβ and panIFNα were strongly induced in response to GFP plasmid transfection (Figure 29A, B). This induction was transient and peaked at 3 hours after transfection. In contrast to the data shown before (Figure 28A, B), type I IFN expression was almost back to basal levels at 24 hours after transfection in these experiments, which is most likely due to the different genetic background of the cells. Whereas for the overexpression experiments WT cells with C57BL/6 background were used, the WT (Oct-6+/+) and Oct-6-deficient cells here are of mixed genetic background. However, absence of Oct-6 did not have any impact on IFNα/β expression.

In WT pMEFs, Egr2 mRNA expression was about 2-fold increased at 3 hours and about 2-fold decreased at 24 hours post transfection (Figure 26C and Figure 29C). Expression levels of Pmp22 mRNA were transiently reduced at 8 hours (Figure 29D) and back to the untreated level at 24 hours post transfection (Figure 29D and Figure 28D). In both cases, the observed effects were independent of Oct-6. Similarly, no effect of Oct-6 on the expression of IFNβ, panIFNα, Egr2 and Pmp22 could be observed in preliminary experiments using poly(I:C) instead of DNA transfection and in response to MCMV infection (Figures App. 3-5).

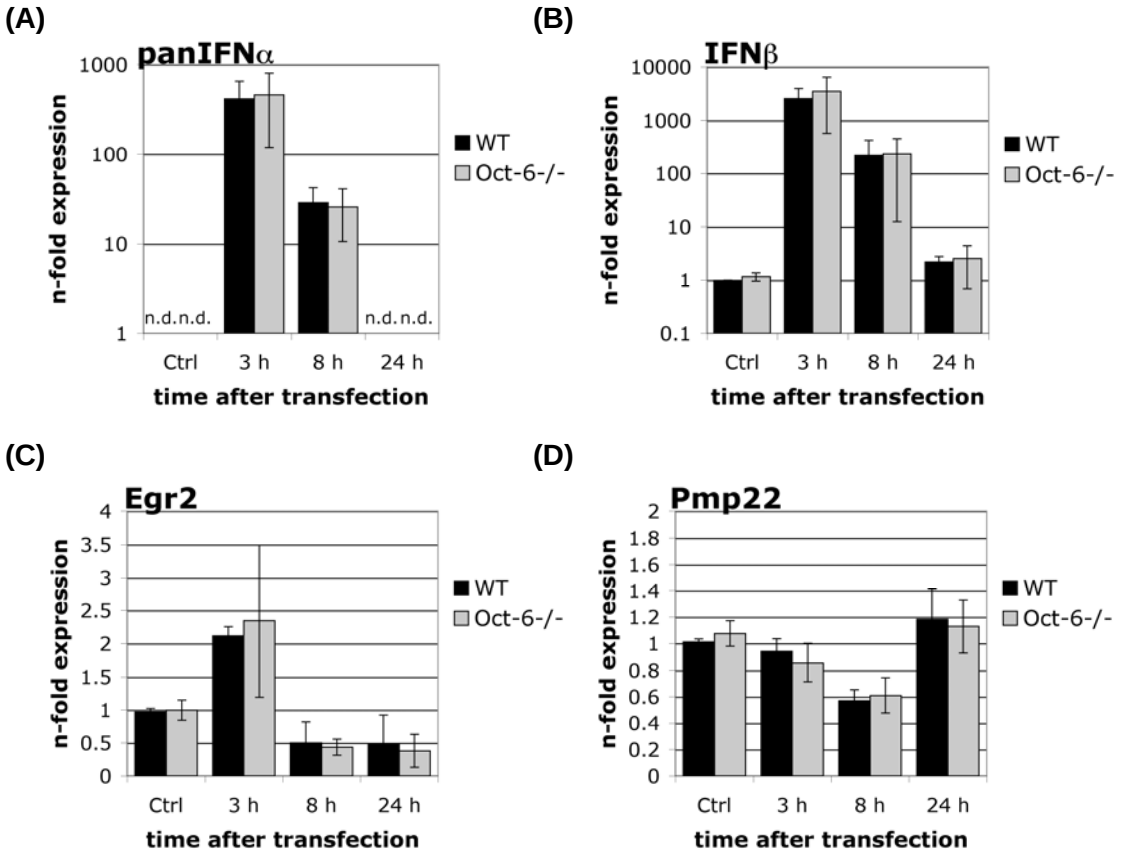

Figure 29: Absence of Oct-6 does not influence the expression patterns of panIFNα, IFNβ, Egr2 and Pmp22 upon GFP transfection in pMEFs. WT and Oct-6-deficient (Oct-6-/-) pMEFs were transfected with enhanced-GFP expression vector (GFP) or were left untransfected (Ctrl). mRNA levels of **(A)** panIFNα, **(B)** IFNβ, **(C)** Egr2 and **(D)** Pmp22 were determined by RT-qPCR at 3, 8, and 24 hours after transfection. N-fold expression values were calculated relative to untransfected WT cells (WT_Ctrl=1) using the standard curve method with Ube2d2 as endogenous control. PanIFNα was not detectable at basal levels, n-fold expression levels were calculated as described in Figure 25 (mean values ± SD from 3 independent experiments).

Candidate target gene expression in Oct-6-deficient macrophages after poly(I:C) treatment

Since a stronger induction of Oct-6 DNA-binding activity in response to type I IFN (Figure 20) and poly(I:C) (Figure 23A) treatment has been observed, loss-of-function experiments were also performed in macrophages. WT and Oct-6-deficient FLMs were treated with poly(I:C) for 8 hours and candidate target gene expression was analysed. IFNβ, panIFNα and iNOS were strongly induced in response to poly(I:C) treatment in FLMs (Figure 30A-C). Egr2 and Pmp22 expression was reduced about 2-fold after poly(I:C) treatment (Figure 30D, E). However, none of the observed effects was dependent on the presence of Oct-6. In addition, preliminary experiments revealed no role for Oct-6 for the expression of these 5 genes in FLMs after longer poly(I:C) treatment, with or without IFNβ or IFNγ pretreatment (Figures App. 6-12).

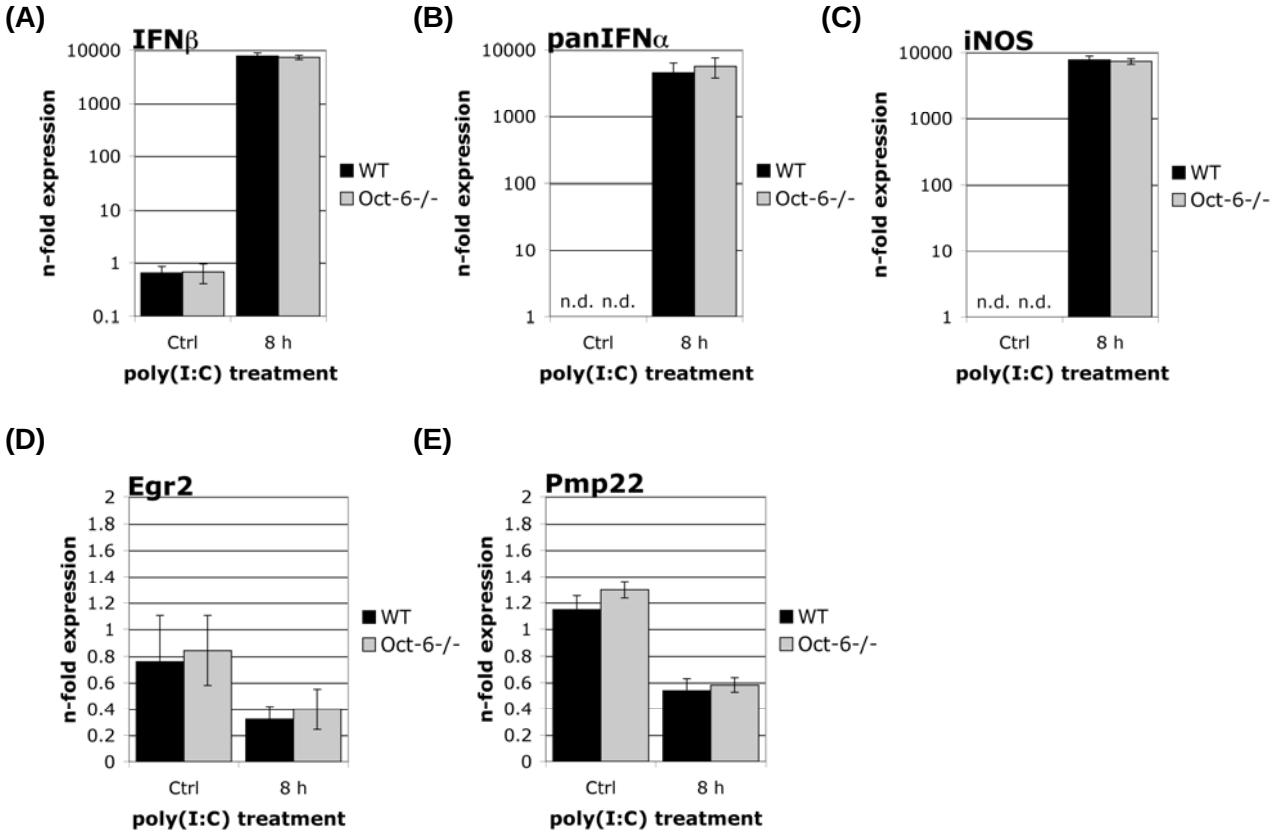

Figure 30: Absence of Oct-6 does not influence the expression of IFNβ, panIFNα, iNOS, Egr2 and Pmp22 in FLMs after poly(I:C) treatment. WT and Oct-6-deficient (Oct-6-/-) FLMs were treated with poly(I:C) (50 µg/ml) for 8 hours or were left untreated (Ctrl). Gene expression of **(A)** IFNβ, **(B)** panIFNα, **(C)** iNOS, **(D)** Egr2 and **(E)** Pmp22 was determined by RT-qPCR. N-fold expression values were calculated relative to the untreated WT cells (WT_Ctrl = 1) using the standard curve method with Ube2d2 as endogenous control. Basal levels for panIFNα and iNOS could not be detected, n-fold expression levels were calculated as described in Figure 25 (mean values ± SD from 3 experiments).

MCMV replication in Oct-6-deficient macrophages

MCMV infection strongly induced Oct-6 expression and DNA-binding activity in macrophages (Figure 23B). In order to investigate the role of Oct-6 also in a more complex cellular readout than the analysis of candidate target gene expression, MCMV replication was analysed comparing WT and Oct-6-deficient FLMs. As already reported for BMMs (Strobl *et al.*, 2005), FLMs were quite resistant to MCMV infection with an increase in viral titres of about 2 logs after 6 days of infection at an MOI of 1 (Figure 31). No differences in viral titres were observed between WT and Oct-6-deficient FLMs. Similarly, no difference was found using an MOI of 0.1 (Figure App. 15).

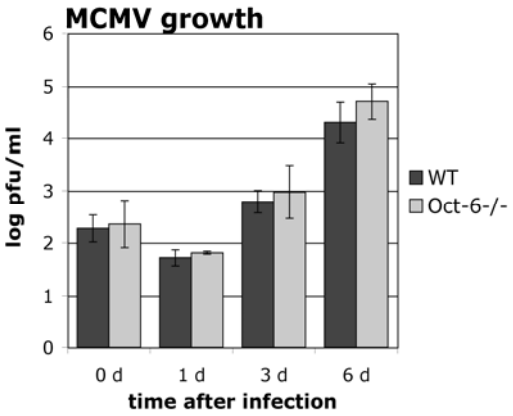

Figure 31: The absence of Oct-6 does not influence MCMV replication rates in FLMs. WT and Oct-6-deficient FLMs were infected with MCMV at an MOI of 1. Supernatants were taken at 1 hour (0 d), 1, 3 and 6 days (d) after infection. Virus titres were determined by plaque forming assays with Stat1-deficient MEFs. Mean values ± SD of 4 independent experiments are shown.

In summary, absence of endogenous Oct-6 had no influence on panIFNα and IFNβ expression in any of the experiments described above, although a striking effect of Oct-6 overexpression on the expression of type I IFNs had been observed. Expression levels of Egr2 and Pmp22, two genes regulated by Oct-6 during Schwann cell development, were not influenced by either overexpression or absence of Oct-6. In addition, endogenous Oct-6 had no detectable impact on MCMV replication.

Microarray analysis: WT versus Oct-6-deficient macrophages after poly(I:C) treatment

In search for potential target genes of Oct-6 a whole genome microarray experiment was performed. In 3 independent experiments WT and Oct-6-deficient FLMs were treated with poly(I:C) for 8 hours. An external institution (Dr. Christian Gülly, Core Facility of Molecular Biology, Centre for Medical Research, Medical University of Graz) was appointed to run and analyse the microarrays (Applied Biosystems, ABI 1700 mouse whole genome microarrays). Poly(I:C) treatment of WT FLMs had a dramatic impact on the transcriptome with approximately 3500 genes (out of 12220 genes included in the analysis) significantly regulated ($p<0.05$; minimal fold change upon treatment of 2; Figure 32). About one third of the 4000 genes were upregulated and the rest of the genes was downregulated.

According to the Gene Ontology (GO) annotation (GeneSpring Expression Analysis 7.3.1 tool, Agilent Technologies), genes involved in immune responses and cell death were significantly enriched in the set of genes up-regulated in response to poly(I:C) treatment (table App. 1). In the set of genes down-regulated in response to poly(I:C) treatment, genes involved in metabolism and cell cycle progression were significantly enriched (table App. 2).

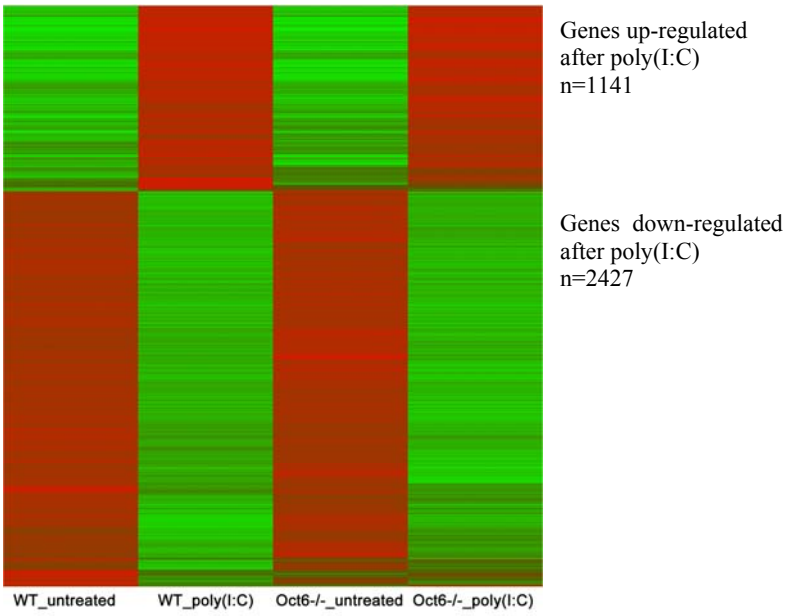

Figure 32: Poly(I:C) treatment has a strong impact on the macrophage transcriptome. Expression patterns of WT and Oct-6-deficient FLMs treated with poly(I:C) (50 µg/ml for 8 hours; 3 independent experiments) are illustrated by heatmaps. Significant differences in gene expression (minimum 2-fold, $p<0.05$; analysed with GeneSpring Expression Analysis tool, 7.3.1, Applied Biosystems) are shown.

A subset of genes (201 genes; tables App. 3, 4) was found to be more than 2-fold differentially expressed between WT and Oct-6-deficient macrophages after poly(I:C) treatment ($p<0.05$). About two thirds of the differentially expressed genes were reduced (125 genes; table App. 3), whereas enhanced gene expression was observed for 86 genes (table App. 4) in Oct-6-deficient FLMs as compared to WT cells. Oct-6 was still detectable in Oct-6-deficient cells, but expression levels were about 5-fold reduced (table 9) as compared to WT cells. Oct-6 deficiency results from a targeted disruption of the DNA-binding domain by insertion of a lacZ/Neo-cassette (Jaegle *et al.*, 1996). A bicistronic mRNA is produced from the targeted locus, which was obviously detected by the Oct-6 microarray probe.

Functional annotation and clustering of the differentially regulated genes was performed using the Gene Functional Classification tool of the database for annotation, visualization and integrated discovery (DAVID; http://david.abcc.ncifcrf.gov/; Dennis *et al.*, 2003; Huang *et al.*, 2008). Of the 201 genes about half (n=97) could be grouped into classes/pathways (table 9). The largest group was "Regulation of transcription" containing 16 genes, most of them down-regulated in the absence of Oct-6, such as Gtf2f2, Egr3, Btg1 and a number of zinc finger proteins. A related category "RNA splicing" contained 3 genes, Sfrs14, Lsm10 and Sf3a1, all of which showed reduced expression in the absence of Oct-6. Another category "Ubiquitin cycle" contained 6 genes, half of which were up-, half downregulated. However, analyses for pathway enrichment could not be performed, because the number of differentially regulated genes was too low as opposed to the vast amount of potential GO-categories and did not yield any significant result. However, we found that Oct-6 exerts positive and

negative regulatory functions on the transcriptional responses to poly(I:C), and it is involved in regulation of a number of different pathways.

Table 9: Genes differentially regulated between WT and Oct-6-deficient FLMs after poly(I:C) treatment grouped according to GO annotation (table continued on the following pages).

Probe ID	FC	*p-value*	Gene Symbol	RefSeq	Description
Regulation of transcription (GO-BP GO:0045449)					
466313	0.3	*0.0173*	**Pou3f1**	NM_011141.1	POU domain, class 3, transcription factor 1
876633	0.3	*0.0075*	**Ctnnd2**	NM_008729.1	catenin (cadherin associated protein), delta 2
834086	0.3	*0.0044*	**Rcor3**	NM_144814.2	REST corepressor 3
515044	0.3	*0.0101*	**Zfp691**	NM_183140.1	zinc finger protein 691
452181	0.3	*0.0433*	**Zmiz1**	NM_175264.2	zinc finger, MIZ-type containing 1
553608	0.3	*0.0014*	**Gtf2f2**	NM_026816.3	general transcription factor IIF, polypeptide 2
315360	0.3	*0.0201*	**Zfp775**	NM_173429.1	zinc finger protein 775
784635	0.3	*0.0077*	**9630041N07Rik**	NM_173387.1	RIKEN cDNA 9630041N07 gene
339824	0.4	*0.0122*	**Egr3**	NM_018781.1	early growth response 3
360325	0.4	*0.0182*	**Foxk2**	NM_001080932.2	forkhead box K2
675560	0.4	*0.0480*	**Zfp414**	NM_026712.1	zinc finger protein 414
883636	0.5	*0.0356*	**Btg1**	NM_007569.2	B-cell translocation gene 1, anti-proliferative
388184	2.3	*0.0176*	**8430426H19Rik**	NM_178875.4	RIKEN cDNA 8430426H19 gene
674148	2.9	*0.0017*	**Snx13**	NM_001014973.2	sorting nexin 13
576988	3.2	*0.0208*	**2810021J22Rik**	NM_172403.2	RIKEN cDNA 2810021J22 gene
906799	3.3	*0.0034*	**E4f1**	NM_007893.1	E4F transcription factor 1
RNA splicing (GO-BP GO:0008380)					
466728	0.4	*0.0481*	**Sfrs14**	NM_172755.2	splicing factor, arginine/serine-rich 14
782547	0.4	*0.00236*	**Lsm10**	NM_138721.1	U7 snRNP-specific Sm-like protein LSM10
685184	0.5	*0.00992*	**Sf3a1**	NM_026175.5	splicing factor 3a, subunit 1
Telomere organization and biogenesis (GO-BP GO:0032200)					
687306	0.3	*0.00876*	**Terc**	NR_001579.1	telomerase RNA component
705683	3.1	*0.00343*	**Pot1b**	NM_028370.1	protection of telomeres 1B
Regulation of Ras protein signal transduction (GO-BP GO:0046578)					
509621	0.4	*0.0077*	**Arhgef11**	NM_001003912.1	Rho guanine nucleotide exchange factor (GEF) 11

Probe ID	FC	*p-value*	Gene Symbol	RefSeq	Description
600711	0.4	*0.0249*	**Tbc1d16**	NM_172443.2	TBC1 domain family, member 16
603800	0.4	*0.0456*	**Arhgef16**	NM_001112744.1	Rho guanine nucleotide exchange factor (GEF) 16
832842	2.6	*0.0206*	**Arhgef4**	NM_183019.2	Rho guanine nucleotide exchange factor 4
G-protein coupled receptor protein signaling pathway (GO-BP GO:0007186)					
461332	0.3	*0.016*	**Olfr1410**	NM_146491.1	olfactory receptor 1410
498376	0.3	*0.0336*	**Olfr982**	NM_146854.1	olfactory receptor 982
538641	0.3	*0.0485*	**Oprd1**	NM_013622.2	opioid receptor, delta 1
900911	0.4	*0.015*	**Olfr1425|Olfr1426**	NM_001011853.1	olfactory receptor 1425|olfactory receptor 1426
371452	0.4	*0.0219*	**Olfr167**	NM_146935.1	olfactory receptor 167
405218	0.4	*0.0321*	**Cysltr2**	NM_133720.1	cysteinyl leukotriene receptor 2
302319	0.4	*0.0143*	**Pcsk1n**	NM_013892.2	proprotein convertase subtilisin/kexin type 1 inhibitor
576856	0.4	*0.0138*	**Olfr1013**	NM_146762.1	olfactory receptor 1013
498112	2.3	*0.0316*	**Cacnb4**	NM_146123.1	calcium channel, voltage-dependent, beta 4 subunit
895890	2.5	*0.00311*	**Olfr598|Olfr597**	NM_001011845.1	olfactory receptor 598|olfactory receptor 597
496110	2.5	*0.0169*	**Olfr310**	NM_001011520.1	olfactory receptor 310
388075	2.8	*0.0427*	**Adra2a**	NM_007417.4	adrenergic receptor. alpha 2a
Monovalent inorganic cation transport (GO-BP GO:0015672)					
455948	0.5	*0.0299*	**Kcnj2**	NM_008425.2	potassium inwardly-rectifying channel, subfamily J, member 2
620798	0.5	*0.0405*	**Catsper3**	NM_029772.1	cation channel, sperm associated 3
554608	0.5	*0.0392*	**Slc8a1**	NM_011406.2	solute carrier family 8 (sodium/calcium exchanger), member 1
Vitamin B6 biosynthetic process (GO-BP GO:0042819)					
480631	0.5	*0.0473*	**Pdxk**	NM_172134.1	pyridoxal (pyridoxine, vitamin B6) kinase
533138	2.9	*0.0472*	**Pnpo**	NM_134021.1	pyridoxine 5'-phosphate oxidase
Ubiquitin cycle (GO-BP GO:0006512)					
628730	0.3	*0.0383*	**Rnf41**	NM_026259.2	ring finger protein 41
643747	0.4	*0.0294*	**Klhl12**	NM_153128.1	kelch-like 12 (Drosophila)
665024	0.5	*0.0434*	**Znrf4**	NM_011483.1	zinc and ring finger 4
381530	2.5	*0.0337*	**Senp5**	NM_177103.4	SUMO/sentrin specific peptidase 5
363922	2.9	*0.0324*	**Yod1**	NM_178691.2	YOD1 OTU deubiquitinating enzyme 1 homologue (S. cerevisiae)NA 9930028C20 gene
308725	4.2	*0.0152*	**Senp8**	NM_027838.2	SUMO/sentrin specific peptidase 8

Probe ID	FC	*p-value*	Gene Symbol	RefSeq	Description
Protein palmitoylation (GO-BP GO:0018345)					
617536	0.2	*0.0124*	**Zdhhc3**	NM_026917.4	zinc finger, DHHC domain containing 3
437482	0.4	*0.0111*	**Zdhhc17**	NM_172554.1	zinc finger, DHHC domain containing 17
Protein kinase activity (GO-MF GO:0004672)					
922907	0.3	*0.0156*	**Map3k12**	NM_009582.2	mitogen activated protein kinase kinase kinase 12
467664	0.3	*0.0256*	**Epha10**	NM_177671.2	Eph receptor A10
851957	0.4	*0.00638*	**Stk40**	NM_028800.2	serine/threonine kinase 40
627826	2.3	*0.0465*	**Prkci**	NM_008857.2	protein kinase C, iota
530372	2.4	*0.0141*	**Epha4**	NM_007936.2	Eph receptor A4
837461	2.4	*0.0336*	**Wnk1**	NM_198703.1	WNK lysine deficient protein kinase 1
357720	2.9	*0.0036*	**Phka1**	NM_008832.2	phosphorylase kinase alpha 1 isoform 1
926998	3.3	*0.00111*	**Rab38**	NM_028238.5	Rab38, member of RAS oncogene family
464717	4.6	*0.00766*	**Dyrk1b**	NM_010092.1	dual-specificity tyrosine-(Y)-phosphorylation regulated kinase 1b
N-methyltransferase activity (GO-MF GO:000817)					
642032	2.9	*0.0374*	**1190005F20Rik**	NM_026876.3	RIKEN cDNA 1190005F20 gene
375317	3.3	*0.0017*	**Setmar**	NM_178391.2	SET domain and mariner transposase fusion gene
Zinc ion binding (GO-MF GO:0008270)					
632096	0.4	*0.0318*	**4933422H20Rik**	NM_001033775.3	RIKEN cDNA 4933422H20 gene
789662	0.4	*0.0232*	**2610507B11Rik**	NM_001002004.1	RIKEN cDNA 2610507B11 gene
871506	0.4	*0.0258*	**Gne**	NM_015828.2	glucosamine
325670	0.4	*0.0463*	**Zfp11**	NM_172462.1	zinc finger protein 11
594289	2.1	*0.0157*	**AU017455**	NM_001033215.2	EST AU017455
375461	2.4	*0.00775*	**2010315B03Rik**	XM_001472446.1	RIKEN cDNA 2010315B03 gene
887858	2.4	*0.00669*	**Ppp1r10**	NM_175934.2	protein phosphatase 1, regulatory subunit 10
721573	2.8	*0.00086*	**Mpi**	NM_025837.2	mannose phosphate isomerase
ATPase activity (GO-MF GO:0016887)					
409901	0.5	*0.0299*	**Vps4b**	NM_009190.2	vacuolar protein sorting 4b (yeast)
807992	2.2	*0.0411*	**Ddx27**	NM_153065.1	DEAD (Asp-Glu-Ala-Asp) box polypeptide 27
556097	2.4	*0.0238*	**Abcd4**	NM_008992.1	ATP-binding cassette, sub-family D (ALD), member 4
Mitochondrion (GO-CC GO:0005739)					

Probe ID	FC	*p-value*	Gene Symbol	RefSeq	Description
331903	0.4	*0.0179*	**4931431F19Rik**	XM_133663.5	RIKEN cDNA 4931431F19 gene
606179	0.4	*0.00383*	**Pars2**	NM_172272.1	prolyl-tRNA synthetase (mitochondrial)(putative)
892845	0.4	*0.0327*	**Slc25a36**	NM_138756.2	solute carrier family 25, member 36
663810	0.4	*0.019*	**Papd1**	NM_026157.1	PAP associated domain containing 1
770438	0.5	*0.0418*	**Slc25a23**	NM_025877.2	solute carrier family 25 (mitochondrial carrier; phosphate carrier), member 23
744134	2.1	*0.017*	**Timm9**	NM_001024853.1	translocase of inner mitochondrial membrane 9 homolog (yeast)
626456	2.4	*0.00167*	**Grpel1**	NM_024478.2	GrpE-like 1, mitochondrial
Endoplasmatic reticulum (GO-CC GO:0005783)					
460096	0.2	*0.0295*	**Caml**	NM_007596.2	calcium modulating ligand
731197	0.3	*0.00332*	**Rcn3**	NM_026555.1	reticulocalbin 3, EF-hand calcium binding domain
670264	0.4	*0.0403*	**Arsg**	NM_028710.2	arylsulfatase G
720766	2.4	*0.0126*	**Duoxa2**	NM_025777.1	dual oxidase maturation factor 2
Integral to membrane (GO-CC GO:0016021)					
608851	0.2	*0.0386*	**Tspan31**	NM_025982.4	tetraspanin 31
360339	0.3	*0.0464*	**Klra2**	NM_008462.4	killer cell lectin-like receptor, subfamily A. member 2
852764	0.4	*0.0497*	**Flrt3**	NM_178382.2	fibronectin leucine rich transmembrane protein 3
925399	0.4	*0.0239*	**Lect1**	NM_010701.1	leukocyte cell derived chemotaxin 1
412730	0.4	*0.0323*	**Tmem86b**	NM_023440.2	transmembrane protein 86B
552370	0.4	*0.0162*	**Tmem183a**	NM_020588.2	transmembrane protein 183A
365471	0.4	*0.00268*	**Col13a1**	NM_007731.1	procollagen, type XIII, alpha 1
564703	0.5	*0.00496*	**Cmtm7**	NM_133978.1	CKLF-like MARVEL transmembrane domain containing 7
828936	0.5	*0.0143*	**E030010A14Rik**	NM_183160.1	RIKEN cDNA E030010A14 gene
754664	2.4	*0.0201*	**Tnfrsf17**	NM_011608.1	tumor necrosis factor receptor superfamily, member 17
513587	2.5	*0.0386*	**Cd276**	NM_133983.2	CD276 antigen
440799	2.7	*0.0451*	**Slc2a1**	NM_011400.1	solute carrier family 2 (facilitated glucose transporter), member 1
760102	3.4	*0.0295*	**Sdc1**	NM_011519.1	syndecan 1
779189	4.0	*0.0169*	**Tmem104**	NM_001033393.1	transmembrane protein 104

97 genes that could be grouped by functional annotation using DAVID bioinformatics ressources; FC: fold change between WT and Oct-6-deficient FLMs after poly(I:C) treatment; within groups sorted by FC; GO-BP: GO biological process; GO-MF: GO molecular function; GO-CC: GO cellular compartment.

Validation of microarray data

Out of the differentially expressed genes, 7 candidate genes (Dapp1, Dyrk1b, E4f1, Lsm10, Map3k12, Stk40, and Zdhhc3) were selected for validation by RT-qPCR. The selection was based on the significance of the fold-difference between the 2 genotypes after poly(I:C) treatment, on the amplitude of the difference, on the amplitude of the induction/reduction of gene expression in the WT and, finally, on the biological function of the respective gene product (table App. 5).

The gene expression differences between WT and Oct-6-deficient FLMs could be verified for 2 genes, namely U7 snRNP-specific Sm-like protein LSM10 (Lsm10) and serine/threonine kinase 40 (Stk40). The expression level of Lsm10 in WT cells was not significantly changed in response to poly(I:C) treatment, whereas in the absence of Oct-6 the expression was reduced by approximately 2-fold (Figure 33A). Stk40 was induced about 7-fold upon poly(I:C) treatment in WT cells, whereas the induction in the absence of Oct-6 was only 3-fold (Figure 33B). For Lsm10 as well as for Stk40 the qPCR data showed high correlation with the microarray data (Figure 33C).

(A) **(B)**

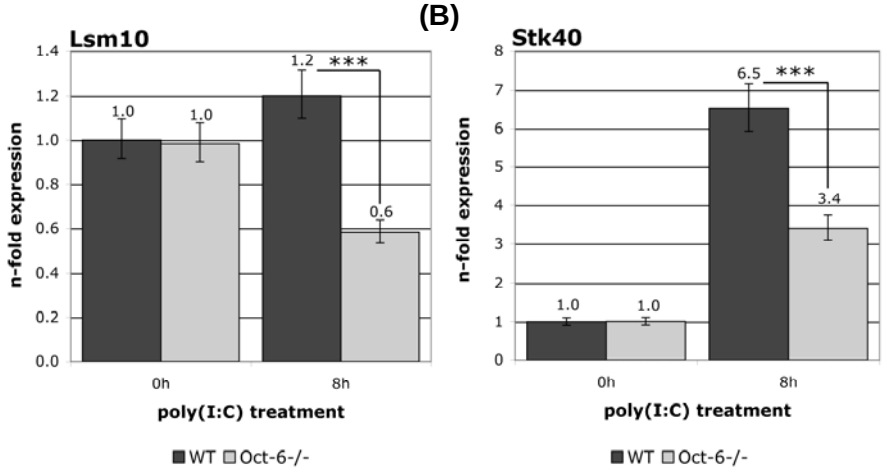

(C)

gene symbol (gene name)	probe_ID RefSeq	WT inducibility (mean ± SD)	Oct6-/- *vs.* WT after poly(I:C) (mean ± SD)	*P-value* for Oct6-/- *vs.* WT after poly(I:C)
Lsm10 (U7 snRNP-specific Sm-like protein LSM10)	782547 NM_138721.1	1.7 ± 0.3	0.40 ± 0.107	*0.0024*
Stk40 (serine/threonine kinase 40)	851957 NM_028800.2	9.6 ± 5.8	0.45 ± 0.094	*0.0064*

Figure 33: Stk40 and Lsm10 are differentially expressed between WT and Oct-6-deficient FLMs after poly(I:C) treatment. WT and Oct-6-deficient FLMs were treated with poly(I:C) (50 µg/ml) for 8 hours, or were left untreated (0h). N-fold expression levels of **(A)** Lsm10 and **(B)** Stk40 relative to untreated WT cells (WT_0h = 1) were determined by RT-qPCR, applying the standard curve method and normalising to Ube2d2 (mean values ± SE of 6 independent experiments are shown; ***, $p<0.001$). **(C)** Microarray data for Lsm10 and Stk40.

For the 5 additional genes tested, the differential expression patterns seen in the microarray could not be reproduced by RT-qPCR (Figures App. 19). A possible reason is that the qPCR assays were not positioned in the same region like the microarray probes. The microarray probes were mostly positioned in the 3' region of the mRNA, for Dyrk1b 2 isoforms differing in the 3' region are known (NCBI, GenBank), for Map3k12 alternative splice variants are described, differing in the 5' part of the mRNA. No differential isoforms are known for Dapp1, E4f1 and Zdhhc3. Differential expression seen in the microarray might still be true for alternative splice forms of the respective gene (Morey *et al.*, 2006).

DISCUSSION

Oct-6 is a transcription factor, which is mainly involved in Schwann cell development (Jaegle *et al.*, 1996; Bermingham *et al.*, 1996), but which has not been related to immunity yet. We found that IFNβ, and to a lesser extent IFNγ, induce expression of Oct-6 in fibroblasts and macrophages, with the expression/DNA-binding activity of Oct-6 being generally stronger in macrophages. Oct-6 expression was not only induced by exogenous IFN, but also in response to poly(I:C) treatment and viral infections. Since this induction of Oct-6 is abolished in the absence of Ifnar1, we conclude that it is dependent on auto-/paracrine type I IFN signalling. Oct-6 expression in response to poly(I:C) treatment or MCMV infection was strongly reduced in IFNβ-deficient macrophages indicating that it is mainly IFNβ that mediates the auto-/paracrine effects. Since Oct-6 expression is completely abolished in Ifnar1-deficient cells, but residual Oct-6 expression is still observed in the absence of IFNβ, we conclude that also IFNαs can contribute to the induction of Oct-6.

With respect to the mechanism of induction, we could show that it is the canonical Jak/Stat signalling pathway which is mediating Oct-6 expression in response to type I IFN, as Oct-6 induction is largely dependent on Stat1, and partially dependent on Tyk2. Irf1, induced by Stat1 after IFN treatment, is known to be required for the expression of a subset of IFN-responsive genes (Honda and Taniguchi, 2006). Involvement of Irf1 in Oct-6 regulation was excluded, as absence of Irf1 had no impact on Oct-6 expression. Therefore we assumed direct involvement of Stat1 in Oct-6 regulation. Notably, strongly delayed and weak Oct-6 expression was observed in the absence of Stat1, arguing for additional IFN activated pathways that also induce low levels of Oct-6. Using ChIP technology, we identified a Stat1-binding region approximately 500 bp upstream of the Oct-6 transcription start site. Two almost perfect GAS and one imperfect ISRE site were predicted within this region. However, at present we cannot tell which Stat1-containing complex binds to which of the predicted elements, i.e. a Stat1/Stat2/Irf9 complex (ISGF3) to the imperfect ISRE site, Stat1/Stat1 homodimers and/or Stat1/Stat3 heterodimers to one or both GAS motifs. Experiments using Stat2- (Park *et al.*, 2000) and/or Irf9-deficient (Kimura *et al.*, 1996) cells would answer the question whether ISGF3 binding to the ISRE is required for regulating Oct-6 expression. Deletion/mutation analyses in reporter gene construct-based systems would be necessary to characterise the exact binding sites. So far, we cannot exclude that other Stat1 binding sites (ISRE and/or GAS motifs) further up- or downstream are also involved in regulation of Oct-6 expression. The question to which extent Stat3 contributes to the regulation of Oct-6 could be addressed by studying Stat3-deficient cells (Alonzi *et al.*, 2001). Oct-6 induction in response to IFNs, *via* the Jak/Stat signalling pathway is a completely novel mechanism for regulating expression of Oct-6. Oct-6 regulation has been characterised best in Schwann cells, where a Schwann cell specific enhancer element located about 12 kb downstream of the Oct-6 transcription start site is solely responsible for correctly timed expression of Oct-6 (Mandemakers *et*

al., 2000). The signals and transcription factors that input on this enhancer element are less well defined. Axonal contact is the major prerequisite, cAMP signalling and activation of NFκB are also involved (Svaren and Meijer, 2008; Birchmeier and Nave, 2008). Only recently, a G-protein coupled receptor family member, Gpr126, was found to be involved in the induction of Oct-6 *via* elevating cAMP levels in zebrafish (Monk *et al.*, 2009). However, ligands, additional receptors and signalling molecules remain to be elucidated. Thus, cytokine- (i.e. IFN-) induced Oct-6 expression in fibroblasts and macrophages is a novel finding and is clearly different from the mechanism responsible for the differentiation-triggered induction of Oct-6 during Schwann cell development.

We could further show that Oct-6 protein induced in response to IFNβ or poly(I:C) treatment localises to the nucleus. Oct-6 contains both, a nuclear localisation and a nuclear export signal, which are located in the POU homeodomain (Baranek *et al.*, 2005). So far, no post-translational modifications have been observed that would impact on Oct-6 localisation and/or transcriptional activity, but it has been hypothesised that regulating the subcellular localisation of Oct-6 can control its transcriptional activity (Baranek *et al.*, 2005). The finding that Oct-6 protein localises to the nucleus of macrophages after IFNβ and poly(I:C) treatment, prompted us to search for target genes, and therefore for the role of Oct-6 in the context of innate immune responses.

Some other POU-transcription factor family members, i.e. Oct-1, Oct-2 or Brn-3a/b, are known to be involved in the regulation of immunity-related genes, such as IFNαs (Mesplède *et al.*, 2005), IFNβ (Haggarty *et al.*, 1991; Du and Maniatis, 1992) and iNOS (Kleinert *et al.*, 2004). Based on the fact that all POU-proteins show similar binding characteristics (Herr and Cleary, 1995), we asked whether these genes are also targets of Oct-6. We further tested whether Egr2 and Pmp22, two genes known to be regulated by Oct-6 during Schwann cell development (Ghazvini *et al.*, 2002; Ryu *et al.*, 2007), are also Oct-6-responsive in fibroblasts and macrophages. Expression of these five candidate target genes was analysed under conditions when Oct-6 was either overexpressed or deleted, i.e. in gain- and loss-of-function studies, respectively. In addition to this candidate target gene approach, a whole genome microarray experiment comparing WT and Oct-6-deficient cells in response to poly(I:C) treatment was performed to more globally search for Oct-6 target genes in the setting of an innate immune response.

When overexpressing Oct-6 and also Oct-1, we found prolonged high-level expression of IFNβ and IFNαs (all subtypes) in contrast to a transient induction of type I IFNs after transfection of control plasmids. This might be due to a direct effect of Oct-6/Oct-1 by their binding to octamer motifs within the regulatory elements of murine IFNα/β genes (Mesplède *et al.*, 2005; Haggarty *et al.*, 1991; Du and Maniatis, 1992). In line with this, we could show weak binding of Oct-6, Oct-1 and Oct-2 to an oligonucleotide probe covering the region -110 to -139 upstream of the IFNβ transcription start site – a preliminary result which needs confirmation. Alternatively, Oct-6/Oct-1 might exert an indirect effect

by either enhancing expression of genes inducing IFNα/β expression, or by repressing genes involved in the shut-off of IFNα/β expression. Our data showing that also Oct-1 had an enhancing effect on type I IFN expression are in contrast to a previous report (Mesplède *et al.*, 2005), where a repressing effect of Oct-1 on basal and virus-induced IFNα expression was observed. These contrasting results might be explained by the different experimental approaches that were followed. Oct-1 was transiently overexpressed in both studies. We analysed endogenous IFNα (all subtypes) expression, whereas Mesplède *et al.* (2005) measured luciferase activity from a co-transfected IFNα-11-specific reporter construct. With a reporter construct the genomic region tested is limited and some *cis*-regulatory elements also impacting on gene regulation might be missing. Mesplède *et al.* (2005) additionally report that in Oct-1-deficient fibroblasts IFNα (all subtypes) expression was enhanced.

In contrast to the striking results of the Oct-6 overexpression experiments, neither IFNα nor IFNβ expression patterns were altered in the absence of Oct-6 in response to DNA transfection in fibroblasts, or after poly(I:C) treatment in macrophages. The reasons for this discrepancy between overexpression and loss-of-function experiments are multiple. Expression of endogenous Oct-6 might be too low to mediate a detectable effect on IFNα/β mRNA expression. Other POU-proteins, i.e. Oct-1 in fibroblasts and Oct-1 and Oct-2 in macrophages, could interfere with or compensate potential effects of Oct-6. In order to follow that question Oct-1/Oct-2 expression could be knocked-down in fibroblasts or macrophages and then the impact of Oct-6 on IFNα/β expression could be analysed. Moreover, it has to be considered that the Oct-6 knockout is generated by the targeted disruption of the DNA-binding domain by insertion of a β-galactosidase/neomycin cassette (Jaegle *et al.*, 1996). No full-length Oct-6 protein can be produced from this mutated allele, but the presence of a truncated Oct-6 protein with residual activity cannot be formally excluded.

Overexpression of Oct-6 in fibroblasts did not have an impact on iNOS expression. Actually, iNOS mRNA could not be detected in fibroblasts in any condition tested. In macrophages, iNOS was strongly induced in response to poly(I:C), but its expression was independent of the presence of Oct-6. A conserved octamer motif is located about 50 bp upstream of the iNOS transcription start site and Oct-1, Oct-2 and Brn3a/b have activating effects on iNOS expression (Kleinert *et al.*, 2004 and references therein). It might well be that either Oct-6 is not able to bind to the iNOS promoter or that a potential effect of the absence of Oct-6 is masked by the presence of other POU-proteins.

The expression of Egr2 and Pmp22, known target genes of Oct-6 in Schwann cells, were not influenced either by overexpression or absence of Oct-6 in fibroblasts and macrophages. Additional factors cooperating with Oct-6 might be necessary to regulate expression of Schwann cell-specific genes. For example, Egr2 is known to be regulated synergistically by Oct-6 and Sox10 in Schwann cells (Svaren and Meijer, 2008) and Sox10 expression has so far not been reported in fibroblasts or

macrophages according to the publicly available gene expression profiles database BioGPS (http://biogps.gnf.org/#goto=genereport&id=6663, December, 2009; Wu *et al.*, 2009).

In order to more globally analyse the role of Oct-6 in the context of an innate immune response, a whole genome microarray experiment was performed comparing the transcriptomes of WT and Oct-6-deficient macrophages treated with poly(I:C). A subset of genes (n=200) was found to be differentially expressed after poly(I:C) treatment in the absence of Oct-6 (minimum fold change = 2; $p<0.05$). Expression levels of about two thirds of those genes were reduced, the rest showed enhanced expression in the absence of Oct-6. This is in accordance with reports in Schwann cells, where Oct-6 can also exert activating (Egr2; Ghazvini *et al.*, 2002) as well as repressing (Pmp22, Mbp, Mpz; Ryu *et al.*, 2007) functions. Functional analysis of the differentially regulated genes revealed that the genes do not belong to one specific pathway, but to a number different ones, e.g. "regulation of transcription", "mRNA splicing" or "ubiquitin cycle". In line with our RT-qPCR data showing no impact of Oct-6 on IFNα/β expression, microarray data did not reveal any differences in IFN and/or ISG expression between WT and Oct-6-deficient cells after poly(I:C) treatment.
Microarray data were validated for two genes, namely Stk40 and Lsm10. Poly(I:C) treatment resulted in an induction of Stk40 expression, which was less pronounced in the absence of Oct-6 indicating that Oct-6 is necessary to amplify the induction of Stk40 mRNA levels. To our knowledge, there are only two reports on Stk40, also known as SINK homologous serine/threonine kinase (SHIK), the first showing that overexpressed Stk40/SHIK inhibits NFκB and p53 mediated transcription (Huang *et al.*, 2003). The second, very recent report, shows that Stk40 is suppressed by another octamer-binding factor, i.e. Oct-4 (Pou5f1), in embryonic stem cells (Li *et al.*, 2010). Stk40 induces differentiation of extraembryonic endoderm *via* activation of the Erk/MAPK pathway. The impact of reduced Stk40 expression on the NFκB, p53 and Erk/MAPK pathway and consequently on the processes of innate immune responses might be an interesting topic for future studies. Lsm10 is not influenced by the treatment in WT cells, but absence of Oct-6 leads to a reduction of Lsm10 levels after poly(I:C) treatment. Thus, Oct-6 is necessary to sustain Lsm10 levels in macrophages after poly(I:C) treatment. Lsm10 encodes a protein of the U7 small nuclear ribonucleoprotein (snRNP) complex, which is involved in formation of the 3'end of canonical histone mRNAs (Schümperli and Pillai, 2004). Canonical histones are expressed in a strictly replication dependent manner and absence of components of the U7 snRNP complex leads to an arrest in G1 phase (Marzluff *et al.*, 2008). As Oct-6 regulates Lsm10 expression, it may consequently be involved in regulating cell cycle progression. Further effort is needed to validate other Oct-6 target genes and address their role in innate immunity.
Cellular POU-proteins are able to regulate transcription of a number of DNA viruses (Latchman, 1999). Oct-6, in particular, is involved in regulating expression of early and late viral gene expression of JC polyomavirus, which is assumed to be responsible for its glial-cell tropism. Oct-6 was strongly

induced in response to MCMV infection in macrophages as well as in fibroblasts (data not shown). We therefore analysed MCMV replication rates in macrophages, but no differences were observed between WT and Oct-6-deficient cells. Thus, we conclude that Oct-6 has no direct effect on MCMV replication in macrophages.

Experiments with the murine Schwann cell line SW10 demonstrated that also in Schwann cells Oct-6 expression is induced in response to IFNβ treatment. However, Oct-6 expression levels/DNA-binding activity in response to IFNβ treatment were rather low, which is probably due to the immature phenotype of this cell line (Hai *et al.*, 2002). It would be worthwhile to study the effect of IFNβ treatment on Oct-6 expression in primary Schwann cells *in vitro* and *in vivo*. *In vivo* experiments would be interesting with respect to cooperative effects of IFNβ treatment and axon-derived signals, e.g. cAMP signalling and NFκB activation (Svaren and Meijer, 2008), known to regulate Oct-6 expression. Oct-6 is also expressed in the myelinating cells of the central nervous system (CNS), the oligodendrocytes, but no effect of the absence of Oct-6 on CNS myelination was reported (Schreiber *et al.*, 1997). It is assumed that other POU-family members expressed in oligodendrocytes, i.e. Brn-1 and Brn-2, can compensate for the loss of Oct-6. However, overexpression of Oct-6 in oligodendrocytes results in a myelination defect in the CNS, indicating that missexpression or altered relative abundances of POU-family members is detrimental for correct CNS development (Jensen *et al.*, 1998). It would be interesting to analyse whether type I IFNs are able to induce expression of Oct-6 also in oligodendrocytes and what the impact on CNS myelination would be. A number of viruses are able to infect the CNS and induce demyelination in humans (e.g. JC polyomavirus, human immunodeficiency virus and measles virus) and in mice (e.g. Theiler's virus, mouse hepatits virus and Semliki forest virus) (Stohlman and Hinton, 2001). Interestingly, neurons have been shown to induce type I IFN expression in response to virus infection in the CNS (Delhaye *et al.*, 2006). In Schwann cells, Oct-6 is also strongly induced during regeneration processes resulting in remyelination after injury. Interestingly, Schwann cells are not only involved in remyelination in the PNS but also in the CNS. Schwann cells invading the CNS after demyelination (Jasmin and Ohara, 2002) or derived from progenitor cells within the CNS (Blakemore, 2005) are able to remyelinate demyelinated axons, thereby sustaining nerve integrity until they are removed by astrocytes and oligodendrocytes can take over to restore a long-lasting myelin sheath (Jasmin and Ohara, 2002). Further studies could address the role of type I IFN production and Oct-6 induction on nerve regeneration, especially in the context of virus induced neuropathologies, but also in the conext of other demyelinating diseases, the most prominent being multiple sclerosis.

SUMMARY

In summary, we have shown for the first time that ***(i)*** the POU-family transcription factor Oct-6 is induced in response to type I and type II IFNs – as opposed to the exclusively developmental context which Oct-6 has so far been related to, that ***(ii)*** this induction is dependent on canonical Jak/Stat signalling, which adds a novel facet to the regulatory elements involved in Oct-6 gene regulation, that ***(iii)*** Oct-6 is induced in fibroblasts and macrophages, cell types that have not been described before to express Oct-6, and that ***(iv)*** Oct-6 is able to modulate the transcriptional responses to poly(I:C) in macrophages. Collectively, these results reveal a novel role for Oct-6 as (co-) activator/repressor of transcription in the context of innate immunity.

REFERENCES

Akira, S., Uematsu, S., and Takeuchi, O. (2006). Pathogen recognition and innate immunity. Cell *124*, 783-801.

Alonzi, T., Maritano, D., Gorgoni, B., Rizzuto, G., Libert, C., and Poli, V. (2001). Essential role of STAT3 in the control of the acute-phase response as revealed by inducible gene inactivation [correction of activation] in the liver. Mol Cell Biol 21, 1621-1632.

Ananko, E., Kondrakhin, Y., Merkulova, T., and Kolchanov, N. (2007). Recognition of interferon-inducible sites, promoters, and enhancers. BMC Bioinformatics *8*, 56.

Andersen, B., Weinberg, W., Rennekampff, O., McEvilly, R., Bermingham, J.J., Hooshmand, F., Vasilyev, V., Hansbrough, J., Pittelkow, M., Yuspa, S., and Rosenfeld, M. (1997). Functions of the POU domain genes Skn-1a/i and Tst-1/Oct-6/SCIP in epidermal differentiation. Genes Dev *11*, 1873-1884.

Ank, N., West, H., and Paludan, S. (2006). IFN-lambda: novel antiviral cytokines. J Interferon Cytokine Res *26*, 373-379.

Arroyo, E., Bermingham, J.J., Rosenfeld, M., and Scherer, S. (1998). Promyelinating Schwann cells express Tst-1/SCIP/Oct-6. J Neurosci *18*, 7891-7902.

Asefa, B., Klarmann, K., Copeland, N., Gilbert, D., Jenkins, N., and Keller, J. (2004). The interferon-inducible p200 family of proteins: a perspective on their roles in cell cycle regulation and differentiation. Blood Cells Mol Dis *32*, 155-167.

Baccarini, M., Bistoni, F., and Lohmann-Matthes, M. (1985). In vitro natural cell-mediated cytotoxicity against Candida albicans: macrophage precursors as effector cells. J Immunol *134*, 2658-2665.

Baranek, C., Sock, E., and Wegner, M. (2005). The POU protein Oct-6 is a nucleocytoplasmic shuttling protein. Nucleic Acids Res *33*, 6277-6286.

Barbalat, R., Lau, L., Locksley, R., and Barton, G. (2009). Toll-like receptor 2 on inflammatory monocytes induces type I interferon in response to viral but not bacterial ligands. Nat Immunol *10*, 1200-1207.

Barber, G. (2001). Host defense, viruses and apoptosis. Cell Death Differ *8*, 113-126.

Baumeister, H., and Meyerhof, W. (2000). The POU domain transcription factor Tst-1 activates somatostatin receptor 1 gene expression in pancreatic beta -cells. J Biol Chem *275*, 28882-28887.

Beck, I., Müller, M., Mentlein, R., Sadowski, T., Mueller, M., Paus, R., and Sedlacek, R. (2007). Matrix metalloproteinase-19 expression in keratinocytes is repressed by transcription factors Tst-1 and Skn-1a: implications for keratinocyte differentiation. J Invest Dermatol *127*, 1107-1114.

Bermingham, J.J., Scherer, S., O'Connell, S., Arroyo, E., Kalla, K., Powell, F., and Rosenfeld, M. (1996). Tst-1/Oct-6/SCIP regulates a unique step in peripheral myelination and is required for normal respiration. Genes Dev *10*, 1751-1762.

Birchmeier, C., and Nave, K. (2008). Neuregulin-1, a key axonal signal that drives Schwann cell growth and differentiation. Glia *56*, 1491-1497.

Blakemore, W. (2005). The case for a central nervous system (CNS) origin for the Schwann cells that remyelinate CNS axons following concurrent loss of oligodendrocytes and astrocytes. Neuropathol Appl Neurobiol *31*, 1-10.

Bogdan, C., Mattner, J., and Schleicher, U. (2004). The role of type I interferons in non-viral infections. Immunol Rev *202*, 33-48.

Bogdan, C., Thüring, H., Dlaska, M., Röllinghoff, M., and Weiss, G. (1997). Mechanism of suppression of macrophage nitric oxide release by IL-13: influence of the macrophage population. J Immunol *159*, 4506-4513.

Bustin, S. (2000). Absolute quantification of mRNA using real-time reverse transcription polymerase chain reaction assays. J Mol Endocrinol *25*, 169-193.

Bustin, S. (2002). Quantification of mRNA using real-time reverse transcription PCR (RT-PCR): trends and problems. J Mol Endocrinol *29*, 23-39.

Carpenter, S., and O'Neill, L. (2007). How important are Toll-like receptors for antimicrobial responses? Cell Microbiol *9*, 1891-1901.

Chiu, Y., Macmillan, J., and Chen, Z. (2009). RNA polymerase III detects cytosolic DNA and induces type I interferons through the RIG-I pathway. Cell *138*, 576-591.

Dailey, L., and Basilico, C. (2001). Coevolution of HMG domains and homeodomains and the generation of transcriptional regulation by Sox/POU complexes. J Cell Physiol *186*, 315-328.

de Veer, M., Holko, M., Frevel, M., Walker, E., Der, S., Paranjape, J., Silverman, R., and Williams, B. (2001). Functional classification of interferon-stimulated genes identified using microarrays. J Leukoc Biol *69*, 912-920.

Decker, T., Kovarik, P., and Meinke, A. (1997). GAS elements: a few nucleotides with a major impact on cytokine-induced gene expression. J Interferon Cytokine Res *17*, 121-134.

Defilippis, V., Alvarado, D., Sali, T., Rothenburg, S., and Früh, K. (2009). Human Cytomegalovirus Induces the Interferon Response Via the DNA Sensor ZBP1. J Virol.

Delhaye, S., Paul, S., Blakqori, G., Minet, M., Weber, F., Staeheli, P., and Michiels, T. (2006). Neurons produce type I interferon during viral encephalitis. Proc Natl Acad Sci U S A *103*, 7835-7840.

Dennis, G.J., Sherman, B., Hosack, D., Yang, J., Gao, W., Lane, H., and Lempicki, R. (2003). DAVID: Database for Annotation, Visualization, and Integrated Discovery. Genome Biol *4*, P3.

Der, S., Zhou, A., Williams, B., and Silverman, R. (1998). Identification of genes differentially regulated by interferon alpha, beta, or gamma using oligonucleotide arrays. Proc Natl Acad Sci U S A *95*, 15623-15628.

Dheda, K., Huggett, J., Bustin, S., Johnson, M., Rook, G., and Zumla, A. (2004). Validation of housekeeping genes for normalizing RNA expression in real-time PCR. Biotechniques *37*, 112-114, 116, 118-119.

Du, W., and Maniatis, T. (1992). An ATF/CREB binding site is required for virus induction of the human interferon beta gene [corrected]. Proc Natl Acad Sci U S A *89*, 2150-2154.

Dunn, T., Ross, I., and Hume, D. (1996). Transcription factor Oct-2 is expressed in primary murine macrophages. Blood *88*, 4072.

Durbin, J.E., Hackenmiller, R., Simon, M.C., and Levy, D.E. (1996). Targeted disruption of the mouse Stat1 gene results in compromised innate immunity to viral disease. Cell *84*, 443-450.

Erlandsson, L., BlumenthalR., Eloranta, M.L., Engel, H., Alm, G., Weiss, S., and Leanderson, T. (1998). Interferon-beta is required for interferon-alpha production in mouse fibroblasts. Curr Biol *8*, 223-226.

Faus, I., Hsu, H., and Fuchs, E. (1994). Oct-6: a regulator of keratinocyte gene expression in stratified squamous epithelia. Mol Cell Biol *14*, 3263-3275.

Friedrich, R., Schlierf, B., Tamm, E., Bösl, M., and Wegner, M. (2005). The class III POU domain protein Brn-1 can fully replace the related Oct-6 during schwann cell development and myelination. Mol Cell Biol *25*, 1821-1829.

Ghazvini, M., Mandemakers, W., Jaegle, M., Piirsoo, M., Driegen, S., Koutsourakis, M., Smit, X., Grosveld, F., and Meijer, D. (2002). A cell type-specific allele of the POU gene Oct-6 reveals Schwann cell autonomous function in nerve development and regeneration. EMBO J *21*, 4612-4620.

Ghislain, J., Desmarquet-Trin-Dinh, C., Jaegle, M., Meijer, D., Charnay, P., and Frain, M. (2002). Characterisation of cis-acting sequences reveals a biphasic, axon-dependent regulation of Krox20 during Schwann cell development. Development *129*, 155-166.

Giulietti, A., Overbergh, L., Valckx, D., Decallonne, B., Bouillon, R., and Mathieu, C. (2001). An overview of real-time quantitative PCR: applications to quantify cytokine gene expression. Methods *25*, 386-401.

Goldring, C., Reveneau, S., Algarté, M., and Jeannin, J. (1996). In vivo footprinting of the mouse inducible nitric oxide synthase gene: inducible protein occupation of numerous sites including Oct and NF-IL6. Nucleic Acids Res *24*, 1682-1687.

Génin, P., Vaccaro, A., and Civas, A. (2009). The role of differential expression of human interferon--a genes in antiviral immunity. Cytokine Growth Factor Rev *20*, 283-295.

Haas, T., Metzger, J., Schmitz, F., Heit, A., Müller, T., Latz, E., and Wagner, H. (2008). The DNA sugar backbone 2' deoxyribose determines toll-like receptor 9 activation. Immunity *28*, 315-323.

Haggarty, A., Camato, R., Paterno, G., Cohen, L., Hiscott, J., and Skup, D. (1991). A developmentally regulated octamer-binding activity in embryonal carcinoma cells which represses beta-interferon expression. Cell Growth Differ *2*, 503-510.

Hai, M., Muja, N., DeVries, G., Quarles, R., and Patel, P. (2002). Comparative analysis of Schwann cell lines as model systems for myelin gene transcription studies. J Neurosci Res *69*, 497-508.

Hasan, U., Chaffois, C., Gaillard, C., Saulnier, V., Merck, E., Tancredi, S., Guiet, C., Brière, F., Vlach, J., Lebecque, S., Trinchieri, G., and Bates, E. (2005). Human TLR10 is a functional receptor, expressed by B cells and plasmacytoid dendritic cells, which activates gene transcription through MyD88. J Immunol *174*, 2942-2950.

He, X., Treacy, M., Simmons, D., Ingraham, H., Swanson, L., and Rosenfeld, M. (1989). Expression of a large family of POU-domain regulatory genes in mammalian brain development. Nature *340*, 35-41.

Herr, W., and Cleary, M. (1995). The POU domain: versatility in transcriptional regulation by a flexible two-in-one DNA-binding domain. Genes Dev *9*, 1679-1693.

Holland, P., Booth, H., and Bruford, E. (2007). Classification and nomenclature of all human homeobox genes. BMC Biol *5*, 47.

Honda, K., Takaoka, A., and Taniguchi, T. (2006). Type I interferon [corrected] gene induction by the interferon regulatory factor family of transcription factors. Immunity *25*, 349-360.

Honda, K., and Taniguchi, T. (2006). IRFs: master regulators of signalling by Toll-like receptors and cytosolic pattern-recognition receptors. Nat Rev Immunol *6*, 644-658.

Horvath, C. (2000). STAT proteins and transcriptional responses to extracellular signals. Trends Biochem Sci *25*, 496-502.

Huang, d.W., Sherman, B., Stephens, R., Baseler, M., Lane, H., and Lempicki, R. (2008). DAVID gene ID conversion tool. Bioinformation *2*, 428-430.

Huang, J., Teng, L., Liu, T., Li, L., Chen, D., Li, F., Xu, L., Zhai, Z., and Shu, H. (2003). Identification of a novel serine/threonine kinase that inhibits TNF-induced NF-kappaB activation and p53-induced transcription. Biochem Biophys Res Commun *309*, 774-778.

Ishii, K., Kawagoe, T., Koyama, S., Matsui, K., Kumar, H., Kawai, T., Uematsu, S., Takeuchi, O., Takeshita, F., Coban, C., and Akira, S. (2008). TANK-binding kinase-1 delineates innate and adaptive immune responses to DNA vaccines. Nature *451*, 725-729.

Jaegle, M., Ghazvini, M., Mandemakers, W., Piirsoo, M., Driegen, S., Levavasseur, F., Raghoenath, S., Grosveld, F., and Meijer, D. (2003). The POU proteins Brn-2 and Oct-6 share important functions in Schwann cell development. Genes Dev *17*, 1380-1391.

Jaegle, M., Mandemakers, W., Broos, L., Zwart, R., Karis, A., Visser, P., Grosveld, F., and Meijer, D. (1996). The POU factor Oct-6 and Schwann cell differentiation. Science *273*, 507-510.

Jasmin, L., and Ohara, P. (2002). Remyelination within the CNS: do schwann cells pave the way for oligodendrocytes? Neuroscientist *8*, 198-203.

Kagan, J., Su, T., Horng, T., Chow, A., Akira, S., and Medzhitov, R. (2008). TRAM couples endocytosis of Toll-like receptor 4 to the induction of interferon-beta. Nat Immunol *9*, 361-368.

Karaghiosoff, M., Neubauer, H., Lassnig, C., Kovarik, P., Schindler, H., Pircher, H., McCoy, B., Bogdan, C., Decker, T., Brem, G., Pfeffer, K., and Muller, M. (2000). Partial impairment of cytokine responses in Tyk2-deficient mice. Immunity *13*, 549-560.

Karaghiosoff, M., Steinborn, R., Kovarik, P., Kriegshäuser, G., Baccarini, M., Donabauer, B., Reichart, U., Kolbe, T., Bogdan, C., Leanderson, T., Levy, D., Decker, T., and Müller, M. (2003). Central role for type I interferons and Tyk2 in lipopolysaccharide-induced endotoxin shock. Nat Immunol *4*, 471-477.

Karikó, K., Ni, H., Capodici, J., Lamphier, M., and Weissman, D. (2004). mRNA is an endogenous ligand for Toll-like receptor 3. J Biol Chem *279*, 12542-12550.

Katsoulidis, E., Li, Y., Mears, H., and Platanias, L. (2005). The p38 mitogen-activated protein kinase pathway in interferon signal transduction. J Interferon Cytokine Res *25*, 749-756.

Kaur, S., Uddin, S., and Platanias, L. (2005). The PI3' kinase pathway in interferon signaling. J Interferon Cytokine Res *25*, 780-787.

Kawai, T., and Akira, S. (2008). Toll-like receptor and RIG-I-like receptor signaling. Ann N Y Acad Sci *1143*, 1-20.

Kimura, T., Kadokawa, Y., Harada, H., Matsumoto, M., Sato, M., Kashiwazaki, Y., Tarutani, M., Tan, R., Takasugi, T., Matsuyama, T., et al. (1996). Essential and non-redundant roles of p48 (ISGF3 gamma) and IRF-1 in both type I and type II interferon responses, as revealed by gene targeting studies. Genes Cells 1, 115-124.

Kleinert, H., Pautz, A., Linker, K., and Schwarz, P. (2004). Regulation of the expression of inducible nitric oxide synthase. Eur J Pharmacol *500*, 255-266.

Kovarik, P., Stoiber, D., Novy, M., and Decker, T. (1998). Stat1 combines signals derived from IFN-gamma and LPS receptors during macrophage activation. EMBO J *17*, 3660-3668.

Krause, C., and Pestka, S. (2007). Historical developments in the research of interferon receptors. Cytokine Growth Factor Rev *18*, 473-482.

Krishnan, J., Selvarajoo, K., Tsuchiya, M., Lee, G., and Choi, S. (2007). Toll-like receptor signal transduction. Exp Mol Med *39*, 421-438.

Kuhn, R., Monuki, E., and Lemke, G. (1991). The gene encoding the transcription factor SCIP has features of an expressed retroposon. Mol Cell Biol *11*, 4642-4650.

Latchman, D. (1999). Regulation of DNA virus transcription by cellular POU family transcription factors. Rev Med Virol *9*, 31-38.

Lee, M., and Kim, Y. (2007). Signaling pathways downstream of pattern-recognition receptors and their cross talk. Annu Rev Biochem *76*, 447-480.

Letertre, C., Perelle, S., Dilasser, F., Arar, K., and Fach, P. (2003). Evaluation of the performance of LNA and MGB probes in 5'-nuclease PCR assays. Mol Cell Probes *17*, 307-311.

Li, L., Sun, L., Gao, F., Jiang, J., Yang, Y., Li, C., Gu, J., Wei, Z., Yang, A., Lu, R., et al. (2010). Stk40 links the pluripotency factor Oct4 to the Erk/MAPK pathway and controls extraembryonic endoderm differentiation. Proc Natl Acad Sci U S A 107, 1402-1407.

Li, P., He, X., Gerrero, M., Mok, M., Aggarwal, A., and Rosenfeld, M. (1993). Spacing and orientation of bipartite DNA-binding motifs as potential functional determinants for POU domain factors. Genes Dev *7*, 2483-2496.

Mandemakers, W., Zwart, R., Jaegle, M., Walbeehm, E., Visser, P., Grosveld, F., and Meijer, D. (2000). A distal Schwann cell-specific enhancer mediates axonal regulation of the Oct-6 transcription factor during peripheral nerve development and regeneration. EMBO J *19*, 2992-3003.

Marzluff, W., Wagner, E., and Duronio, R. (2008). Metabolism and regulation of canonical histone mRNAs: life without a poly(A) tail. Nat Rev Genet *9*, 843-854.

Meijer, D. (2009). Neuroscience. Went fishing, caught a snake. Science *325*, 1353-1354.

Meijer, D., Graus, A., and Grosveld, G. (1992). Mapping the transactivation domain of the Oct-6 POU transcription factor. Nucleic Acids Res *20*, 2241-2247.

Meijer, D., Graus, A., Kraay, R., Langeveld, A., Mulder, M., and Grosveld, G. (1990). The octamer-binding factor Oct6: cDNA cloning and expression in early embryonic cells. Nucleic Acids Res *18*, 7357-7365.

Mesplède, T., Island, M., Christeff, N., Petek, F., Doly, J., and Navarro, S. (2005). The POU transcription factor Oct-1 represses virus-induced interferon A gene expression. Mol Cell Biol *25*, 8717-8731.

Mirsky, R., Parkinson, D., Dong, Z., Meier, C., Calle, E., Brennan, A., Topilko, P., Harris, B., Stewart, H., and Jessen, K. (2001). Regulation of genes involved in Schwann cell development and differentiation. Prog Brain Res *132*, 3-11.

Monk, K., Naylor, S., Glenn, T., Mercurio, S., Perlin, J., Dominguez, C., Moens, C., and Talbot, W. (2009). A G protein-coupled receptor is essential for Schwann cells to initiate myelination. Science *325*, 1402-1405.

Monuki, E., Kuhn, R., and Lemke, G. (1993). Repression of the myelin P0 gene by the POU transcription factor SCIP. Mech Dev *42*, 15-32.

Monuki, E., Weinmaster, G., Kuhn, R., and Lemke, G. (1989). SCIP: a glial POU domain gene regulated by cyclic AMP. Neuron *3*, 783-793.

Morey, J., Ryan, J., and Van Dolah, F. (2006). Microarray validation: factors influencing correlation between oligonucleotide microarrays and real-time PCR. Biol Proced Online *8*, 175-193.

Muller, U., Steinhoff, U., Reis, L.F., Hemmi, S., Pavlovic, J., Zinkernagel, R.M., and Aguet, M. (1994). Functional role of type I and type II interferons in antiviral defense. Science *264*, 1918-1921.

Nakhaei, P., Genin, P., Civas, A., and Hiscott, J. (2009). RIG-I-like receptors: sensing and responding to RNA virus infection. Semin Immunol *21*, 215-222.

Neumann, M., Fries, H., Scheicher, C., Keikavoussi, P., Kolb-Mäurer, A., Bröcker, E., Serfling, E., and Kämpgen, E. (2000). Differential expression of Rel/NF-kappaB and octamer factors is a hallmark of the generation and maturation of dendritic cells. Blood *95*, 277-285.

Nissen, R., and Yamamoto, K. (2000). The glucocorticoid receptor inhibits NFkappaB by interfering with serine-2 phosphorylation of the RNA polymerase II carboxy-terminal domain. Genes Dev *14*, 2314-2329.

Panne, D. (2008). The enhanceosome. Curr Opin Struct Biol *18*, 236-242.

Park, C., Li, S., Cha, E., and Schindler, C. (2000). Immune response in Stat2 knockout mice. Immunity 13, 795-804.

Phillips, K., and Luisi, B. (2000). The virtuoso of versatility: POU proteins that flex to fit. J Mol Biol *302*, 1023-1039.

Pokrovskaja, K., Panaretakis, T., and Grandér, D. (2005). Alternative signaling pathways regulating type I interferon-induced apoptosis. J Interferon Cytokine Res *25*, 799-810.

Reis, L.F., Ruffner, H., Stark, G., Aguet, M., and Weissmann, C. (1994). Mice devoid of interferon regulatory factor 1 (IRF-1) show normal expression of type I interferon genes. EMBO J *13*, 4798-806.

Reményi, A., Tomilin, A., Schöler, H., and Wilmanns, M. (2002). Differential activity by DNA-induced quarternary structures of POU transcription factors. Biochem Pharmacol *64*, 979-984.

Renner, K., Sock, E., Bermingham, J.J., and Wegner, M. (1996). Expression of the gene for the POU domain transcription factor Tst-1/Oct6 is regulated by an estrogen-dependent enhancer. Nucleic Acids Res *24*, 4552-4557.

Ryan, A., and Rosenfeld, M. (1997). POU domain family values: flexibility, partnerships, and developmental codes. Genes Dev *11*, 1207-1225.

Ryu, E., Wang, J., Le, N., Baloh, R., Gustin, J., Schmidt, R., and Milbrandt, J. (2007). Misexpression of Pou3f1 results in peripheral nerve hypomyelination and axonal loss. J Neurosci *27*, 11552-11559.

Sadler, A., and Williams, B. (2008). Interferon-inducible antiviral effectors. Nat Rev Immunol *8*, 559-568.

Sadzak, I., Schiff, M., Gattermeier, I., Glinitzer, R., Sauer, I., Saalmüller, A., Yang, E., Schaljo, B., and Kovarik, P. (2008). Recruitment of Stat1 to chromatin is required for interferon-induced serine phosphorylation of Stat1 transactivation domain. Proc Natl Acad Sci U S A *105*, 8944-8949.

Scherer, S., Wang, D., Kuhn, R., Lemke, G., Wrabetz, L., and Kamholz, J. (1994). Axons regulate Schwann cell expression of the POU transcription factor SCIP. J Neurosci *14*, 1930-1942.

Schindler, C., Levy, D., and Decker, T. (2007). JAK-STAT signaling: from interferons to cytokines. J Biol Chem *282*, 20059-20063.

Schroder, K., Hertzog, P., Ravasi, T., and Hume, D. (2004). Interferon-gamma: an overview of signals, mechanisms and functions. J Leukoc Biol *75*, 163-189.

Schröder, M., Baran, M., and Bowie, A. (2008). Viral targeting of DEAD box protein 3 reveals its role in TBK1/IKKepsilon-mediated IRF activation. EMBO J *27*, 2147-2157.

Schümperli, D., and Pillai, R. (2004). The special Sm core structure of the U7 snRNP: far-reaching significance of a small nuclear ribonucleoprotein. Cell Mol Life Sci *61*, 2560-2570.

Shivdasani, R., and Orkin, S. (1996). The transcriptional control of hematopoiesis. Blood *87*, 4025-4039.

Smyth, G. (2004). Linear models and empirical bayes methods for assessing differential expression in microarray experiments. Stat Appl Genet Mol Biol *3*, Article3.

Soulat, D., Bürckstümmer, T., Westermayer, S., Goncalves, A., Bauch, A., Stefanovic, A., Hantschel, O., Bennett, K., Decker, T., and Superti-Furga, G. (2008). The DEAD-box helicase DDX3X is a

critical component of the TANK-binding kinase 1-dependent innate immune response. EMBO J *27*, 2135-2146.

Stark, G. (2007). How cells respond to interferons revisited: from early history to current complexity. Cytokine Growth Factor Rev *18*, 419-423.

Stohlman, S., and Hinton, D. (2001). Viral induced demyelination. Brain Pathol *11*, 92-106.

Strobl, B., Bubic, I., Bruns, U., Steinborn, R., Lajko, R., Kolbe, T., Karaghiosoff, M., Kalinke, U., Jonjic, S., and Müller, M. (2005). Novel functions of tyrosine kinase 2 in the antiviral defense against murine cytomegalovirus. J Immunol *175*, 4000-4008.

Sugihara, T., Kudryavtseva, E., Kumar, V., Horridge, J., and Andersen, B. (2001). The POU domain factor Skin-1a represses the keratin 14 promoter independent of DNA-binding. A possible role for interactions between Skn-1a and CREB-binding protein/p300. J Biol Chem *276*, 33036-33044.

Svaren, J., and Meijer, D. (2008). The molecular machinery of myelin gene transcription in Schwann cells. Glia *56*, 1541-1551.

Takaoka, A., and Yanai, H. (2006). Interferon signalling network in innate defence. Cell Microbiol *8*, 907-922.

Takeuchi, O., and Akira, S. (2007). Recognition of viruses by innate immunity. Immunol Rev *220*, 214-224.

Terenzi, F., Hui, D., Merrick, W., and Sen, G. (2006). Distinct induction patterns and functions of two closely related interferon-inducible human genes, ISG54 and ISG56. J Biol Chem *281*, 34064-34071.

Topilko, P., Schneider-Maunoury, S., Levi, G., Baron-Van Evercooren, A., Chennoufi, A., Seitanidou, T., Babinet, C., and Charnay, P. (1994). Krox-20 controls myelination in the peripheral nervous system. Nature *371*, 796-799.

Uematsu, S., and Akira, S. (2007). Toll-like receptors and Type I interferons. J Biol Chem *282*, 15319-15323.

Uzé, G., and Monneron, D. IL-28 and IL-29: newcomers to the interferon family. Biochimie *89*, 729-734.

van Boxel-Dezaire, A., Rani, M., and Stark, G. (2006). Complex modulation of cell type-specific signaling in response to type I interferons. Immunity *25*, 361-372.

Vilaysane, A., and Muruve, D. (2009). The innate immune response to DNA. Semin Immunol *21*, 208-214.

Wu, C., Orozco, C., Boyer, J., Leglise, M., Goodale, J., Batalov, S., Hodge, C., Haase, J., Janes, J., Huss, J.r., et al. (2009). BioGPS: an extensible and customizable portal for querying and organizing gene annotation resources. Genome Biol 10, R130.

Zhang, Z., and Schluesener, H. (2006). Mammalian toll-like receptors: from endogenous ligands to tissue regeneration. Cell Mol Life Sci *63*, 2901-2907.

Zwart, R., Broos, L., Grosveld, G., and Meijer, D. (1996). The restricted expression pattern of the POU factor Oct-6 during early development of the mouse nervous system. Mech Dev *54*, 185-194.

APPENDIX

Preliminary Results

Various additional experiments were performed in order to either check for Oct-6 expression or to investigate a role of Oct-6 in innate immunity. No independent repeats were performed for these experiments.

Screening of various murine cell types for expression of Oct-6

In order to test, whether Oct-6 is also expressed in other cell types, B-cells, T-cells, NK-cells, BMMs and FLMs were treated with IFNβ and the composition of the octamer-binding factors was analysed by a bandshift assay. The preliminary results showed, that as expected, Oct-1 was present in all cell types and major expression of Oct-2 was found in B-cells and macrophages (Figure App. 1). Under basal conditions Oct-6 was not detected in any cell type. In contrast to fibroblasts and macrophages Oct-6 DNA-binding activity was not induced in B-cells, T-cells or NK-cells.

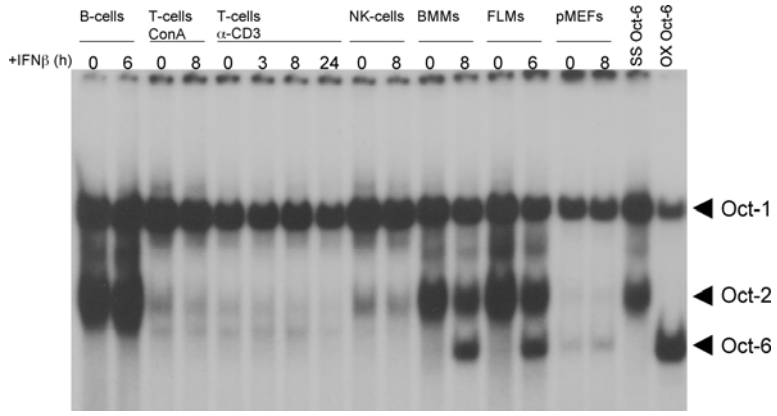

Figure App. 1: Oct-6 is induced in pMEFs and macrophages, but not in the other cell types tested. B-cells (α-CD19 MACSed from splenocytes), T-cells (splenocytes activated with ConA or α-CD3ε), NK-cells (α-Dx5 MACSed from splenocytes), BMMs, FLMs and pMEFs were treated with IFNβ (1000 U/ml) for the indicated times. Whole cell extracts were analysed by a bandshift assay with an octamer motif-containing oligonucleotide (SS: supershift with an α-Oct-6 antibody from BMMs_IFNβ_8h; OX: overexpression of Oct-6 in a MEF line).

Comparison of the induction of Oct-6 in BMMs and FLMs

Due to the perinatal lethal phenotype of Oct-6-deficient mice, we had to establish fetal liver-derived macrophage (FLM) cultures as an alternative macrophage population instead of BMMs which we routinely use. In a preliminary experiment we prooved, that IFNβ and poly(I:C) also induced Oct-6 DNA-binding activity in FLMs (Figure App. 2).

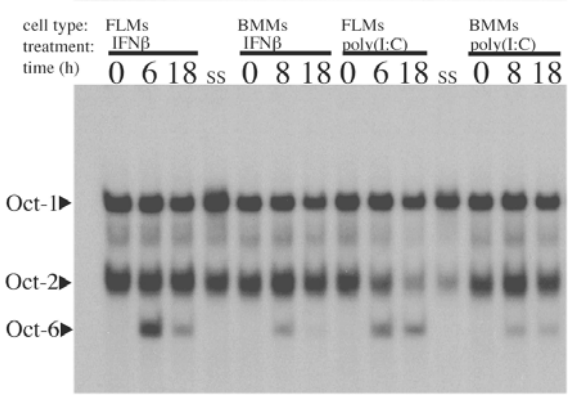

Figure App. 2: Oct-6 DNA-binding activity in response to IFNβ or poly(I:C) treatment is also induced in FLMs. FLMs and BMMs were treated with IFNβ (1000 U/ml), poly(I:C) (50 µg/ml) for the indicated times, or left untreated. Whole cell lysates were analysed by a bandshift assay using an oligonucleotide containing the octamer consensus motif (SS: supershift of the FLM_IFNβ_6h and FLM_poly(I:C)_6h lysate with an α-Oct-6 specific antibody).

Candidate target gene expression in pMEFs: poly(I:C) transfection (with or without IFNβ pretreatment), MCMV infection

In addition to the DNA transfection experiments described in the results section, preliminary experiments analysing the effect of Oct-6 deficiency in pMEFs on candidate target gene expression in response to poly(I:C) transfection with or without IFNβ pretreatment, and after MCMV infection were performed.

As expected, transfection of pMEFs with poly(I:C) resulted in a strong increase of IFNβ and panIFNα expression (Figures App. 3A, B), whereas Egr2 expression seemed to be slightly reduced 24 hours after poly(I:C) transfection (Figure App. 3C) and Pmp22 expression levels were unchanged (Figure App. 3D). No effect of the absence of Oct-6 on target gene expression could be observed.

Figure App. 3 – continued on the following page.

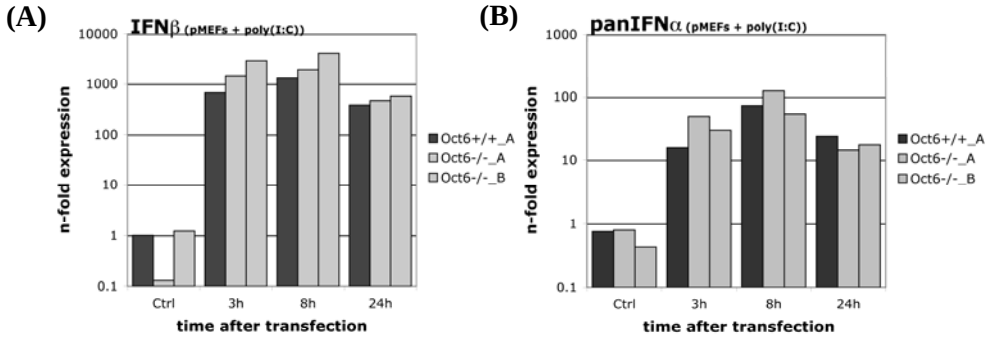

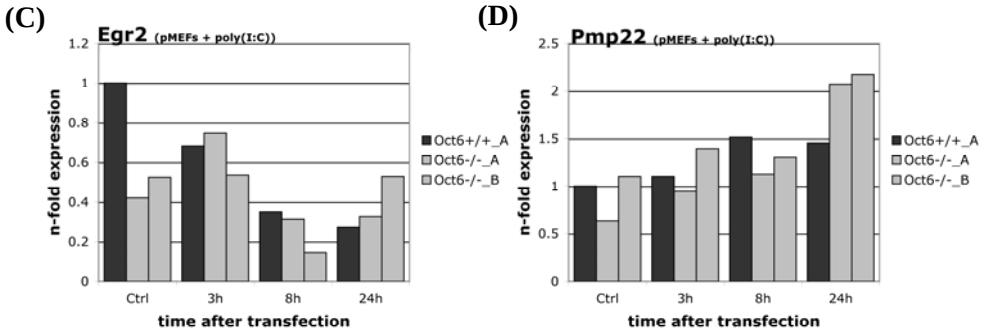

Figure App. 3: Absence of Oct-6 has no impact on candidate target gene expression in pMEFs after poly(I:C) treatment. WT (Oct6+/+) and Oct-6-deficient (Oct6-/-) pMEFs (from separate fetuses ("A", "B")) were transfected with poly(I:C) (200 ng/10^6 cells). After the indicated times total RNA was isolated. Changes in **(A)** IFNβ, **(B)** panIFNα, **(C)** Egr2 and **(D)** Pmp22 mRNA compared to the untransfected (Ctrl) WT sample were determined by RT-qPCR, calculating n-fold expression levels by the ΔΔCt method normalising to Ube2d2 (only unicates were run for each sample).

In order to increase Oct-6 levels, pMEFs were treated with IFNβ followed by poly(I:C) transfection, but again no difference in candidate target gene expression between the genotypes was observed (Figure App. 4A, B).

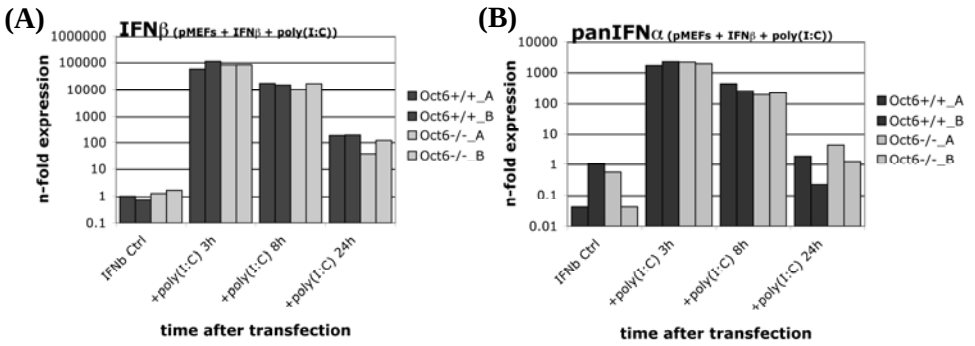

Figure App. 4: Absence of Oct-6 has no impact on IFNα/β expression in pMEFs after poly(I:C) treatment with IFNβ pretreatment. WT (Oct6+/+) and Oct-6-deficient (Oct6-/-) pMEFs (from separate fetuses ("A", "B")) were treated with IFNβ (1000 U/ml for 14 hours) followed by transfection with poly(I:C) (200 ng/10^6 cells). After the indicated times total RNA was isolated. Changes in **(A)** IFNβ and **(B)** panIFNα mRNA compared to the untransfected (Ctrl) WT sample were determined by RT-qPCR, calculating n-fold expression levels by the ΔΔCt method normalising to Ube2d2 (only unicates were run for each sample).

Furthermore WT and Oct-6-deficient pMEFs were infected with MCMV and candidate gene expression was analysed. As expected, IFNβ expression was highly increased in response to MCMV infection (Figure App. 5A), whereas expression of panIFNα was only slightly increased (Figure App. 5B). Expression of Egr2 was not influenced by viral infection (Figure App. 5C), Pmp22 mRNA levels were slightly increased (about 2-fold) 12 hours after infection (Figure App. 5D). However, candidate target gene expression was independent of Oct-6.

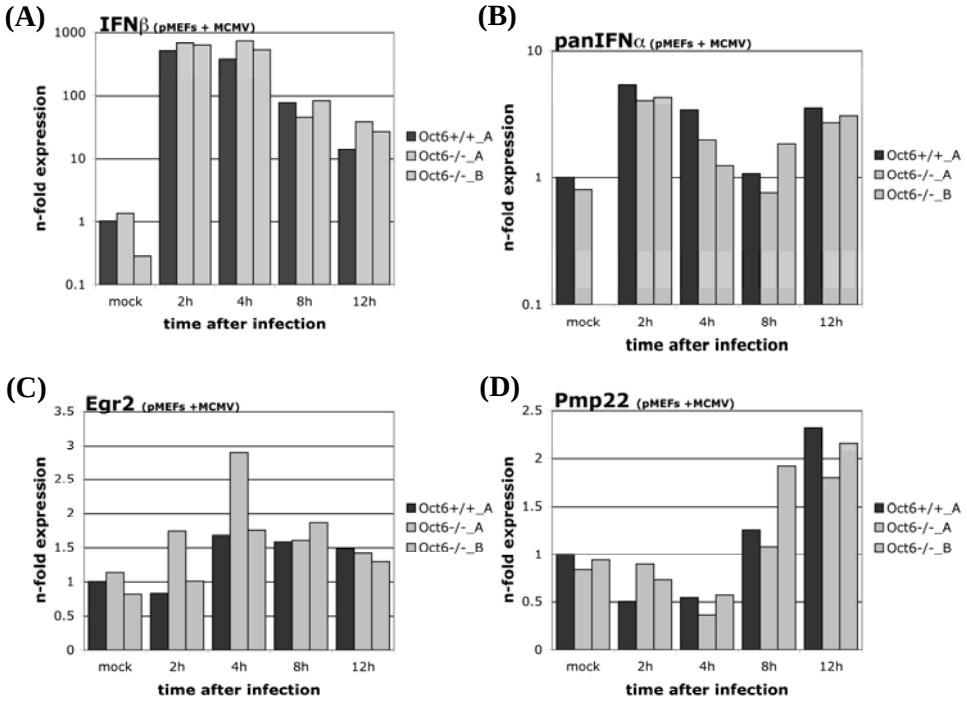

Figure App. 5: Absence of Oct-6 has no impact on candidate target gene expression in pMEFs after MCMV infection. WT (Oct6+/+) and Oct-6-deficient (Oct6-/-) pMEFs (from separate fetuses ("A", "B")) were infected with MCMV at an MOI of 1. After the indicated times total RNA was isolated. Changes in **(A)** IFNβ, **(B)** panIFNα, **(C)** Egr2 and **(D)** Pmp22 mRNA compared to the uninfected (mock) WT sample were determined by RT-qPCR, calculating n-fold expression levels by the ΔΔCt method normalising to Ube2d2 (only unicates were run for each sample).

Candidate target gene expression in FLMs: poly(I:C) kinetic and titration (with or without IFN pretreatment)

In addition to the 8 hours poly(I:C) treatment described in the results section, preliminary experiments analysing the effect of Oct-6 deficiency in FLMs on candidate target gene expression were performed. These experiments included (a) a detailed kinetic of poly(I:C) treatment, (b) down-titration of poly(I:C), (c) IFNβ and IFNγ treatments prior to poly(I:C) stimulation.

In order to test if Oct-6 is involved in gene regulation at another time than 8 hours after poly(I:C) treatment, a timecourse experiment was performed. As expected and already shown in the results (Figure 27A, B), expression of IFNα/β was highly induced in response to poly(I:C) treatment, with a 1000-fold induction reached already after 3 hours, peaking 6 hours of treatment (Figures App. 6A, B). Similarly, expression levels of iNOS were strongly induced in response to poly(I:C) treatment (Figure App. 6C). Expression levels of Egr2 (Figure App. 6D) and Pmp22 (Figure App. 6E) varied considerably between the different FLM preparations. Expression of both genes was clearly reduced upon poly(I:C) treatment. However, all observed expression patterns were not influenced by the presence/absence of Oct-6 at any time point tested.

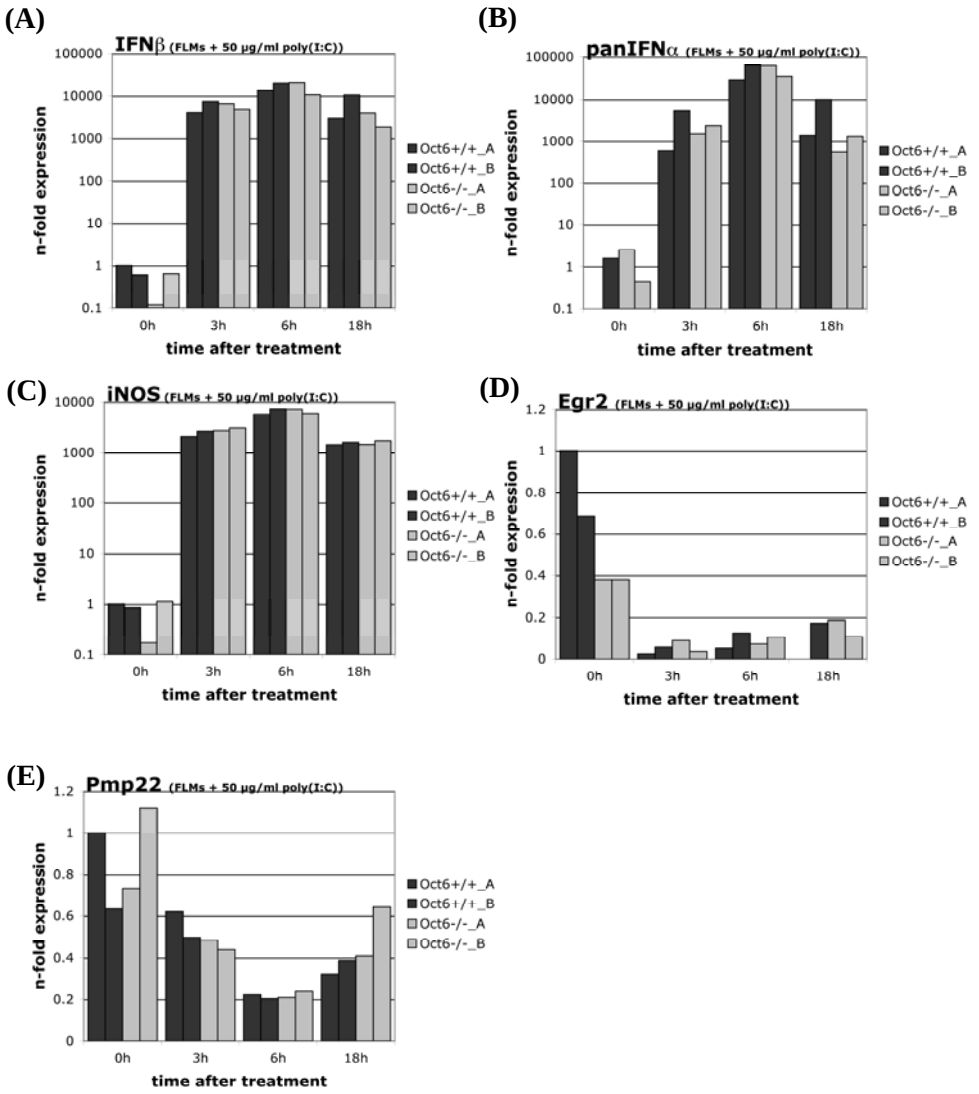

Figure App. 6: Absence of Oct-6 has no impact on candidate target gene expression in FLMs after poly(I:C) treatment (kinetic). WT (Oct6+/+) and Oct-6-deficient (Oct6-/-) FLMs (from separate fetuses ("A", "B")) were treated with poly(I:C) (50 µg/ml) for the indicated times. Changes in **(A)** IFNβ, **(B)** panIFNα, **(C)** iNOS, **(D)** Egr2 and **(E)** Pmp22 mRNA levels compared to an untreated (Ctrl) WT sample were determined by RT-qPCR, calculating n-fold expression levels by the ΔΔCt method normalising to Ube2d2 (only unicates were run for each sample).

Considering that Oct-6 expression under the conditions tested so far might be too low to show an effect on target gene expression, FLMs were pretreated with IFNβ or IFNγ for different times prior to poly(I:C) treatment to increase Oct-6 expression. Treatment with IFNβ or IFNγ alone does not induce IFNα/β expression (Figures App. 7-9A, B). After poly(I:C) treatment expression of IFNα/β mRNA is highly induced independent of the pretreatment. Expression of iNOS is induced one hour after poly(I:C) treatment with short (4 hours) IFNβ pretreatment (Figure App. 7C). With a long (12 gours) IFNβ pretreatment, iNOS induction in response to poly(I:C) is delayed (Figure App. 8C). In both cases IFNβ treatment alone did not induce iNOS expression. In contrast, IFNγ treatment alone induced high

amounts of iNOS (App. 9C), poly(I:C) treatment could further increase iNOS expression after IFNγ pretreatment. Expression patterns of IFNβ, IFNα and iNOS were independent of the presence/absence of Oct-6 upon any treatment tested.

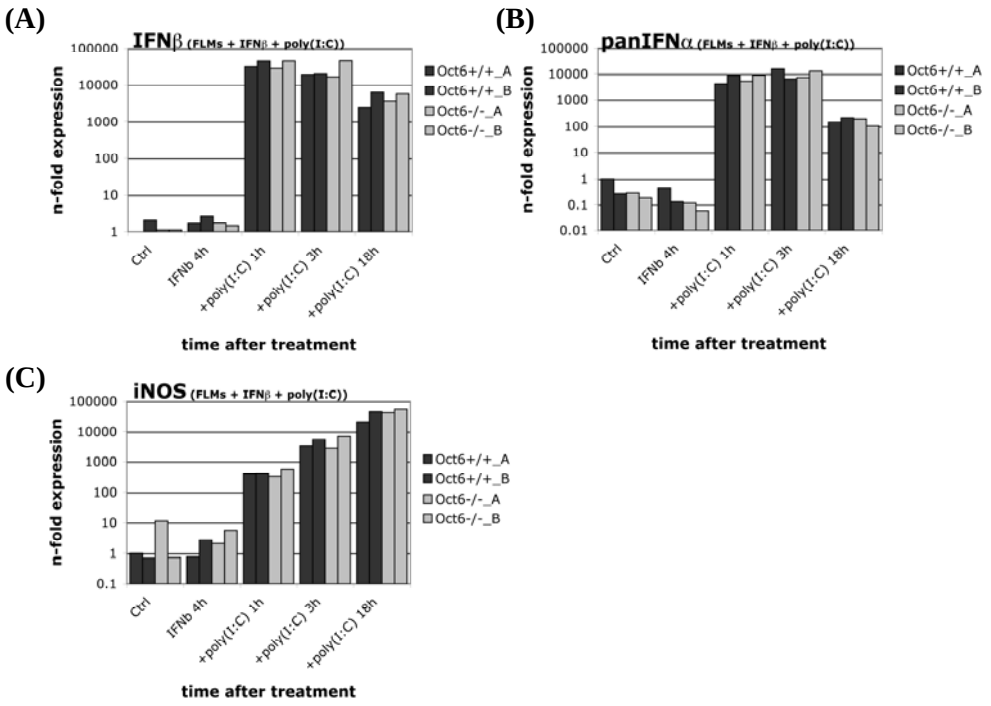

Figure App. 7: Absence of Oct-6 has no impact on candidate target gene expression in FLMs after short IFNβ pretreatment followed by poly(I:C) treatment. WT (Oct6+/+) and Oct-6-deficient (Oct6-/-) FLMs (from separate fetuses ("A", "B")) were treated with IFNβ (1000 U/ml) for 4 hours, followed by poly(I:C) (50 µg/ml) treatment for the indicated times. Changes in **(A)** IFNβ, **(B)** panIFNα and **(C)** iNOS mRNA levels compared to an untreated (Ctrl) WT sample were calculated as decribed in Figure App. 6.

Figure App. 8 – condtinued on the following page.

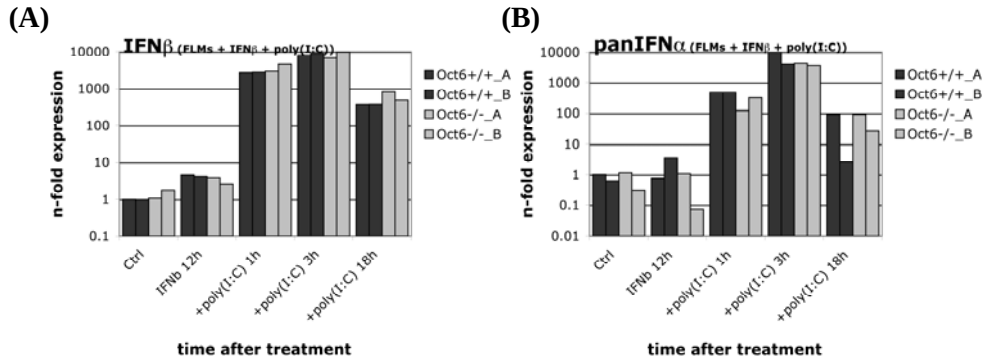

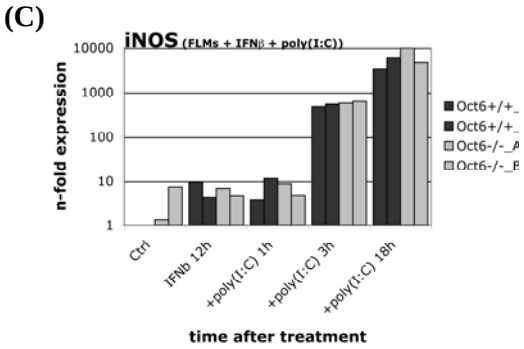

Figure App. 8: Absence of Oct-6 has no impact on candidate target gene expression in FLMs after long IFNβ pretreatment followed by poly(I:C) treatment. WT (Oct6+/+) and Oct-6-deficient (Oct6-/-) FLMs (from separate fetuses ("A", "B")) were treated with IFNβ (1000 U/ml) for 12 hours, followed by poly(I:C) (50 µg/ml) treatment for the indicated times. Changes in **(A)** IFNβ, **(B)** panIFNα and **(C)** iNOS mRNA levels compared to an untreated (Ctrl) WT sample were calculated as decribed in Figure App. 6.

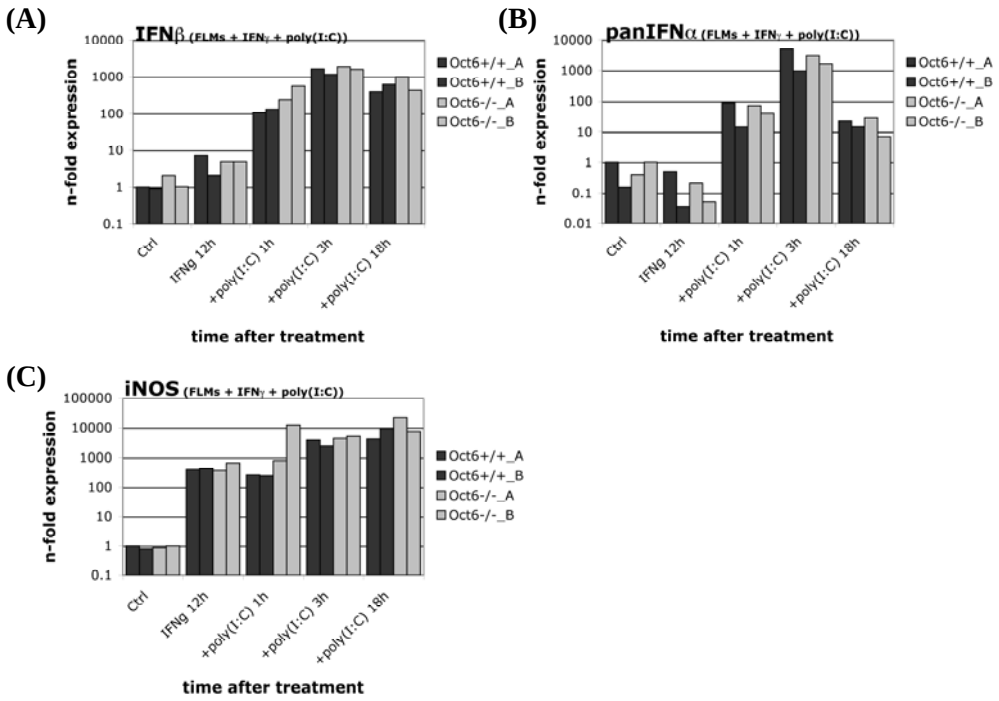

Figure App. 9: Absence of Oct-6 has no impact on candidate target gene expression in FLMs after long IFNγ pretreatment followed by poly(I:C) treatment. WT (Oct6+/+) and Oct-6-deficient (Oct6-/-) FLMs (from separate fetuses ("A", "B")) were treated with IFNγ (1000 U/ml) for 12 hours, followed by poly(I:C) (50 µg/ml) treatment for the indicated times. Changes in **(A)** IFNβ, **(B)** panIFNα and **(C)** iNOS mRNA levels compared to an untreated (Ctrl) WT sample were calculated as described in Figure App. 6.

Based on the hypothesis that the standard poly(I:C) concentration of 50 µg/ml might be too high and thus leading to a saturation effect in IFNα/β expression, consequently masking a potential effect of the absence of Oct-6, the amount of poly(I:C) was gradually reduced to concentrations as low as 5 ng/ml. Similar high amounts of IFNβ mRNA were induced with 50 µg/ml (Figure App. 6A) poly(I:C) and with concentrations as low as 500 ng/ml (Figure App. 10A, B). An effect of poly(I:C) reduction on IFNβ mRNA induction was observed with 50 ng/ml (Figure App. 10C) and 5 ng/ml poly(I:C) (Figure App. 10D). Induction of IFNα was similarly high with 50 µg/ml (Figure App. 6B) and 5 µg/ml (Figure App. 11A) poly(I:C). With reduction of poly(I:C) to 50 ng/ml (Figure App. 11B, C), panIFNα induction was lower, with 5 ng/ml poly(I:C) panIFNα was not detectable (data not shown). However, no differences in IFNα/β expression between WT and Oct-6-deficient FLMs could be observed at any concentration or time point.

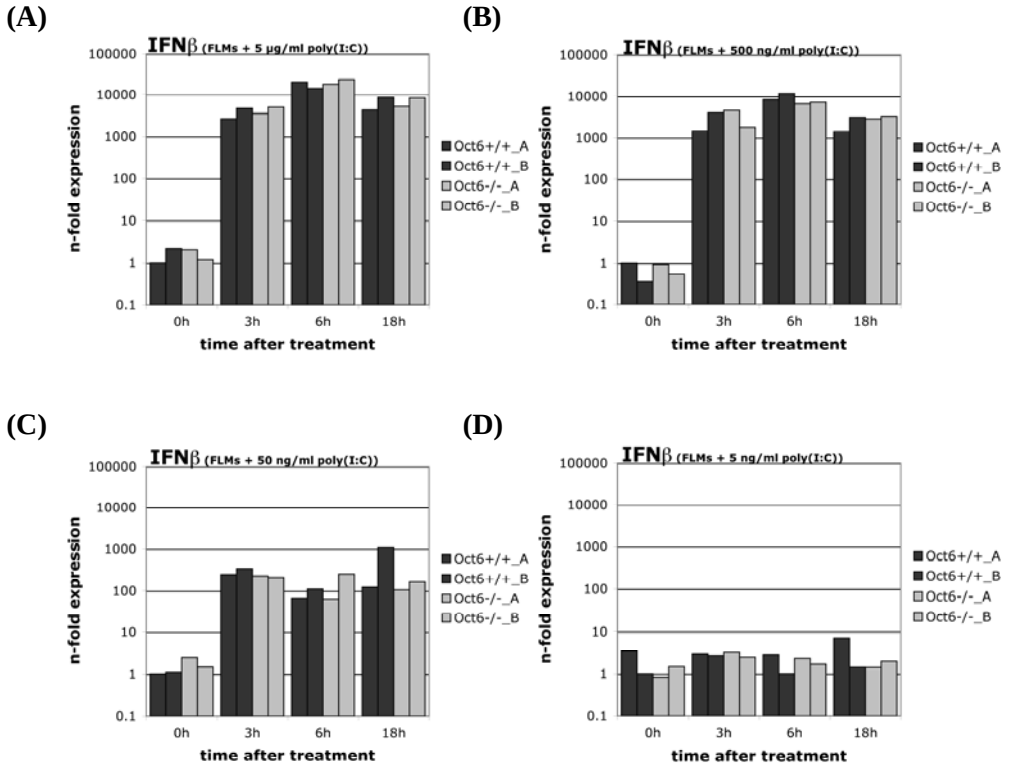

Figure App. 10: Absence of Oct-6 has no impact on IFNβ expression in response to various concentrations of poly(I:C) in FLMs. WT (Oct6+/+) and Oct-6-deficient (Oct6-/-) FLMs (from separate fetuses ("A", "B")) were treated with **(A)** 5 µg/ml, **(B)** 500 ng/ml, **(C)** 50 ng/ml or **(D)** 5 ng/ml poly(I:C) for the indicated times. Changes in IFNβ mRNA compared to an untreated WT sample were calculated as described in Figure App. 6.

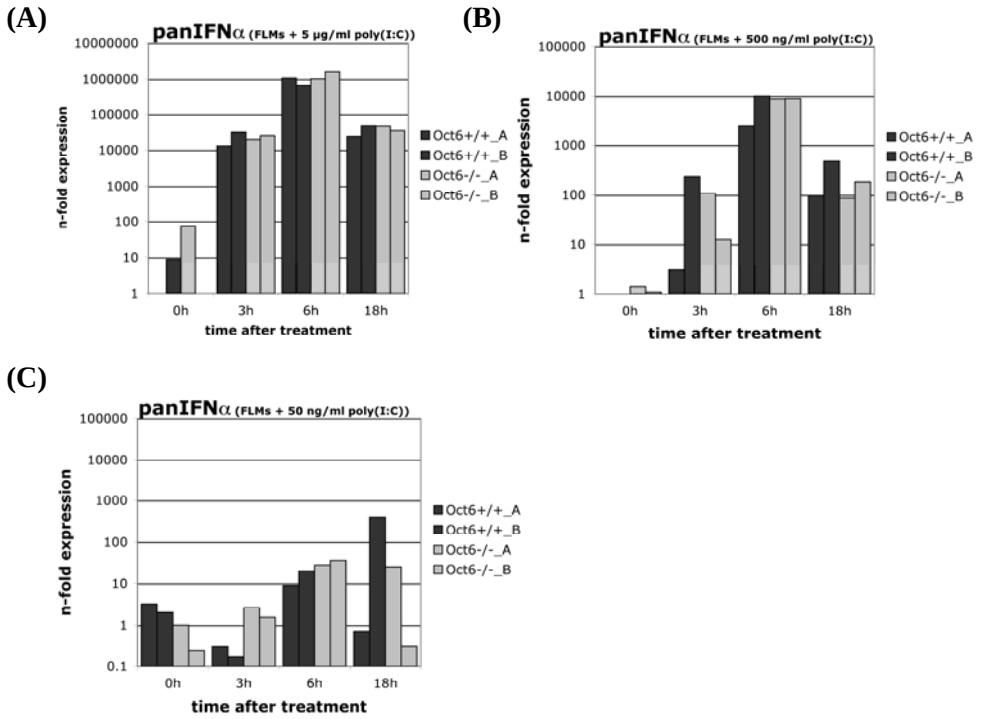

Figure App. 11: Absence of Oct-6 has no impact on panIFNα expression in response to poly(I:C) treatment in FLMs. Experimental setup and calculation of n-fold expression levels as described in Figure App. 10 and 6, respectively.

Expression of IFNα subtypes in Oct-6-deficient FLMs

Based on a report claiming that Oct-1 represses distinct IFNα subtypes (Mesplede *et al.*, 2005), expression levels of IFNα-1 and IFNα-2 in WT and Oct-6-deficient FLMs were determined by semiquantitative PCR. Preliminary results showed, that IFNα-subtypes were induced after treatment with poly(I:C) alone (Figure App. 12A) or with IFNβ pretreatment prior to poly(I:C) treatment (Figure App. 12B). No differences in IFNα subtype expression between the genotypes could be observed.

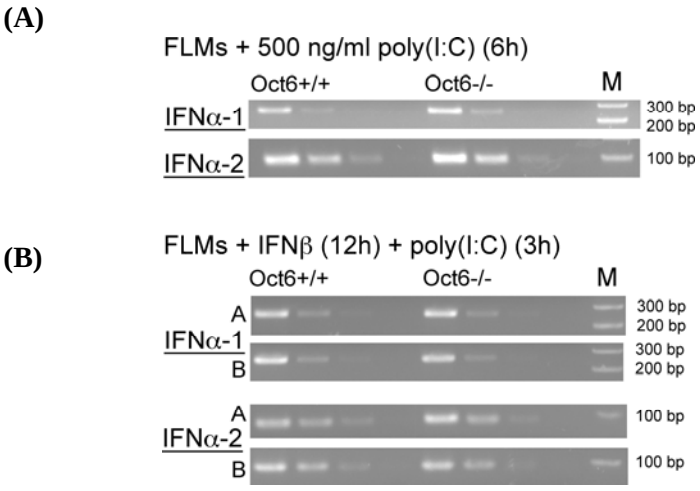

Figure App. 12: Absence of Oct-6 does not influence the expression of IFNα-1 and IFNα-2. WT (Oct-6+/+) and Oct-6-deficient (Oct-6-/-) FLMs (separate cell preparations "A", "B") were **(A)** treated with poly(I:C) (500 ng/ml), or **(B)** pretreated with IFNβ (1000 U/ml) followed by poly(I:C) treatment (50 µg/ml). Expression of IFNα-1 and IFNα-2 was determined by semiquantitative PCR: 5-fold dilution series of the respective cDNAs were amplified and the amplification products were separated on a 2% agarose gel stained with ethdium bromide (M: size marker). Similar expression of the endogenous control Ube2d2 has been checked by qPCR before (data not shown).

Binding of POU-transcription factors to consensus motifs in the IFNβ promoter

A number of potential octamer-binding sites are present in the murine IFNβ promoter (Haggarty *et al.*, 1991). In bandshift experiments, using two oligonucleotide probes covering the regions -110 to -139 (IFNβ_1) and -78 to -113 (IFNβ_2) (Figure App. 13A), we tested wether Oct-6 is able to bind to the motifs within the murine IFNβ promoter. FLMs were treated with poly(I:C) and whole cell extracts were used to shift an oligonucleotide containing the standard octamer consensus motif (OCT), IFNβ_1 or IFNβ_2. As expected and shown before, strong binding of Oct-6 was observed with the OCT-probe. Weak binding of Oct-6, but also of Oct-1 and Oct-2, to IFNβ_1 could be observed (Figure App. 13B). No binding pattern resembling the Oct-protein pattern was observed with the IFNβ_2 probe.

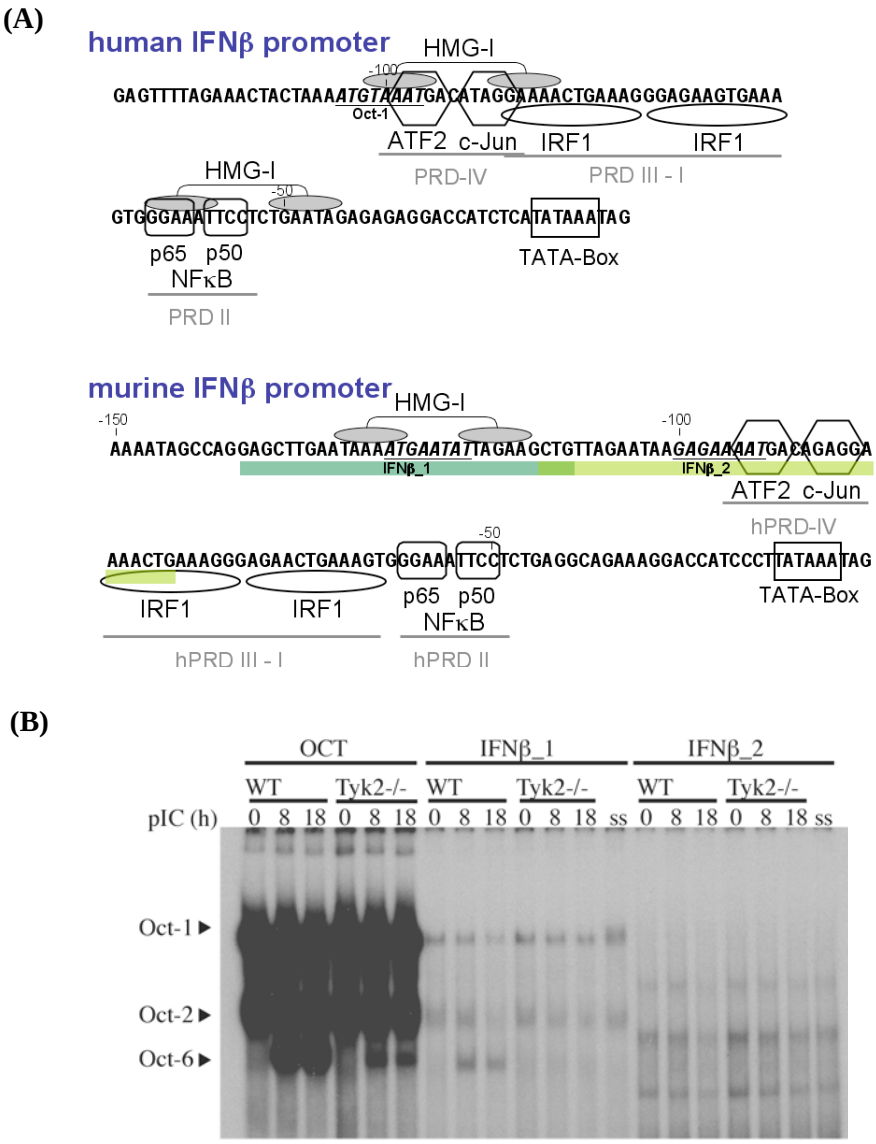

Figure App. 13: POU-proteins are able to bind to consensus motifs of the murine IFNβ promoter. (A) Comparison between the human (Du and Maniatis, 1992) and the murine IFNβ promoter with the respective transcription factor binding sites (potential octamer motifs: italic and underlined). The two oligonucleotides (IFNβ_1 and IFNβ_2) used for the bandshift experiment are indicated. **(B)** WT and Tyk2-/- BMMs were treated with poly(I:C) (50 µg/ml) for the indicated times. Whole cell extracts were analysed by a bandshift assay with an octamer motif-containing probe (OCT) and two oligonucleotides covering potential octamer motifs in the murine IFNβ promoter (IFNβ_1 and IFNβ_2), (SS: Supershift of WT_8h lysates with an α-Oct-6 antibody).

Activation of signalling pathways in Oct-6-deficient FLMs

In order to test effects of the absence of Oct-6 on the activation of pathways involved in the response to poly(I:C) treatment, NFκB and p38 mitogen-associated protein kinas (MAPK) activation was analysed in WT and Oct-6-deficient macrophages. Preliminary results showed that NFκB was similarly activated (serine-536 phosphorylation of the p65 subunit; Figure App. 14A).

Also after pretreatment with IFNβ for 2 days followed by poly(I:C) treatment similar activation of NFκB (Figure App. 14B) was observed in WT and Oct-6-deficient macrophages. Also activation of p38 MAPK observed in response to poly(I:C) and combined IFNβ pre-/poly(I:C) treatment (Figures App 14C, D) was similar in WT and Oct-6-deficient cells.

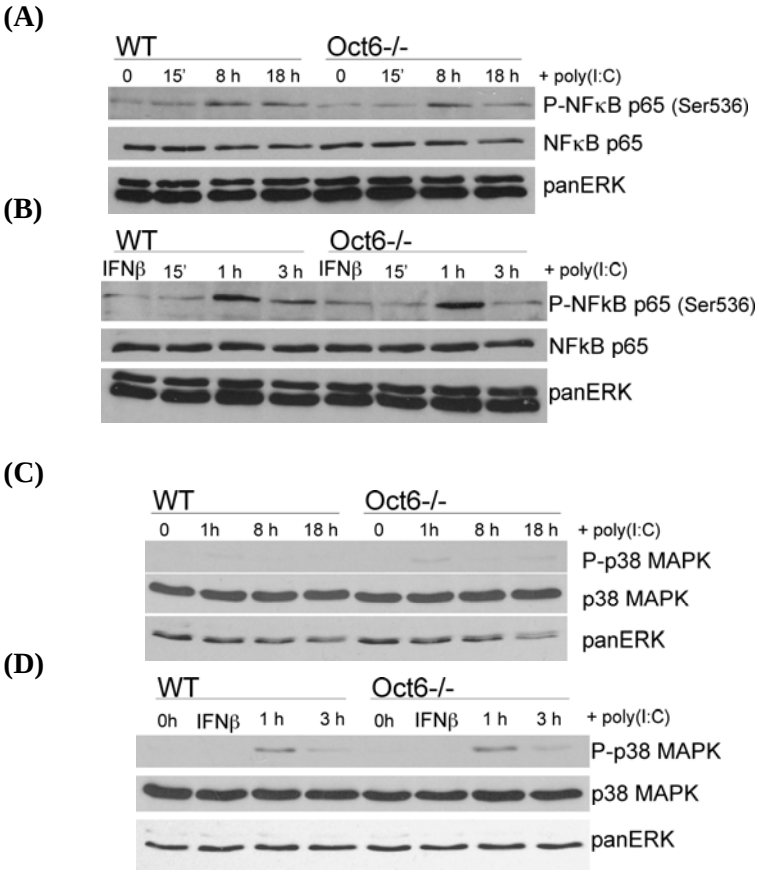

Figure App. 14: Activation of the NFκB- and the p38 MAPK-pathway are not influenced by the absence of Oct-6. WT and Oct-6-deficient FLMs were **(A, C)** treated with poly(I:C) (50 μg/ml), or **(B, D)** pretreated with IFNβ (1000 U/ml for two days) followed by poly(I:C) treatment for the indicated times. Whole cell extracts were analysed by western blot with antibodies detecting **(A)** Serine-536-phosphorylated (Ser536-P) NFκB p65, **(B)** NFκB p65, **(C)** phosphorylated (P) p38 MAPK and **(D)** p38 MAPK. All blots were reprobed with an α-panERK specific antibody to control for equal loading.

MCMV replication in Oct-6-deficient FLMs: lower MOI, standard MOI with or without IFN pretreatment

In addition to the standard MOI of 1 for MCMV infections, lower virus dose (i.e. MOI of 0.1) and IFN treatment prior to infection was analysed in WT *versus* Oct-6-deficient FLMs. As expected, MCMV replicated to lower titres at a lower MOI (Figure App. 15A compare to Figure 28 in the results section) and IFNβ as well as IFNγ pretreatment reduced viral replication (Figure App. 15B-D, compare to Figure 28). Preliminary data showed no effect of Oct-6 on MCMV replication under any of those conditions.

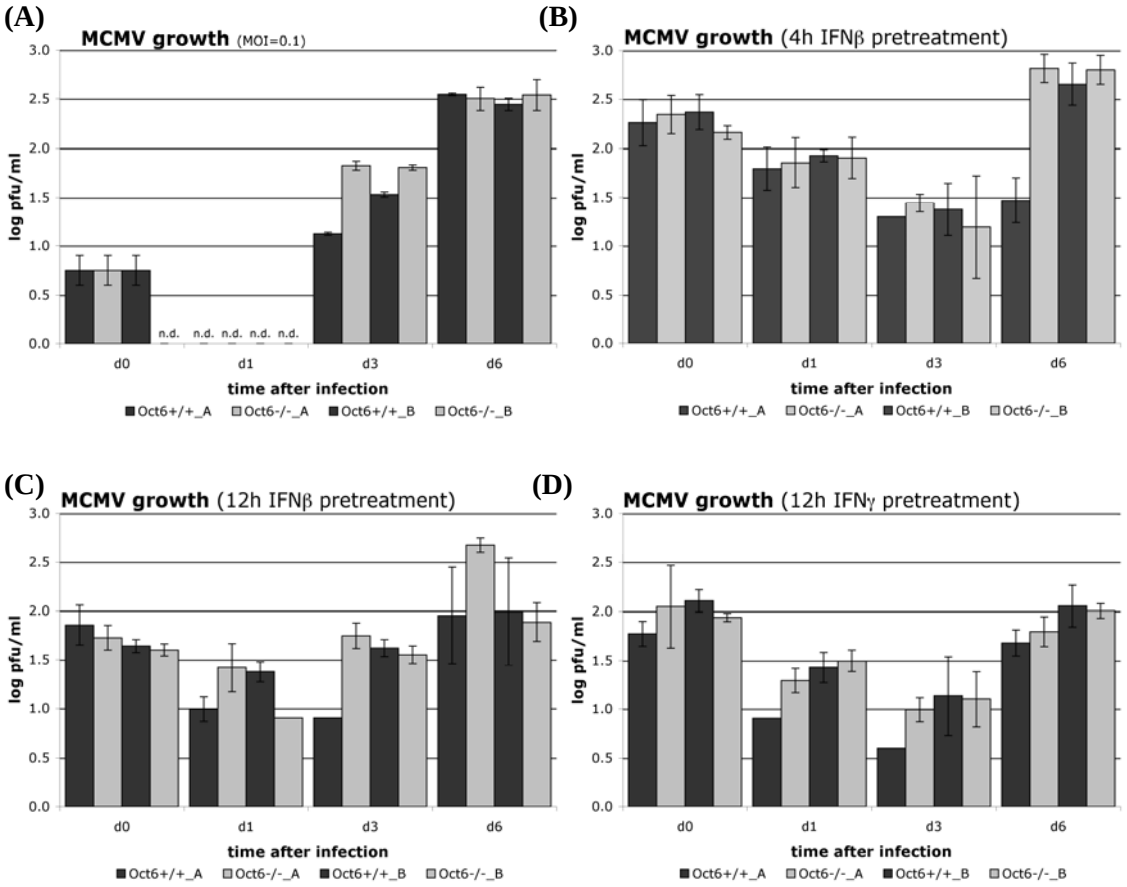

Figure App. 15: The absence of Oct-6 does not influence MCMV replication in FLMs. WT and Oct-6-deficient FLMs (separate FLM preparations "A", "B") were **(A)** infected with MCMV (MOI=0.1), **(B)** pretreated with IFNβ for 4 hours, **(C)** for 12 hours or **(D)** pretreated with IFNγ for 12 hours followed by infection with MCMV (MOI=1). Supernatants were taken one hour (d0), 1, 3 and 6 days (d) after infection. Virus titres were determined in a plaque forming assays on Stat1-deficient MEFs. Mean values ± SD of technical duplicates are shown.

Details of microarray results

Functional annotation of genes regulated in response to poly(I:C)

Poly(I:C) treatment had a major impact on the macrophage transcriptome as about 1200 genes were up- and 2300 genes downregulated in WT FLMs. Functional annotation and statistical analysis (GeneSpring Expression Analysis 7.3.1 tool, Agilent Technologies) revealed that genes upregulated in response to poly(I:C) were significantly enriched in immunity-related GO-categories, such as "defense response", "immune response" or "response to virus" (table App. 1). In contrast, genes downregulated after poly(I:C) treatment were enriched in metabolism-related GO-categories, e.g. "DNA metabolism", "macromolecule metabolism" or "biopolymer metabolism" (table App. 2).

Genes involved in “apoptosis” and “cell death” were up-regulated, whereas genes necessary for “cell cycle” and “mitosis” were down-regulated in response to poly(I:C) underlining the proapoptotic nature of an antiviral response in this case provoked by poly(I:C) treatment.

Table App. 1: GO “biological process” categories upregulated in WT upon poly(I:C) treatment (top 30 categories; sorted by significance of enrichment).

Category	*p-Value*	Genes in Category	% of Genes in Category	Genes in List in Category	% of Genes in List in Category
GO:9607: response to biotic stimulus	*3.10E-67*	711	5.2	163	24.2
GO:6952: defense response	*5.95E-60*	680	5.0	151	22.4
GO:6955: immune response	*6.66E-53*	558	4.1	129	19.2
GO:43207: response to external biotic stimulus	*4.30E-32*	377	2.8	83	12.3
GO:9613: response to pest. pathogen or parasite	*2.03E-31*	358	2.6	80	11.9
GO:9605: response to external stimulus	*1.08E-24*	539	3.9	89	13.2
GO:9615: response to virus	*6.37E-23*	45	0.3	26	3.9
GO:6950: response to stress	*6.55E-17*	790	5.8	96	14.3
GO:9611: response to wounding	*2.26E-13*	265	1.9	45	6.7
GO:6954: inflammatory response	*3.29E-13*	143	1.0	32	4.8
GO:45087: innate immune response	*3.55E-13*	54	0.4	20	3.0
GO:19883: antigen presentation. endogenous antigen	*1.97E-11*	13	0.1	10	1.5
GO:6915: apoptosis	*7.41E-11*	469	3.4	58	8.6
GO:16265: death	*1.19E-10*	513	3.8	61	9.1
GO:12501: programmed cell death	*1.58E-10*	478	3.5	58	8.6
GO:50896: response to stimulus	*1.69E-10*	2408	17.6	183	27.2
GO:8219: cell death	*1.76E-10*	505	3.7	60	8.9
GO:19882: antigen presentation	*2.66E-10*	40	0.3	15	2.2
GO:19885: antigen processing. endogenous antigen via MHC class I	*3.12E-10*	12	0.1	9	1.3
GO:42107: cytokine metabolism	*1.27E-08*	51	0.4	15	2.2
GO:30333: antigen processing	*1.69E-08*	32	0.2	12	1.8
GO:50776: regulation of immune response	*1.92E-08*	102	0.7	21	3.1
GO:42981: regulation of apoptosis	*3.25E-07*	291	2.1	36	5.3
GO:42089: cytokine biosynthesis	*4.55E-07*	49	0.4	13	1.9
GO:50874: organismal physiological process	*4.67E-07*	2154	15.8	154	22.9
GO:7243: protein kinase cascade	*5.01E-07*	165	1.2	25	3.7
GO:1817: regulation of cytokine production	*5.24E-07*	42	0.3	12	1.8
GO:1816: cytokine production	*5.37E-07*	66	0.5	15	2.2
GO:43067: regulation of programmed cell death	*5.82E-07*	298	2.2	36	5.3
GO:7249: I-kappaB kinase/NF-kappaB cascade	*1.36E-06*	31	0.2	10	1.5

Table App. 2: GO "biological process" categories downregulated in WT upon poly(I:C) treatment (top 30 categories; sorted by significance of enrichment).

Category	*p-Value*	Genes in Category	% of Genes in Category	Genes in List in Category	% of Genes in List in Category
GO:50875: cellular physiological process	*1.15E-29*	9300	68.1	1109	81.0
GO:6259: DNA metabolism	*4.57E-28*	520	3.8	138	10.1
GO:44238: primary metabolism	*3.40E-27*	6143	45.0	804	58.7
GO:44237: cellular metabolism	*1.76E-25*	6427	47.0	826	60.3
GO:8152: metabolism	*7.04E-25*	6804	49.8	861	62.9
GO:43170: macromolecule metabolism	*1.51E-23*	3860	28.3	549	40.1
GO:43283: biopolymer metabolism	*1.08E-22*	2424	17.7	381	27.8
GO:7049: cell cycle	*4.02E-21*	607	4.4	138	10.1
GO:278: mitotic cell cycle	*4.97E-17*	181	1.3	59	4.3
GO:279: M phase	*7.24E-17*	172	1.3	57	4.2
GO:6139: nucleobase, nucleoside, nucleotide and nucleic acid metabolism	*7.46E-17*	2837	20.8	407	29.7
GO:51301: cell division	*3.97E-16*	199	1.5	61	4.5
GO:7067: mitosis	*7.83E-15*	122	0.9	44	3.2
GO:87: M phase of mitotic cell cycle	*1.10E-14*	123	0.9	44	3.2
GO:6281: DNA repair	*9.04E-13*	153	1.1	47	3.4
GO:51276: chromosome organization and biogenesis	*1.51E-12*	265	1.9	66	4.8
GO:9058: biosynthesis	*3.05E-12*	1123	8.2	184	13.4
GO:6974: response to DNA damage stimulus	*5.25E-12*	188	1.4	52	3.8
GO:6323: DNA packaging	*1.33E-11*	240	1.8	60	4.4
GO:9719: response to endogenous stimulus	*1.93E-11*	194	1.4	52	3.8
GO:6996: organelle organization and biogenesis	*1.66E-10*	928	6.8	153	11.2
GO:6260: DNA replication	*2.65E-10*	105	0.8	34	2.5
GO:7001: chromosome organization and biogenesis (sensu Eukaryota)	*9.43E-10*	252	1.8	58	4.2
GO:16070: RNA metabolism	*2.25E-09*	386	2.8	77	5.6
GO:44249: cellular biosynthesis	*3.09E-09*	998	7.3	157	11.5
GO:16126: sterol biosynthesis	*1.49E-08*	25	0.2	14	1.0
GO:7059: chromosome segregation	*3.63E-08*	34	0.2	16	1.2
GO:6396: RNA processing	*4.59E-08*	306	2.2	62	4.5
GO:6364: rRNA processing	*1.37E-07*	41	0.3	17	1.2
GO:16072: rRNA metabolism	*2.08E-07*	42	0.3	17	1.2

Detailed list of Oct-6 target genes in FLMs after poly(I:C) treatment

A subset of 201 genes was found to be differentially regulated between WT and Oct-6-deficient FLMs after poly(I:C) treatment, 125 reduced (table App. 3), 86 induced (table App. 4). These results indicate that Oct-6 exerts positive and negative functions in regulating transcriptional responses to poly(I:C).

Table App. 3: Genes significantly reduced in the absence of Oct-6 in FLMs after poly(I:C) treatment (at least 2-fold change (FC), *p<0.05*; genes sorted by FC).

Probe_ID	FC	*p-value*	Gene Symbol	RefSeq	Description
617536	0.18	*0.0124*	Zdhhc3	NM_026917.4	zinc finger. DHHC domain containing 3
460096	0.20	*0.0295*	Caml	null	calcium modulating ligand
853119	0.22	*0.0029*	LOC623921	null	null
681506	0.23	*0.0324*	Eef1a2	NM_007906.2	eukaryotic translation elongation factor 1 alpha 2
608851	0.23	*0.0386*	Tspan31	null	tetraspanin 31
701281	0.23	*0.0086*	Prmt6	null	protein arginine N-methyltransferase 6
923656	0.24	*0.0366*	Lrpb7	NM_013588.1	leucine rich protein. B7 gene
461196	0.25	*0.0000*	Trmt2b	NM_172540.1	TRM2 tRNA methyltransferase 2 homolog B (S. cerevisiae)
360339	0.25	*0.0464*	Klra2	null	killer cell lectin-like receptor. subfamily A. member 2
687306	0.25	*0.0088*	Terc	null	telomerase RNA component
466313	0.26	*0.0173*	Pou3f1	NM_011141.1	POU domain. class 3. transcription factor 1
475048	0.27	*0.0435*	U2af1-rs2	null	U2 small nuclear ribonucleoprotein auxiliary factor (U2AF) 1. related sequence 2
496065	0.28	*0.0108*	3021401C12Rik	null	RIKEN cDNA 3021401C12 gene
653822	0.28	*0.0454*	Kif3a	null	kinesin family member 3A
461332	0.28	*0.0160*	Olfr1410	NM_146491.1	olfactory receptor 1410
778122	0.29	*0.0149*	2200001I15Rik	NM_183278.1	RIKEN cDNA 2200001I15 gene
834612	0.29	*0.0462*	Oit1	null	oncoprotein induced transcript 1
876633	0.30	*0.0075*	Ctnnd2	NM_008729.1	catenin (cadherin associated protein). delta 2
731197	0.31	*0.0033*	Rcn3	NM_026555.1	reticulocalbin 3. EF-hand calcium binding domain
498376	0.31	*0.0336*	Olfr982	NM_146854.1	olfactory receptor 982
834086	0.31	*0.0044*	Rcor3	NM_144814.2	REST corepressor 3
602262	0.31	*0.0350*	A930011G23Rik	null	RIKEN cDNA A930011G23 gene
922907	0.32	*0.0156*	Map3k12	NM_009582.2	mitogen activated protein kinase kinase kinase 12
515044	0.32	*0.0101*	Zfp691	NM_183140.1	zinc finger protein 691
452181	0.32	*0.0433*	Zmiz1	NM_175264.2	zinc finger, MIZ-type containing 1
556058	0.32	*0.0136*	Rgag4	NM_183318.1	retrotransposon gag domain containing 4

Probe_ID	FC	*p-value*	Gene Symbol	RefSeq	Description
553608	0.32	*0.0014*	Gtf2f2	null	general transcription factor IIF, polypeptide 2/
430244	0.33	*0.0004*	1700088E04Rik	null	RIKEN cDNA 1700088E04 gene
806282	0.33	*0.0098*	Plin	NM_175640.1	perilipin
315360	0.33	*0.0201*	Zfp775	NM_173429.1	zinc finger protein 775
489609	0.33	*0.0317*	2210404J11Rik	NM_183133.1	RIKEN cDNA 2210404J11 gene
538641	0.33	*0.0485*	Oprd1	NM_013622.2	opioid receptor. delta 1
628730	0.34	*0.0383*	Rnf41	NM_026259.2	ring finger protein 41
600102	0.34	*0.0233*	Tstd2	NM_173033.2	thiosulfate sulfurtransferase (rhodanese)-like domain containing 2
924325	0.34	*0.0373*	Zfp96	NM_016684.1	zinc finger protein 96
525473	0.34	*0.0493*	Sprr2b	null	small proline-rich protein 2B
467664	0.34	*0.0256*	Epha10	NM_177671.2	Eph receptor A10
784635	0.34	*0.0077*	9630041N07Rik	NM_173387.1	RIKEN cDNA 9630041N07 gene
339824	0.35	*0.0122*	Egr3	NM_018781.1	early growth response 3
900911	0.35	*0.0150*	Olfr1425|Olfr1426	NM_001011853.1	olfactory receptor 1425|olfactory receptor 1426
371452	0.36	*0.0219*	Olfr167	NM_146935.1	olfactory receptor 167
523384	0.36	*0.0345*	BC067068	NM_207522.1	cDNA sequence BC067068
509621	0.36	*0.0077*	Arhgef11	NM_001003912.1	Rho guanine nucleotide exchange factor (GEF) 11
632096	0.36	*0.0318*	4933422H20Rik	null	RIKEN cDNA 4933422H20 gene
331903	0.37	*0.0179*	4931431F19Rik	null	RIKEN cDNA 4931431F19 gene
778997	0.37	*0.0226*	Akr1e1	null	aldo-keto reductase family 1. member E1
405218	0.37	*0.0321*	Cysltr2	NM_133720.1	cysteinyl leukotriene receptor 2
501689	0.38	*0.0015*	Zfp605	null	zinc finger protein 605
733175	0.38	*0.0172*	Fam119a	NM_025964.2	family with sequence similarity 119, member A
481636	0.38	*0.0003*	Dnalc1	null	dynein, axonemal, light chain 1
600711	0.38	*0.0249*	Tbc1d16	null	TBC1 domain family. member 16
826596	0.39	*0.0180*	Rrp8	NM_025897.1	ribosomal RNA processing 8, methyltransferase, homolog (yeast)
643747	0.39	*0.0294*	Klhl12	NM_153128.1	kelch-like 12 (Drosophila)
698795	0.39	*0.0344*	Prlpe	null	prolactin-like protein E
555651	0.39	*0.0267*	Fanca	null	Fanconi anemia. complementation group A
516875	0.39	*0.0008*	Sgtb	NM_144838.1	small glutamine-rich tetratricopeptide repeat (TPR)-containing. beta
437482	0.39	*0.0111*	Zdhhc17	null	zinc finger. DHHC domain containing 17
789662	0.39	*0.0232*	2610507B11Rik	NM_001002004.1	RIKEN cDNA 2610507B11 gene
302319	0.39	*0.0143*	Pcsk1n	NM_013892.2	proprotein convertase subtilisin/kexin type 1 inhibitor

Probe_ID	FC	*p-value*	Gene Symbol	RefSeq	Description
466728	0.40	*0.0481*	Sfrs14	NM_172755.2	splicing factor. arginine/serine-rich 14
852764	0.40	*0.0497*	Flrt3	NM_178382.2	fibronectin leucine rich transmembrane protein 3
925399	0.40	*0.0239*	Lect1	NM_010701.1	leukocyte cell derived chemotaxin 1
782547	0.40	*0.0024*	Lsm10	NM_138721.1	U7 snRNP-specific Sm-like protein LSM10
603800	0.40	*0.0456*	Arhgef16	null	Rho guanine nucleotide exchange factor (GEF) 16
461234	0.40	*0.0314*	BB014433	NM_001007591.1	est
876790	0.40	*0.0147*	End2	null	ES neuronal differentiation 2
871506	0.40	*0.0258*	Gne	NM_015828.2	glucosamine
525897	0.41	*0.0363*	2610507I01Rik	null	RIKEN cDNA 2610507I01 gene
327644	0.41	*0.0215*	LOC636981	null	null
730850	0.41	*0.0141*	MGC60818	NM_001004181.1	null
325670	0.41	*0.0463*	Zfp11	NM_172462.1	zinc finger protein 11
412730	0.41	*0.0323*	Tmem86b	null	transmembrane protein 86B
659293	0.42	*0.0012*	Polm	NM_017401.1	polymerase (DNA directed). mu
670264	0.42	*0.0403*	Arsg	NM_028710.2	arylsulfatase G
335731	0.42	*0.0278*	BC028801	null	cDNA sequence BC028801
606179	0.42	*0.0038*	Pars2	NM_172272.1	prolyl-tRNA synthetase (mitochondrial)(putative)
473747	0.42	*0.0308*	4930525D18Rik	null	RIKEN cDNA 4930525D18 gene
892845	0.42	*0.0327*	Slc25a36	NM_138756.2	solute carrier family 25. member 36
552370	0.42	*0.0162*	Tmem183a	null	transmembrane protein 183A
606800	0.42	*0.0191*	Hbq1	NM_175000.1	hemoglobin. theta 1
663810	0.42	*0.0190*	Papd1	NM_026157.1	PAP associated domain containing 1
928427	0.43	*0.0160*	Lmo6	NM_175097.2	LIM domain only 6
366561	0.43	*0.0477*	Zfp788	NM_023363.1	zinc finger protein 788
576856	0.43	*0.0138*	Olfr1013	NM_146762.1	olfactory receptor 1013
360325	0.43	*0.0182*	Foxk2	null	forkhead box K2
509117	0.43	*0.0312*	Gm10033	NM_194351.1	predicted gene 10033
686810	0.44	*0.0211*	Pik3ca	NM_008839.1	phosphatidylinositol 3-kinase. catalytic. alpha polypeptide
354059	0.44	*0.0309*	Tpbpb	null	trophoblast specific protein beta/
846824	0.44	*0.0349*	B020017C02Rik	null	RIKEN cDNA B020017C02 gene
872447	0.44	*0.0356*	Gm7036	null	predicted gene 7036
748759	0.44	*0.0094*	Kazald1	NM_178929.2	Kazal-type serine peptidase inhibitor domain 1
365471	0.44	*0.0027*	Col13a1	NM_007731.1	procollagen. type XIII. alpha 1

Probe_ID	FC	*p-value*	Gene Symbol	RefSeq	Description
553168	0.44	*0.0263*	E430024I08Rik	null	RIKEN cDNA E430024I08 gene
675560	0.44	*0.0480*	Zfp414	NM_026712.1	zinc finger protein 414
469286	0.45	*0.0158*	5730409N16Rik	null	RIKEN cDNA 5730409N16 gene
851957	0.45	*0.0064*	Stk40	NM_028800.2	serine/threonine kinase 40
359762	0.45	*0.0097*	Ccdc27	null	coiled-coil domain containing 27
875269	0.45	*0.0323*	Gins4	NM_024240.3	GINS complex subunit 4 (Sld5 homolog)
342055	0.46	*0.0267*	LOC552874	null	null
743810	0.46	*0.0136*	6720463M24Rik	NM_175265.2	RIKEN cDNA 6720463M24 gene
724366	0.46	*0.0463*	2610027F03Rik	null	RIKEN cDNA 2610027F03 gene
457912	0.46	*0.0185*	D730001M18Rik	null	RIKEN cDNA D730001M18 gene
564703	0.46	*0.0050*	Cmtm7	null	CKLF-like MARVEL transmembrane domain containing 7
455948	0.46	*0.0299*	Kcnj2	NM_008425.2	potassium inwardly-rectifying channel. subfamily J. member 2
685184	0.46	*0.0099*	Sf3a1	null	splicing factor 3a. subunit 1
883636	0.46	*0.0356*	Btg1	null	B-cell translocation gene 1. anti-proliferative
853912	0.46	*0.0205*	Etl4	null	enhancer trap locus 4/
770438	0.47	*0.0418*	Slc25a23	NM_025877.2	solute carrier family 25 (mitochondrial carrier; phosphate carrier). member 23
620798	0.47	*0.0405*	Catsper3	NM_029772.1	cation channel. sperm associated 3
828936	0.47	*0.0143*	E030010A14Rik	NM_183160.1	RIKEN cDNA E030010A14 gene
929052	0.47	*0.0166*	Inpp5f	NM_178641.3	inositol polyphosphate-5-phosphatase F
614945	0.48	*0.0413*	1190002A17Rik	null	RIKEN cDNA 1190002A17 gene
552424	0.48	*0.0020*	Ptpn9	NM_019651.1	protein tyrosine phosphatase. non-receptor type 9
483305	0.48	*0.0467*	Gm1419	null	gene model 1419. (NCBI)
409901	0.48	*0.0299*	Vps4b	null	vacuolar protein sorting 4b (yeast)
581904	0.49	*0.0254*	Ism1	null	isthmin 1 homolog (zebrafish)
480631	0.49	*0.0473*	Pdxk	NM_172134.1	pyridoxal (pyridoxine. vitamin B6) kinase
554608	0.49	*0.0392*	Slc8a1	null	solute carrier family 8 (sodium/calcium exchanger), member 1/
773254	0.49	*0.0327*	1700012B07Rik	null	RIKEN cDNA 1700012B07 gene
577782	0.49	*0.0298*	Dnajb1	null	DnaJ (Hsp40) homolog, subfamily C, member 1/
495637	0.49	*0.0062*	Dapp1	NM_011932.1	dual adaptor for phosphotyrosine and 3-phosphoinositides 1
659670	0.50	*0.0141*	BC026645	null	cDNA sequence BC026645
665024	0.50	*0.0434*	Znrf4	NM_011483.1	zinc and ring finger 4
852467	0.50	*0.0093*	Btbd5	NM_025707.1	BTB (POZ) domain containing 5
858839	0.50	*0.0182*	Klhdc2	NM_027117.1	kelch domain containing 2

Table App. 4: Genes significantly enhanced in the absence of Oct-6 in FLMs after poly(I:C) treatment (at least 2-fold change (FC), *p<0.05*; genes sorted by FC).

Probe_ID	FC	*p-value*	Gene Symbol	RefSeq	Description
464717	4.62	*0.0077*	Dyrk1b	NM_010092.1	dual-specificity tyrosine-(Y)-phosphorylation regulated kinase 1b
482821	4.62	*0.0176*	4933411E02Rik	null	RIKEN cDNA 4933411E02 gene
308725	4.24	*0.0152*	Senp8	null	SUMO/sentrin specific peptidase 8
779189	3.97	*0.0169*	Tmem104	null	transmembrane protein 104
575351	3.64	*0.0022*	Klhdc8b	NM_030075.1	kelch domain containing 8B
462774	3.44	*0.0414*	Ccdc69	NM_177471.2	coiled-coil domain containing 69
760102	3.41	*0.0295*	Sdc1	NM_011519.1	syndecan 1
615421	3.40	*0.0267*	Kptn	NM_133727.1	kaptin
441148	3.39	*0.0004*	BC048403	NM_173022.2	cDNA sequence BC048403
676377	3.35	*0.0360*	Pgap1	null	post-GPI attachment to proteins 1
926998	3.35	*0.0011*	Rab38	NM_028238.5	Rab38. member of RAS oncogene family
438223	3.32	*0.0169*	2900093K20Rik	null	RIKEN cDNA 2900093K20 gene
906799	3.31	*0.0034*	E4f1	NM_007893.1	E4F transcription factor 1
515079	3.29	*0.0325*	Dis3l2	NM_153530.1	DIS3 mitotic control homolog (S. cerevisiae)-like 2
375317	3.28	*0.0017*	Setmar	NM_178391.2	SET domain and mariner transposase fusion gene
576988	3.19	*0.0208*	2810021J22Rik	null	RIKEN cDNA 2810021J22 gene
755758	3.19	*0.0316*	Vnn1	NM_011704.1	vanin 1
786159	3.18	*0.0029*	Ahcyl2	NM_021414.3	S-adenosylhomocysteine hydrolase-like 2
831829	3.13	*0.0288*	Ccdc28a	NM_144820.1	coiled-coil domain containing 28A
862084	3.11	*0.0438*	Gramd4	NM_172611.1	GRAM domain containing 4
705683	3.07	*0.0034*	Pot1b	null	protection of telomeres 1B
304938	3.02	*0.0276*	5730405O12Rik	null	RIKEN cDNA 5730405O12 gene
652183	3.02	*0.0040*	Aggf1	NM_025630.2	angiogenic factor with G patch and FHA domains 1
456695	2.98	*0.0231*	4930505K14Rik	null	RIKEN cDNA 4930505K14 gene
780025	2.97	*0.0293*	4930529M08Rik	NM_175280.2	RIKEN cDNA 4930529M08 gene
642032	2.94	*0.0374*	1190005F20Rik	null	RIKEN cDNA 1190005F20 gene
363922	2.93	*0.0324*	Yod1	NM_178691.2	YOD1 OTU deubiquitinating enzyme 1 homologue (S. cerevisiae)NA 9930028C20 gene
674148	2.90	*0.0017*	Snx13	null	sorting nexin 13
357720	2.89	*0.0036*	Phka1	null	phosphorylase kinase alpha 1 isoform 1
313803	2.87	*0.0168*	Rnh1	null	ribonuclease/angiogenin inhibitor 1

Probe_ID	FC	*p-value*	Gene Symbol	RefSeq	Description
533138	2.86	*0.0472*	Pnpo	NM_134021.1	pyridoxine 5'-phosphate oxidase
553200	2.84	*0.0212*	Sesn3	null	sestrin 3
924582	2.83	*0.0389*	Capn1	NM_007600.2	calpain 1
721573	2.81	*0.0009*	Mpi	null	mannose phosphate isomerase
388075	2.76	*0.0427*	Adra2a	null	adrenergic receptor. alpha 2a
326700	2.76	*0.0235*	Crsp7	null	cofactor required for Sp1 transcriptional activation. subunit 7
436262	2.73	*0.0242*	1110031I02Rik	NM_025402.1	RIKEN cDNA 1110031I02 gene
440799	2.65	*0.0451*	Slc2a1	NM_011400.1	solute carrier family 2 (facilitated glucose transporter). member 1
726921	2.63	*0.0431*	1110004E09Rik	NM_026502.1	RIKEN cDNA 1110004E09 gene
916478	2.63	*0.0420*	Ibrdc2	NM_146042.2	IBR domain containing 2
406158	2.63	*0.0212*	Il17c	NM_145834.1	interleukin 17C
316450	2.62	*0.0349*	Dlgh2	NM_011807.1	discs. large homolog 2 (Drosophila)
832842	2.55	*0.0206*	Arhgef4	null	Rho guanine nucleotide exchange factor 4/
496110	2.55	*0.0169*	Olfr310	NM_001011520.1	olfactory receptor 310
344219	2.55	*0.0479*	Pon2	NM_183308.1	paraoxonase 2
513587	2.54	*0.0386*	Cd276	NM_133983.2	CD276 antigen
896781	2.54	*0.0310*	LOC634451	null	discontinued
794783	2.53	*0.0060*	4921525O09Rik	null	RIKEN cDNA 4921525O09 gene
358405	2.53	*0.0020*	9930038B18Rik	NM_176929.3	RIKEN cDNA 9930038B18 gene
895890	2.52	*0.0031*	Olfr598lOlfr597	NM_001011845.1	olfactory receptor 598lolfactory receptor 597
453496	2.50	*0.0407*	Strbp	NM_009261.1	spermatid perinuclear RNA binding protein
401839	2.49	*0.0271*	Defb5	NM_030734.1	defensin beta 5
381530	2.48	*0.0337*	Senp5	null	SUMO/sentrin specific peptidase 5
837461	2.45	*0.0336*	Wnk1	NM_198703.1	WNK lysine deficient protein kinase 1
626456	2.44	*0.0017*	Grpel1	NM_024478.2	GrpE-like 1. mitochondrial
556097	2.43	*0.0238*	Abcd4	NM_008992.1	ATP-binding cassette. sub-family D (ALD). member 4
754664	2.43	*0.0201*	Tnfrsf17	NM_011608.1	tumor necrosis factor receptor superfamily. member 17
720766	2.42	*0.0126*	Duoxa2	NM_025777.1	dual oxidase maturation factor 2
887858	2.40	*0.0067*	Ppp1r10	NM_175934.2	protein phosphatase 1. regulatory subunit 10
375461	2.39	*0.0078*	2010315B03Rik	null	RIKEN cDNA 2010315B03 gene
530372	2.37	*0.0141*	Epha4	NM_007936.2	Eph receptor A4
563861	2.37	*0.0450*	Disc1	null	disrupted in schizophrenia 1 isoform 1/ disrupted in schizophrenia 1 isoform 2/
668249	2.34	*0.0196*	Rhobtb1	null	Rho-related BTB domain containing 1

Probe_ID	FC	*p-value*	Gene Symbol	RefSeq	Description
498112	2.32	*0.0316*	Cacnb4	NM_146123.1	calcium channel. voltage-dependent. beta 4 subunit
388184	2.31	*0.0176*	8430426H19Rik	null	RIKEN cDNA 8430426H19 gene
909303	2.29	*0.0162*	Coq4	NM_178693.2	coenzyme Q4 homolog (yeast)
627826	2.25	*0.0465*	Prkci	NM_008857.2	protein kinase C. iota
379623	2.21	*0.0167*	Narg2	NM_145618.3	NMDA receptor-regulated gene 2
765948	2.18	*0.0081*	Pdzd4	null	PDZ domain containing 4/
807992	2.16	*0.0411*	Ddx27	NM_153065.1	DEAD (Asp-Glu-Ala-Asp) box polypeptide 27
347501	2.16	*0.0109*	Tesc	NM_021344.2	tescalcin
594289	2.14	*0.0157*	AU017455	null	est AU017455
387041	2.13	*0.0149*	Cxx1c	NM_028375.2	CAAX box 1 homolog C (human)
420073	2.12	*0.0022*	Lrdd	NM_022654.1	leucine-rich and death domain containing
744134	2.10	*0.0170*	Timm9	null	translocase of inner mitochondrial membrane 9 homolog (yeast)
885026	2.05	*0.0285*	Afap1l2	NM_146102.1	actin filament associated protein 1-like 2

Validation of microarray data: supplemental data

As shown in the results, 2 out of 7 genes were positively validated for differential expression between WT and Oct-6-deficient macrophages after poly(I:C) treatment (Figure 33). For the rest of the genes, namely Dapp1, Dyrk1b, E4f1, Map3k12 and Zdhhc3, microarray results (table App. 5) could not be reproduced by RT-qPCR (Figure App. 17A-E). According to the microarray data, expression levels of Dyrk1b and Zdhhc3 were not altered upon treatment in WT cells, but up- or downregulated in the absence of Oct-6, but RT-qPCR results showed similar regulation of mRNA levels in both genotypes. Microarray data showed a reduction of E4f1 and Map3k12 expression levels after treatment in WT cells, but constant or less reduced levels in the absence of Oct-6, respectively. RT-qPCR showed similar reduction of E4f1 and Map3k12 expression in both genotypes.

According to the microarray data, Dapp1 was induced about 3-fold in WT FLMs. In the absence of Oct-6, expression levels of Dapp1 were about 2-fold lower after poly(I:C) treatment in comparison the WT situation. RT-qPCR analysis showed that Dapp1 is neither induced in the WT, nor is it reduced in the absence of Oct-6 (Figure App. 17A).

A possible reason for the discrepancy between microarray and RT-qPCR results is that the qPCR assays were not positioned in the same region as the microarray probes. The microarray results might still be right for alternative splice forms (Morey *et al.*, 2006). In order to test this possibility, it would be necessary to design qPCR assays located within the respective microarray probe sequence.

Table App. 5: Microarray data for the genes showing different expression patterns in microarray *versus* RT-qPCR analysis.

gene symbol (gene name)	probe_ID RefSeq	WT inducibility (mean ± SD)	Oct6-/- *vs.* WT after poly(I:C) (mean ± SD)	*P-value* for Oct6-/- *vs.* WT after poly(I:C)
Dapp1 (dual adaptor for phospho-tyrosine and 3-phospho-inositides 1)	495637 NM_011932.1	3.1 ± 1.6	0.49 ± 0.096	*0.0062*
Dyrk1b (dual-specificity tyrosine-(Y)-phosphorylation regulated kinase 1b)	464717 NM_010092.1	1.1 ± 0.4	4.8 ± 2.45	*0.0077*
E4f1 (E4F transcription factor 1)	906799 NM_007893.1	0.3 ± 1.5	3.3 ± 0.38	*0.0034*
Map3k12 (mitogen-activated protein kinase kinase kinase 12)	922907 NM_009582.2	0.3 ± 0.1	0.39 ± 0.108	*0.0156*
Zdhhc3 (zinc finger, DHHC domain containing 3)	617536 NM_026917.4	1.0 ± 0.2	0.23 ± 0.131	*0.0124*

Figure App. 17 – continued on the following page.

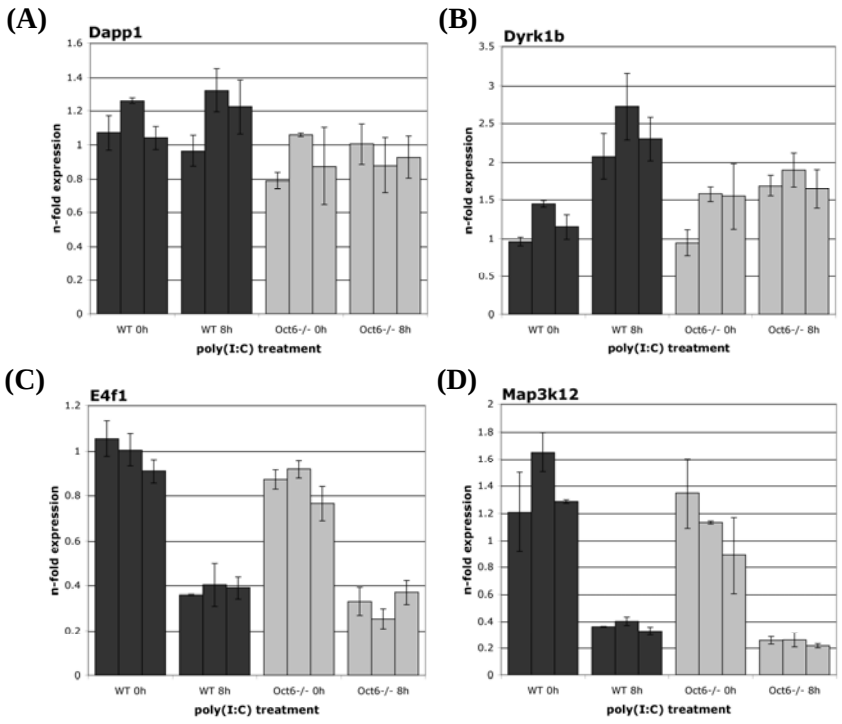

(E)

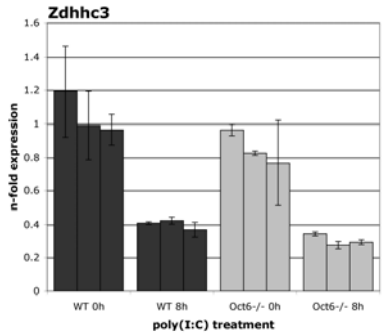

Figure App. 17: RT-qPCR data for the genes showing different expression patterns in microarray *versus* RT-qPCR analysis. WT and Oct-6-deficient FLMs were treated with poly(I:C) (50 µg/ml) for 8 hours. For validation, cDNA of the same RNA samples that had been analysed on the microarray, was used. N-fold expression levels of **(A)** Dapp1, **(B)** Dyrk1b, **(C)** E4f1, **(D)** Map3k12 and **(E)** Zdhhc3 were determined by RT-qPCR, applying the ΔΔCt method, normalising to Ube2d2 (mean values of technical duplicates ± SD are shown).

CURRICULUM VITAE

Name: Elisabeth Hofmann

Nationality: Austrian

Date of birth: January, 16th 1980

Place of birth: Graz, Austria

Education:

since October 2005: PhD thesis in the Laboratory of Dr. Birgit Strobl/Prof. Dr. Mathias Müller, titled: "*The role of Tyk2 in type I interferon signalling: identification and characterisation of novel target genes*".

October 2002 – April 2005: Diploma thesis at the Institute of Animal Breeding and Genetics, University of Veterinary Medicine, Laboratory of Dr. Ralf Steinborn/Prof. Dr. Mathias Müller, titled: "*mRNA profiling of immune responses*".

October 2001 – October 2002: studies of Biology with focus on Microbiology and Genetics at the University of Vienna

October 1998 – July 2001: studies of Biology, with focus on Microbiology at the Karl-Franzens-University in Graz.

June 1998: Matura, passed "with excellent success"

Publications:

Vogl C., Flatt T., Fuhrmann B., Hofmann E., Wallner B., Stiefvater R., Kovarik P., Strobl B., and Müller M. (2010). Transcriptome analysis reveals a major impact of tyrosine kinase 2 (Tyk2) on the expression of interferon responsive and metabolic genes.
– *BMC Genomics,* accepted.

Hofmann E., Reichart U., Gausterer C., Guelly C., Meijer D., Müller M., and Strobl B. (2010). Octamer-binding factor 6 (Oct-6/Pou3f1) is an interferon-inducible protein and contributes to dsRNA-mediated innate immune responses.
– submitted.

Published abstracts:

Hofmann E., Reichart U., Gausterer C., Meijer D., Müller M., and Strobl B. (2008). OCT-6 (POU3F1, SCIP, TST-1) is an interferon-inducible protein. Cytokine *43,* 242.

Hofmann E., Reichart U., Gausterer C., Guelly C., Meijer D., Müller M., and Strobl B. (2009). Oct-6 is an interferon-inducible protein and contributes to the transcriptional responses to poly(I:C). Cytokine *48,* 88.

Meetings:

Cytokines 2006: 6th Joint meeting of the International Cytokine Society (ISC), the International Society for Interferon and Cytokine Research (ISICR) and the European Cytokine Society (ECS).

Cytokines 2008: 7th Joint Conference of the International Cytokine Society and the International Society for Interferon and Cytokine Research: Cytokines in cancer, inflammation and infectious diseases: translating science into health. – Poster presentation.

Cytokines 2009: Tri-Society Annual Conference of the Society for Leukocyte Biology, the International Cytokine Society and the International Society for Interferon and Cytokine Research: Cellular and cytokine interactions in health and disease. – Poster presentation.

LEBENSLAUF

Name: Elisabeth Hofmann
Nationalität: Österreicherin
Geburtsdatum: 16. Jänner 1980
Geburtsort: Graz, Österreich

Ausbildung:

seit Oktober 2005: Dissertation im Labor von Dr. Birgit Strobl/Prof. Dr. Mathias Müller, mit dem Titel: "*The role of Tyk2 in type I interferon signalling: identification and characterisation of novel target genes*".

Oktober 2002 – April 2005: Diplomarbeit am Institut für Tierzucht und Genetik der Veterinärmedizinischen Universität Wien, im Labor von Dr. Ralf Steinborn/Prof. Dr. Mathias Müller, mit dem Titel: "*mRNA profiling of immune responses*".

Oktober 2001 – Oktober 2002: Studium der Biologie, Studienzweig Mikrobiologie und Genetik an der Universität Wien

Oktober 1998 – Juli 2001: Studium der Biologie, Studienzweig Mikrobiologie an der Karl-Franzens-University Graz.

Juni 1998: Matura, "mit Auszeichnung" bestanden

Publikationen:

Vogl C., Flatt T., Fuhrmann B., Hofmann E., Wallner B., Stiefvater R., Kovarik P., Strobl B., and Müller M. (2010). Transcriptome analysis reveals a major impact of tyrosine kinase 2 (Tyk2) on the expression of interferon responsive and metabolic genes. – *BMC Genomics,* accepted.

Hofmann E., Reichart U., Gausterer C., Guelly C., Meijer D., Müller M., and Strobl B. (2010). Octamer-binding factor 6 (Oct-6/Pou3f1) is an interferon-inducible protein and contributes to dsRNA-mediated innate immune responses.
– submitted.

Publizierte Abstracts:

Hofmann E., Reichart U., Gausterer C., Meijer D., Müller M., and Strobl B. (2008). OCT-6 (POU3F1, SCIP, TST-1) is an interferon-inducible protein. Cytokine *43,* 242.

Hofmann E., Reichart U., Gausterer C., Guelly C., Meijer D., Müller M., and Strobl B. (2009). Oct-6 is an interferon-inducible protein and contributes to the transcriptional responses to poly(I:C). Cytokine *48,* 88.

Konferenzen:

Cytokines 2006: 6th Joint meeting of the International Cytokine Society (ISC), the International Society for Interferon and Cytokine Research (ISICR) and the European Cytokine Society (ECS).

Cytokines 2008: 7th Joint Conference of the International Cytokine Society and the International Society for Interferon and Cytokine Research: Cytokines in cancer, inflammation and infectious diseases: translating science into health. – Poster Präsentation.

Cytokines 2009: Tri-Society Annual Conference of the Society for Leukocyte Biology, the International Cytokine Society and the International Society for Interferon and Cytokine Research: Cellular and cytokine interactions in health and disease. – Poster Präsentation.

POSTERS

Cytokines 2008, Montréal

Oct-6 (Pou3f1, Tst-1, SCIP) is an interferon-inducible protein

Elisabeth Hofmann[1], Ursula Reichart[1], Christian Gausterer[1], Dies Meijer[2], Mathias Müller[1,3] and Birgit Strobl[1]

[1]Department for Biomedical Sciences, Institute of Animal Breeding and Genetics, University of Veterinary Medicine Vienna, Austria,
[2]Department of Cell Biology and Genetics, Erasmus University Medical Center Rotterdam, Netherlands
[3]University Center Biomodels Austria, University of Veterinary Medicine Vienna, Austria.

Introduction

Octamer binding factor 6 (Oct-6) belongs to the Pit-Oct-Unc (POU)-family of transcription factors and can either positively or negatively influence gene expression. So far, expression of Oct-6 was described to be confined to embryonic stem cells, neuronal subpopulations, myelinating glia, pancreatic islets, and epidermal keratinocytes. Oct-6 is strictly regulated and plays a crucial role in the progression from pro-myelinating to myelinating Schwann cells, whereas its role in the other cell types is less clear (1).
We report here that Oct-6 is an interferon β (IFNβ) inducible protein and we present detailed kinetics and molecular requirements for Oct-6 induction in fibroblasts and macrophages.

Schematic structure of Oct-6.
The POU-domain is highly conserved amongst the members of the POU-family. Transcription factors belonging to this family recognise and bind to a common octamer consensus motif (ATGCAAAT) (2).

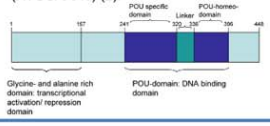

The POU-family of transcription factors.

class	members
I	Pit-1
II	Oct-1, Oct-2, Skn-1a
III	**Oct-6, Brn-1, Brn-2, Brn-4**
IV	Brn-3a, Brn-3b, Brn-3c
V	Oct-4, Sprm-1
VI	Brn-5, Wtsl

Results

IFNβ induces Oct-6 expression in murine fibroblasts (MEFs).

Tyrosine kinase 2 (Tyk2) is required for full induction.

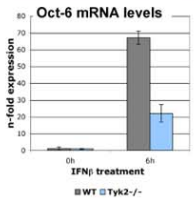

Wildtype (WT) and Tyk2 deficient MEF cell lines were treated with IFNβ (500 U/ml) for 6 h. Expression of Oct-6 mRNA was analysed by RT-qPCR. Results from three independent cell lines *per* genotype are depicted (mean values +/- SD).

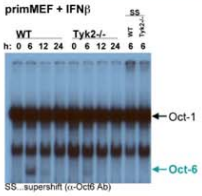

WT and Tyk2 deficient primary MEFs were treated with IFNβ (1000 U/ml) for the indicated times. Electrophoretic mobility shift assays (EMSAs) were performed with a probe containing the octamer consensus motif. Identity of Oct-6 was confirmed by supershift with α-Oct-6 antibody (Santa Cruz).

IFNβ induces Oct-6 expression in macrophages.

The induction is completely dependent on signal transducer and activator of transcription (STAT1).

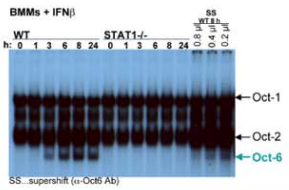

WT and STAT1 deficient bone marrow-derived macrophages (BMMs) were treated with IFNβ (1000 U/ml) for the indicated times. EMSAs were performed with a probe containing the octamer consensus motif. Identity of Oct-6 was confirmed by supershift with indicated amounts of α-Oct-6 antibody (Santa Cruz).

Murine Cytomegaglovirus (MCMV) infection induces Oct-6 expression in macrophages.

The induction is completely dependent on the presence of IFNα/β receptor 1 (Ifnar1) and partially dependent on Tyk2 and IFNβ.

WT, Tyk2-/- and Ifnar1-/- BMMs were infected with MCMV (moi=1) for the indicated times. Oct-6 mRNA expression was analysed by RT-qPCR. Results from one representative experiment (n=2) are shown (mean values +/- SD of technical duplicates).

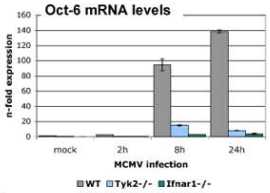

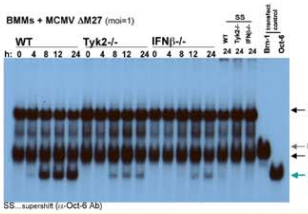

WT, Tyk2-/- and IFNβ-/- BMMs were infected with MCMV ΔM27 (moi=1) for the indicated times. EMSAs were performed with a probe containing the octamer motif. Identity of Oct-6 was confirmed by supershift with α-Oct-6 antibody (Santa Cruz) and Oct-6 overexpression.

Oct-6 localizes to the nucleus upon IFNβ and poly(I:C) treatment.

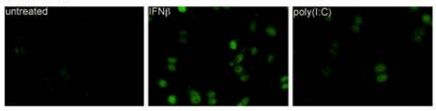

Fetal liver macrophages (FLMs) were grown on glass slides, treated with IFNβ (1000 U/ml) or poly(I:C) (50 µg/ml), or left untreated. After 8 h they were fixed with formaldehyde (4%) and permeabilised with methanol. Oct-6 was detected by immunofluorescence with α-Oct-6 primary antibody (Santa Cruz) and fluorescently labeled α-goat IgG secondary antibody (Alexa).

Oct-6 overexpression strongly induces IFNβ mRNA.

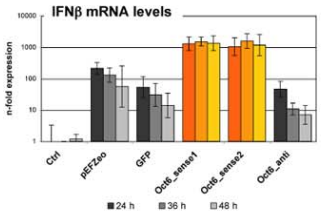

Primary MEFs were transfected with 10 µg of empty vector (pEFZeo), enhanced-GFP expression vector (Amaxa; GFP), two different plasmids for Oct-6 expression (Oct6_sense1/2) and a plasmid containing Oct-6 cDNA in antisense direction (Oct6_anti). As a control untransfected cells (Ctrl) were analysed. IFNβ mRNA levels were determined by RT-qPCR at 24, 36, and 48 h after transfection. Mean values (+/- SD) derived from 3 independent experiments are shown.

Summary and conclusions

- Oct-6 is an IFNα/β and IFNγ inducible protein in at least two different cell types (murine fibroblasts and macrophages).
- Induction of Oct-6 by IFNβ is dependent on STAT1 and partially dependent on Tyk2.
- Murine Cytomegalovirus infection and poly(I:C) treatment lead to the expression of Oct-6 in an IFNα/β receptor (Ifnar1) dependent manner.
- Oct-6 translocates to the nucleus upon IFNβ and poly(I:C) treatment.
- Overexpression of Oct-6 in primary fibroblasts strongly upregulates IFNβ mRNA levels.
- **Oct-6 expression and activity are not as restricted as previously thought.**
- **Data suggest novel functions of Oct-6 in innate immunity.**

References
1.Jaegle M., Mandemakers W., Broos L., Zwart R., Karis A., Visser P., Grosveld F., Meijer D. (1996). The POU factor Oct-6 and Schwann cell differentiation. *Science*, 273:507-510.
2.Phillips K. and Luisi B.(2000). The virtuoso of versatility: POU proteins that flex to fit. *Journal of Molecular Biology*, 302:1023-1039.

Acknowledgement
MM is funded by the Austrian Science Fund (FWF) SFB F28 Jak-Stat Signalling. Biomodels Austria is supported by the Federal Austrian Ministry of Science and Research (BM.W_F° GZ200.11/1-VI/1/2004). BS was partially supported by the Austrian Science Fund (FWF, P15892).

Cytokines 2009, Lisbon

Oct-6 (Pou3f1, Tst-1, SCIP) is an interferon-inducible protein and contributes to the transcriptional responses to poly(I:C)

Elisabeth Hofmann[1], Ursula Reichart[1], Christian Gausterer[1], Christian Gülly[2], Dies Meijer[3], Mathias Müller[1,4] and Birgit Strobl[1]

[1]*Institute of Animal Breeding and Genetics, Department for Biomedical Sciences, University of Veterinary Medicine Vienna, Austria,*
[2]*Center for Medical Research, Medical University Graz, Austria,*
[3]*Department of Cell Biology and Genetics, Erasmus University Medical Center Rotterdam, Netherlands,*
[4]*University Center Biomodels Austria, University of Veterinary Medicine Vienna, Austria.*

Introduction

Octamer binding factor 6 (Oct-6) belongs to the Pit-Oct-Unc (POU)-family of transcription factors and can either positively or negatively influence gene expression. Oct-6 plays a crucial role in terminal differentiation of myelinating Schwann cells. Its expression is tightly controlled on the transcriptional level, but the factors and *cis*-acting elements involved are largely unknown. Tissue-specific and time-dependent expression is regulated by distal enhancer elements (1).

We report here that Oct-6 is an interferon- (IFN-) inducible protein and we present detailed kinetics and molecular requirements for Oct-6 induction in macrophages. Moreover, we show involvement of Oct-6 in the transcriptional control of a subset of genes in response to poly(I:C) treatment of macrophages.

DNA binding of POU-proteins.
The POU-domain is highly conserved amongst the members of the POU-family. Transcription factors belonging to this family recognise and bind to a common octamer consensus motif (ATGCAAAT) (2).

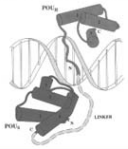

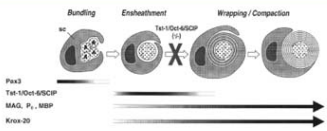

Role of Oct-6 in Schwann cell development.
Knock out of Oct-6 results in a perinatally lethal phenotype, which is due to breathing defects. Schwann cells deficient for Oct-6 are transiently arrested in a pre-myelinating stage (1, 3).

Results

IFNβ, poly(I:C) and MCMV induce Oct-6 expression/activity in macrophages

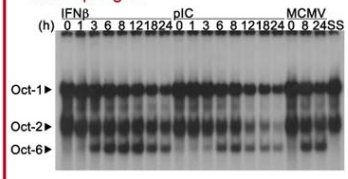

Wild type (WT) bone marrow-derived macrophages (BMMs) were treated with IFNβ (1000 U/ml), poly(I:C) (pIC; 50 µg/ml) or were infected with murine cytomegalovirus (MCMV; moi=1) for the indicated times. EMSAs were performed with an octamer motif containing oligonucleotide. (SS: supershift of the IFNβ_8h sample (lane 5) with an α-Oct-6 antibody (Santa Cruz)).

Expression of Oct-6 in response to poly(I:C) is mediated by autocrine/paracrine IFNα/β signalling

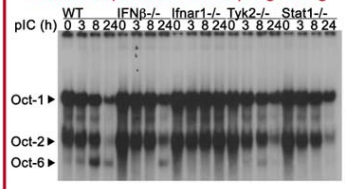

WT, IFNβ-, Ifnar1-, Tyk2- and Stat1-deficient BMMs were treated with poly(I:C) (pIC; 50 µg/ml) for the indicated times. EMSAs were performed with an octamer motif containing oligonucleotide.

Stat1 binds to the Oct-6 promoter after IFN treatment

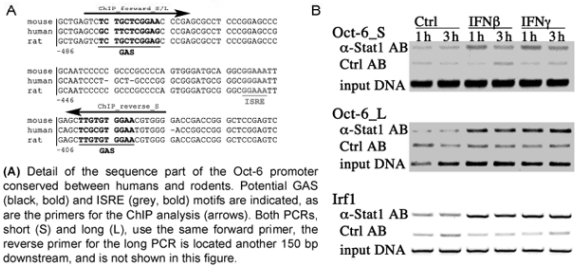

(A) Detail of the sequence part of the Oct-6 promoter conserved between humans and rodents. Potential GAS (black, bold) and ISRE (grey, bold) motifs are indicated, as are the primers for the ChIP analysis (arrows). Both PCRs, short (S) and long (L), use the same forward primer, the reverse primer for the long PCR is located another 150 bp downstream, and is not shown in this figure.

(B) WT BMM were treated with IFNβ (500 U/ml) and IFNγ (200 U/ml) for 1h and 3h, or left untreated (Ctrl). ChIP against Stat1 (α-Stat1 AB) with unspecific rabbit serum as control (Ctrl AB) was performed, followed by two different PCRs for the Oct-6 promoter (S and L), and a PCR for the Irf1 promoter as a control.

Oct-6 localises to the nucleus after IFNβ or poly(I:C) treatment

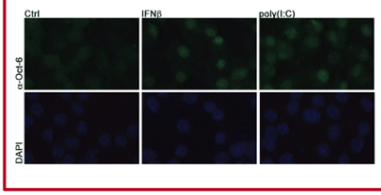

WT BMMs were grown on glass slides, treated with IFNβ (1000 U/ml) or poly(I:C) (50 µg/ml), or left untreated (Ctrl). After 6h cells were fixed with formaldehyde (4%) and permeabilised with methanol. Oct-6 was detected by immuno-fluorescence with an α-Oct-6 primary antibody (Santa Cruz) and a fluorescently labeled α-goat IgG secondary antibody (Alexa). Nuclei were stained with DAPI.

Oct-6 is involved in transcriptional regulation of the responses to poly(I:C) treatment - microarray analysis

- WT *versus* Oct-6-/- fetal liver-derived macrophages (FLMs)
- Untreated *versus* poly(I:C) treated (pIC; 50 µg/ml for 8h)

Numbers of genes differentially regulated (at least 2-fold, $p<0.05$)

WT_Ctrl *vs.* WT_pIC (treatment effect)	3570
WT_Ctrl *vs.* WT_pIC - upregulated	1142
WT_Ctrl *vs.* WT_pIC - downregulated	2428
WT_pIC *vs.* Oct-6-/-_pIC (genotype effect)	222
WT_pIC *vs.* Oct-6-/-_pIC - upregulated	85
WT_pIC *vs.* Oct-6-/-_pIC - downregulated	137

ABI 1700 mouse whole genome microarray expression system (Applied Biosystems).

Oct-6 has activating as well as repressing functions in modulating the transcriptional responses to poly(I:C).

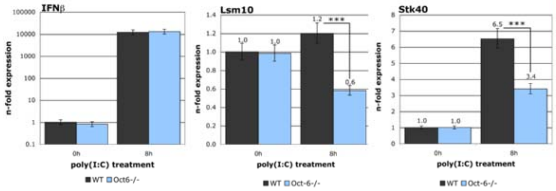

WT and Oct-6-/- FLMs were treated with poly(I:C) (50 µg/ml) for 8h. Target gene expression (Lsm10: U7 snRNP-specific Sm-like protein LSM10; Stk40: serine/threonine kinase 40) was analysed by RT-qPCR. Results from six independent experiment are shown (mean values ± SE; *** indicates $p<0.001$).

Summary and conclusions

- Oct-6 is induced by IFNα/β and IFNγ treatment.
- Murine cytomegalovirus infection and poly(I:C) treatment induce expression of Oct-6 in a type I IFN dependent manner.
- Induction of Oct-6 is dependent on Jak/Stat signalling.
- Stat1 binds to a conserved region in the Oct-6 promoter containing potential GAS and ISRE motifs.
- **Oct-6 expression and activity are not as restricted as previously thought.**
- Microarray analysis reveals involvement of Oct-6 in the regulation of transcriptional responses to poly(I:C).
- **Data suggest novel functions of Oct-6 in innate immunity.**

References
1. Jaegle M., Mandemakers W., Broos L., Zwart R., Karis A., Visser P., Grosveld F., Meijer D. (1996). The POU factor Oct-6 and Schwann cell differentiation. *Science*, 273:507-510.
2. Herr W., Cleary MA. (1995). The POU domain: versatility in transcriptional regulation by a flexible two-in-one DNA-binding domain. *Genes Dev.*, 9(14):1679-93.
3. Bermingham JR. Jr., Scherer SS., O'Connell S., Arroyo E., Kalla KA., Powell FL.,Rosenfeld MG. (1996). Tst-1/Oct-6/SCIP regulates a unique step in peripheral myelination and is required for normal respiration. *Genes Dev.* 10(14):1751-62.

Acknowledgement
MM and BS are funded by the Austrian Science Fund (FWF) SFB F28 Jak-Stat Signalling. Biomodels Austria is supported by the Federal Austrian Ministry of Science and Research (BM.W_f GZ200.11/1-VI/1/2004).